UNICAMP

Thaís dos Santos Pegoretti

Environmental and sound analysis of the acoustic treatment of vehicle compartments

Análise ambiental e sonora do tratamento acústico de habitáculos de veículos

74/2014

CAMPINAS
2014

i

UNIVERSIDADE ESTADUAL DE CAMPINAS

FACULDADE DE ENGENHARIA MECÂNICA

Thaís dos Santos Pegoretti

Environmental and sound analysis of the acoustic treatment of vehicle compartments

Análise ambiental e sonora do tratamento acústico de habitáculos de veículos

Doctoral Thesis presented to the School of Mechanical Engineering of the University of Campinas in partial fulfillment of the requirements for the degree of Doctor in Mechanical Engineering, in the Area of Solid Mechanics and Mechanic of Design.

Tese de Doutorado apresentada à Faculdade de Engenharia Mecânica da Universidade Estadual de Campinas como parte dos requisitos exigidos para obtenção do título de Doutora em Engenharia Meânica, na Área Mecânica dos Sólidos e Projeto Mecânico.

Orientador: Prof. Dr. José Roberto de França Arruda
Coorientador: Pierre Lamary

ESTE EXEMPLAR CORRESPONDE À VERSÃO FINAL DA TESE DEFENDIDA PELA ALUNA Thaís dos Santos Pegoretti, E ORIENTADA PELO PROF. DR. José Roberto de França Arruda.

....

ASSINATURA DO ORIENTADOR

CAMPINAS
2014

iii

UNIVERSIDADE ESTADUAL DE CAMPINAS

FACULDADE DE ENGENHARIA MECÂNICA

COMISSÃO DE PÓS-GRADUAÇÃO EM ENGENHARIA MECÂNICA

DEPARTAMENTO DE MECÂNICA COMPUTACIONAL
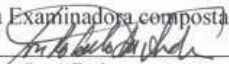
TESE DE DOUTORADO

Environmental and sound analysis of the acoustic treatment of vehicle compartments

Análise ambiental e sonora do tratamento acústico de habitáculos de veículos

Autora: Thaís dos Santos Pegoretti
Orientador: José Roberto de França Arruda
Co-orientador: Pierre Lamary

A Banca Examinadora composta pelos membros abaixo aprovou esta Tese:
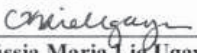
_____
Prof. Dr. José Roberto de França Arruda, Presidente
DMC/FEM/UNICAMP

_____
Prof. Dr. José Maria Campos dos Santos
DMC/FEM/UNICAMP

_____
Prof. Dr. Renato Pavanello
DMC/FEM/UNICAMP

_____
Profa. Dra. Cássia Maria Lie Ugaya
UTFPR

_____
Prof. Dr. Marcus Antônio Viana Duarte
FEMEC/UFU

Campinas, 21 de Julho de 2014.

To my husband, Felipe.

Acknowledgments

I would like to say thanks

To my advisor, Dr. José Roberto de França Arruda.

To my co-advisor, Dr. Pierre Lamary from UFC.

To Dr. Daniel Brissaud for accepting me at G-SCOP and for contributing with my work.

To Dr. Fabrice Mathieux, for the continuous encouragement throughout these four years.

To my family.

To my laboratory colleagues: Dani, Marcela, Jaque, Nilson and Ana.

To CNPq, for the financial support.

Genius is one percent inspiration, ninety nine percent perspiration.

Thomas Alva Edison

Resumo

PEGORETTI, Thaís dos Santos. Análise ambiental e sonora do tratamento acústico de habitáculos de veículos. 2014. 122p. Tese de Doutorado. Faculdade de Engenharia Mecânica, Universidade Estadual de Campinas, Campinas.

Este trabalho tem como objetivo desenvolver uma metodologia capaz de adicionar critérios ambientais à fase de pré-projeto de um tratamento acústico veicular. Essa integração foi realizada através de uma otimização multiobjetivo baseada em um algoritmo genético. Um caso real foi analisado com a metodologia proposta. Ele consiste em um painel acústico multicamadas aplicado em um automóvel de passeio. O método da matriz de transferência é usado para o cálculo do comportamento acústico do painel. Neste método é feita a hipótese simplificadora de painel de área infinita, o que permite um custo computacional muito menor do que modelos de elementos finitos. Para a modelagem de materiais poroelásticos, utiliza-se o modelo de Johnson-Champoux-Allard, que inclui os fenômenos de dispersão de energia resultante da interação térmica e viscosa entre as fases sólida e fluida. O custo computacional menor do modelo é essencial para a otimização. Foram estabelecidos como objetivos da otimização a curva de perda de transmissão desejada e os resultados da análise do ciclo de vida do painel. Uma curva de perda de transmissão em função de bandas de oitava foi estabelecida como um critério de desempenho acústico mínimo. Para os critérios ambientais, o impacto de um painel existente foi estabelecido como máximo. A análise do ciclo de vida quantifica o impacto do produto em relação a diversos aspectos. Na metodologia proposta três critérios foram selecionados inicialmente: aquecimento global, destruição de recursos abióticos e toxicidade da água doce. Finalmente, apenas um deles foi utilizado na otimização, o aquecimento global, pois os critérios máximos estabelecidos para os demais eram facilmente atingidos ao longo da otimização. A otimização multiobjetivos gera como resultado uma frente de Pareto com um conjunto de soluções, e cabe ao projetista escolher a melhor opção, analisando-a em relação ao impacto ambiental e a outros aspectos, tais como disponibilidade e custo.

Palavras-chave: Materiais poroelasticos., Análise do ciclo de vida, Otimização multiobjetivo.

Abstract

PEGORETTI, Thaís dos Santos. Environmental and sound analysis of the acoustic treatment of vehicle compartments. 2014. 122p. Tese de doutorado. Faculdade de Engenharia Mecânica, Universidade Estadual de Campinas, Campinas.

This work aims at developing a methodology capable of adding environmental criteria to the pre-design of a vehicular acoustic treatment. This integration was accomplished through a multi-objective optimization based on a genetic algorithm. A real case study was analyzed with the proposed methodology. It consists of a multilayered acoustic panel applied in passenger vehicles. The transfer matrix method is used to calculate the acoustic behavior of the panel. In this method the panel area is infinite. It provides a lower computational cost than finite element models, which can take into account the real dimensions of the panel. The Johnson-Champoux-Allard model was used for poroelastic material modeling. It includes the energy loss generated by the viscous and the thermal interactions between the solid and the fluid media. The lower computational cost of the model is essential for the optimization. The desired acoustic transmission and results of the life cycle analysis of the panel were established as the optimization objectives. A transmission loss curve in octave bands was defined as a minimum noise performance criterion. For the environmental criteria, an existing panel behavior was established as the maximum. The life cycle assessment quantifies the product impact with respect to many aspects. In the proposed methodology, three criteria were initially selected: global warming, abiotic depletion, and fresh water aquatic ecotoxicity. Finally, only one of them was used in the optimization, the global warming, because the maximum values established for the other criteria were easily achieved during the optimization. The multi-objective optimization provides a Pareto front solutions set, and it is up to the designer to choose the best option, analyzing the solution set with relation to environmental impact and other aspects, such as availability and cost.

Keywords: Poroelastic materials, life cycle assessment, Multi-objective optimization.

List of Illustrations

List of Tables

List of most used symbols and abbreviations

Symbol	Description	Unit
$j = \sqrt{-1}$	Imaginary number	-
ω	Frequency	Hz
c_0	Sound propagation velocity	ms^{-1}
μ	Viscosity	$kgm^{-1}s^{-1}$
μ_L and λ	Lamé coefficients	-
ϕ_P	Porosity	Dimensionless
α_∞	Tortuosity	Dimensionless
σ_R	Flow resistivity	$Nm^{-4}s$
Λ	Viscous characteristic length	m
Λ'	Thermal characteristic length	m
ϕ	Longitudinal sound wave displacement potential	-
ψ	Shear wave displacement potential	-
k	Bulk modulus	
ρ	Density	kgm^{-3}
$\bar{\bar{\sigma}}_{ij,j}^{S}$	Solid stress tensor	-
$\bar{\bar{\sigma}}_{ij,j}^{F}$	Fluid stress tensor	-
$\bar{\epsilon}^{F}$	Fluid deformations	-
$\bar{\epsilon}^{S}$	Solid deformations	-
$\vec{u}^{F}$	Fluid displacement	-
$\vec{u}^{S}$	Solid displacement	-

Abbreviation	Description
A	Acidification
AD	Abiotic depletion
E	Eutrophication
EF	Elementary flow
FU	Functional unit
FWAE	Fresh water aquatic ecotoxocity
LCA	Life cycle assessment
LCIA	Life cycle impact assessment
OLD	Ozone layer depletion
TE	Terrestrial ecotoxicity

TABLE OF CONTENTS

1 Introduction

The design phase of a product is determinant for its performance with relation to its main function and also concerning other fields such as economy, environment, society, etc. This step of the production process is specifically developed according to the context: country where the product will be sent, available suppliers and clients that the industry desires to reach. So, at this moment, designers should keep in mind all the consequences related to manufacturing, using and disposing of hundreds or thousands of samples. The choice of a design solution among others depends on a criteria set composed of their main concern fields. Generally, different weights are given to each field depending on its importance, in order to facilitate the decision.

The systematic design has composed the engineering curricula for decades (POLAK, 1976), (PAHL E BEITZ, 1992), (JONES, 1992). However, it is not usually practiced in the industry. Eder (1998) presents tree reasons for that:

1. Most industries work with a restricted quantity of products. Therefore, engineers believe they already know the possible design solutions for this family of products. Moreover, generally a narrow quantity of suppliers is available, what restricts the design project.

2. The industry has no time and no staff to waste in a complicated process that is not guaranteed to generate a better design.

3. There is a resistance to making changes on the actual industrial design process in order to include systematic design concepts.

Jones (1992) mentions two traditional design methods: Craft evolution and Design by drawing. The first one refers to the design through a long process of craft work, while the second names the design by making scale drawings. The latter takes a long time to achieve an optimal design, and the production is not involved in the trial-and-error process, it is replaced by scale drawings. It is interesting to mention that complex designs such as the rowing boat, the violin, and the axe were achieved using craft design, and the craftsmen generally cannot give adequate reasons for the decisions they take. It is possible to conclude that the design process also includes art and sensibility, and the methods and the tools generally only guide the design team. So, ideally, an equilibrium between free art and design procedures should to be followed in the industry.

Seven modern design methods are listed by Jones (1992). Some of them are: systematic search, value analysis, systems engineering, and boundary searching. Most of them include the optimization idea, however not using directly an optimization numerical tool. The systematic search is the closest to a single objective optimization, even including weighting factors among the objectives. However, no theoretical model is used for each objective value calculation. Generally, in the industry, the design team asks the other departments to predict approximate objective values. Recent works develop mathematical tools based on optimization in the design process, but including theoretical models in the objective functions calculation.

1.1 Related works

Komly *et al.* (2012) developed a mathematical model based on Life Cycle Assessment (LCA) results to assess the environmental efficiency of the end-of-life management of polyethylene terephthalate (PET) bottles. They applied multi-objective optimization, genetic algorithm, and decision making in this work. The multi-objective problem consists in finding the allocation of bottles between valorization paths that minimize the environmental impacts of bottle end-of-lives. The LCA impact categories studied are: abiotic depletion, acidification, and global warming.

Tang *et al.* (2010) optimize shape, sizing and material selection for three examples through a multi-objective optimization involving mixed variables. One of them is a square plate with a central hole subjected to thermal and static loads. Structural performance and weight are their criteria, so both the maximum stress and the total plate weight are minimized. They could obtain a stress distribution of the final design that enabled them to see how the stress concentration phenomena transfer from the edge to the hole in the original design and this distribution changed significantly in the final design with an obvious quantitative decrease.

Acoustic multilayered panel manufacturers need to face the following problem: to select materials and to combine layers. Tanneau *et al.* (2006) analyze these multilayered panels including acoustic performance and mass criteria. They develop a single objective optimization with genetic algorithm maximizing the transmission loss and minimizing the total mass. The variables are the layer thicknesses. The material choice and the number of layers is fixed. They concluded that the optimization is an efficient tool for this kind of problem.

Lee e Kim (2007) maximized transmission loss of a poroelastic layer sequence using one-dimensional topology optimization. The material layout is optimized with given design space, loading and boundary conditions. The air and a poroelastic material are defined as material options and different layouts are obtained depending on the analyzed frequency range. The optimized foam layouts outperform nominal foam performances for all frequency bands considered.

Lind-Nordgren e Goransson (2010) also consider acoustic performance and mass as their criteria. Given a fixed multilayered configuration, they replace an air layer by a porous material one optimizing its micro properties: porosity, Young Modulus, viscous characteristic length, and static flow resistivity. Pressure level (weighted through A and C weighting) and mass are minimized. In order to show that a more flexible optimization model would provide more alternatives of solutions, they state that: "Rather than to optimize only one foam layer it would be natural to want to optimize an entire multilayered panel, where the number of layers, the thickness of each layer and the foam properties of each layer are all variables to be considered."

These examples illustrate the industry necessity for tools that quantify and compare the product performance in different aspects to facilitate decision making. Ideally, these tools should provide a solutions set that lies among designers project limitations, so they could choose from this group the optimal solutions considering the decision moment and the context.

1.2 Aim of this work

This work aims at developing a methodology that enables sound panel designers to analyze their products considering their environmental performance. A multi-objective optimization (DEB, 2001) generates a group of design solutions for a multilayered panel applied in vehicles given an acoustic minimum and an environmental maximum objectives. The novelty of this work is to include the environmental criteria in the design phase of the acoustic panel. The developed methodology can be expanded to other products and to other fields, resulting in a powerful tool for designers and, afterwards, for decision makers.

This is a transversal work that begins with poroelastic material acoustics and Life Cycle Assessment (LCA) research fields. Uncertainty analyzes can be made at this point in order to analyze the models sensitivity to the input data. Then, poroelastic materials acoustic and environmental
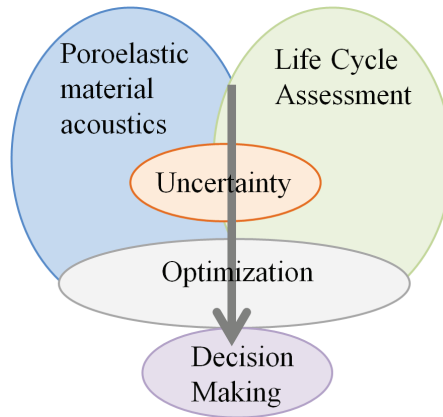
Figure 1.1: Transversal progression of this work passing by different research fields.

assessments are joined through a multi-objective optimization that yields the final choice of the optimal solution. This transversal passage is illustrated in Figure 1.1

1.3 Brief methodology

In the acoustics field, first the Biot model that was used in order to study poroelastic materials is applied in the Transfer Matrix method, with *TMTX* software. It was developed by PhD Pierre Lamary and PhD Olivier Tanneau in Matlab® environment. Using this method, it was possible to predict the transmission loss and the absorption of fluid, solid, and poroelastic materials. Moreover it was also possible to analyze sequential combinations of these fields that compose multilayered acoustic panels. Three recycled cotton felts and a loaded rubber were characterized at *CTTM* ("Centre de Transfert de Technologie du Mans"), in Le Mans, France, so the acoustic behavior of the real case study panel models could be simulated and compared.

In the environmental field, the life cycle assessment of three panel models was made. Two allocation splits for the recycled cotton were used: "50/50" and "100/0", and two end-of-life scenarios were analyzed: landfill and incineration with energy recovery. The calculation was made in SimaPro® version 7.3.3 environment, with *EcoInvent* V2 database and CML 2002 Life cycle impact assessment method, regarding the following impact categories: Abiotic Depletion, Acidification, Eutrophication, Global Warming, Ozone Layer Depletion, Fresh Water Aquatic Ecotoxicity, and Terrestrial Ecotoxicity.

Uncertainty analyzes were separately developed in both models. In the acoustic model, the influence of the porous material flow resistivity parameter variation in a single layer panel transmission loss was studied. A random variable approach was achieved with the Monte Carlo method and a random field approach was reached with the Karhunen-Loève expansion. Simulations were developed in Matlab® environment. In the environmental model, the raw material quantities were considered as random variables, and their influence in the impact assessment results was observed through the mean and the coefficient of variation of each impact category. The Monte Carlo method tool available in SimaPro® was used.

In order to join both models, a surface response based on a second degree polynomial was adjusted to fit the environmental model. One surface response was developed for each material layer type present in the real case study. So a multilayered panel environmental impact calculation was simplified as the sum of the impacts of each one of its layers.

The multi-objective optimization was developed in Matlab®, using its optimization toolbox. The creation, the mutation, and the crossover functions were modified, because it was necessary to deal with discrete (material type) and continuous (layer thickness) variables. The transmission loss performance was maximized, while the environmental impact was minimized. The number of layers, the materials database, and the maximum multilayered panel thickness were defined and an optimal solution set was calculated. The solutions were disposed in a bidimensional Pareto front, according to their environmental and acoustic scores. Thus the design team is able to analyze each solution in detail and to choose the best option according to the choice moment and to other concerns, such as cost and availability.

1.4 Real case study

Acoustic panels (also called dashes or front body panels) are analyzed in this work. The dashes are produced by *Coplac*®, an industry located in the city of Itu, state of São Paulo, Brazil. The company seized the opportunity to use scraps of jeans from local manufacturers to produce its automobile equipment. Currently, the three panel types are produced and applied in different vehicle models. Nowadays, a panel composed of recycled cotton fibers is used in an automobile model called *Agile*®. Their external size and shape are dictated by the car geometry.
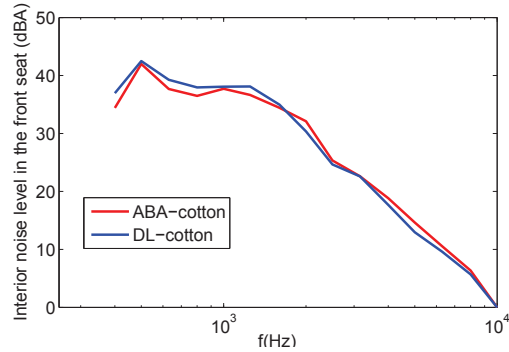
Figure 1.2: Interior vehicle sound level and loudness guaranteed by ABA-cotton and DL-cotton acoustic panels. The scale of the Y-axis is omitted for confidentiality reasons.

The three design options for the acoustic panels analyzed in this work are:

1. A Dual-Layer panel mainly made of polyurethane (PU), called DL-PU; this is the "status-quo" option because is a widely used solution that uses non-renewable materials;

2. An Absorption-Barrier-Absorption panel mainly made of recycled textile, called ABA-cotton; this is the first innovative option;

3. A Dual-Layer panel mainly made of recycled textile, called DL-cotton; this is the second innovative option.

During tests at the *General Motors*® facility, the noise level curve (shown in Fig. 1.2) was measured at the front seat of the vehicle when an acoustic source emitted sound waves from the engine component of the vehicle and with the panels well placed in the dashboard.

The loudness concept (KINSLER, 1982) - an attribute of hearing sensation for sounds that can be ordered in a scale that extends between quiet and loud - can be used here as a basis for comparison between the curves. Different quantitative loudness measures try to adjust sound measurements to correspond to the loudness perceived by the human ear, for instance: the complex Zwicker loudness model (MOORE E GLASBERG, 1996) and the simpler A-weighting method (BARRON, 2003). The loudness perceived by the vehicle passengers is calculated through A-weighting, when the vehicles are assembled with the two recycled fibers' options of panel.
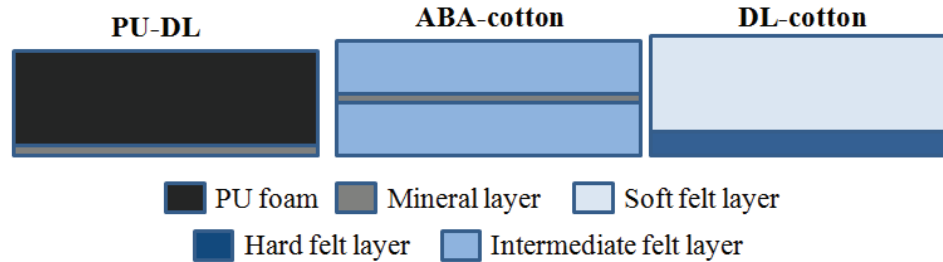
Figure 1.3: Lateral view scheme of the DL-PU, ABA and DL-cotton panels, from the left to the right.

The DL-PU panel was used as a reference for ABA-cotton and DL-cotton, as it already guarantees a satisfactory noise level. The values of loudness obtained for the panels were quite close: 71,9dBA for the ABA-cotton panel and 72,2dBA for the DL-cotton panel. This difference cannot be perceived by the passengers. Therefore, the acoustic performances were considered equal for this study, as a first approximation, making possible to define a Functional Unit for the three systems.

Lateral view schemes of the acoustic panels are illustrated in Figure 1.3. They consist of PU foam, mineral mixture (cement, calcite and low density polyethylene), and felt mixture (scraps of jeans' manufacturers (cotton fibers), scraps of the panel production (cotton fibers + polyethylene (PE)) and low density PE). The exact composition of raw material in each layer cannot be mentioned here for confidentiality reasons. There are two models: DL and ABA and the thickness of each layer vary according to the design project. The mineral layer is identical in DL-PU and in ABA-cotton panels. There are also three types of felt layers depending on their density: hard, soft and intermediate. The hard felt is denser and it isolates the noise, while the soft layer dissipates it. The intermediate layer behaves as isolator and dissipator; however its performance is medium in both criteria. Panels' specific characteristics will be detailed in the following section.

1.4.1 DL-PU panel

The DL-PU panel is composed of a PU foam layer and a mineral layer, as shown in Figure 1.3. The total input material mass of this product is 13.3kg, though, after the panel is pressed and cut in order to obtain the desired geometry/shape, which has holes, it loses 3.5kg, and the DL-PU panel final mass is 9.9kg.

Mass (kg)	DL-PU	ABA-cotton	DL-cotton
Input materials	13.3	13.7	7.7
PU-foam	4.4	0	0
Mineral mixture	8.9	4.8	0
Felt mixture	0	8.9	7.7
Production scraps	3.5	3.6	2.0
Final Product	9.9	10.1	5.7

Table 1.1: Total masses, mixtures, and scraps of the panels.

1.4.2 ABA-cotton panel

The ABA-cotton panel is a sandwich of a mineral layer between two intermediate felt layers. The 8.9kg mineral layer is pressed with 4.8kg of intermediate felt layers. 3.6kg of scraps are generated and its final mass is of 10.1kg. The scraps of felt return to the production process.

1.4.3 DL-cotton panel

The third panel is the DL-cotton panel, which consists of two felt layers with different densities: one layer of hard felt and the other one of soft felt. The total input material mass of these layers is 7.7kg and the panel production generates 2.0kg of scraps, so the DL panel final mass is 5.7kg. The DL-cotton panel has been developed by *Coplac*® as an evolution of the ABA-cotton panel, aiming at similar acoustic performance without calcite or cement, thanks to specific materials and design architecture. This evolution was developed for cost and weight reduction: a reduction of 13% in the panel price was obtained by the evolution from ABA-cotton panel to DL-cotton panel.

Table 1.1 summarizes input material, production scraps and final product masses for the three products.

1.5 Outline

In Chap. 2 porous material acoustics background is exposed. Equivalent Fluid model, Biot model, and the Transfer Matrix method are detailed. The characterized parameters of the poroelas-

tic material are listed and results of simulations using the Equivalent Fluid model are presented. In Chap. 3 the Life Cycle Assessment methodology theory is summarized, a discussion about natural fibers is made, and an example addressing the influence of modeling in LCA results is presented. Chapter 4 contains the real case study LCA. The results follow the life cycle phases sequence: production, production + use, production + use + landfill end-of life, and production + use + incineration with energy recovery end-of life. The LCA uncertainty analysis is included in this chapter. In Chap. 5 a preliminary uncertainty analysis of the acoustic model is made, using a Monte Carlo method and the Karhunen-Loève expansion. In this preliminary uncertainty integration, the influence of flow resistivity variation along the panel thickness in the material transmission loss is evaluated. Environmental assessment and acoustic performance are put together in Chapter 6. A multi-objective optimization considering mixed variables is made in order to encounter the best multilayered acoustic panel solution for the real case study. Finally, in Chapter 7, final discussions are made and conclusions are presented.

2   Porous Material Acoustic background

In this chapter porous materials characteristics are presented. Then, equivalent fluid model (Biot's model), and behavior equations are introduced. Finally, the transfer matrix method for transmission loss and absorption prediction is explained, also including the continuity relationships. Next, the characterization method is briefly discussed and the parameters obtained for three felts and one loaded rubber are listed. Finally, simulations using the software *TMTX* for absorption, transmission loss and insertion loss are presented. This software was developed by PhD Pierre Lamary and PhD Olivier Tanneau, applying the Transfer Matrix method **??** in Matlab® environment.

2.1   Poroelastic medium description

A porous medium is a material composed of skeletal (also called matrix or frame) and pores. The pores are generally filled with a fluid that can be liquid or gas, while the skeleton is solid (generally constituted by fibers or by a polymeric matrix) (Allard, 1993). Some examples of porous materials are: foams, bones, ceramics, and rocks. Poroelastic materials are commonly applied in buildings, vehicles and airplanes for sound absorption and insulation.

When modeling this type of material, the presence of two phases generates the necessity of considering the solid-fluid interface. Thermal and viscous dissipation effects of the fluid makes the porous medium to behave as acoustically dissipative and absorbent. If skeleton movements are neglected, a porous medium can be modeled as an equivalent fluid (see Section 2.2).

To study the wave propagation in porous materials, it is necessary to assume some hypotheses (Dauchez, 1999):

H1: **Macroscopic scale**: in a microscopic scale, the medium is full of complexities and variations. So, observing it in a macroscopic scale and considering a volume element with a sufficient quantity of pores, its statistic characteristics does not significantly vary. Therefore one considers that the material is locally homogeneous.

H2: **Large wavelength**: wavelength must be larger than the volume element size, so it is

possible to apply continuous medium tools.

H3: **Linear elasticity**: stress-strain relations are linear.

H4: **Harmonic regime**: the variables that describe the movement have an harmonic temporal relation in the form $e^{j\omega t}$, so that instantaneous quantities $a(t)$ are expressed in function of complex amplitudes a by: $a(t) = \Re(ae^{j\omega t})$

A poroelastic material contains 3 parameter groups.

1. Saturating fluid: it is described by the static volumetric mass (ρ_0), the sound velocity c_0, the viscosity μ, the Prandt number N_{Pr}, the loss factor η, etc. The complete list of parameters is presented in Tab. 2.1.

2. Mechanic skeleton behavior: it is characterized by the volumetric mass ρ_1, the Young Modulus E, and the Poisson coefficient ν.

3. Solid-fluid interactions: it includes elastic, inertial, viscous and thermal interactions. To understand these interactions, it is necessary to know the following parameters:

Porosity (ϕ_P) expresses a fraction of the volume fluid (V_f) over the total volume (V_t): ($\phi_P = \frac{V_f}{V_t}$) that lies between 0 (solid medium) and 1 (fluid medium). It influences physical properties such as: density, thermal conductivity and mechanical resistance. (Allard, 1993) states that "For most of fibrous materials and plastic foams with open bubbles, the porosity lies very close to one". Porosity is dimensionless.

Tortuosity (α_∞) is a measure of the axial axis deviation of the pores along the wave propagation direction of the porous material. It permits to describe the inertial coupling translated as an increase in the fluid volumetric mass. An equivalent fluid density is defined such as: $\rho_e = \alpha_\infty \rho_0$. The tortuosity minimum value is 1 and it is dimensionless.

Flow resistivity (σ_R) describes the viscous interactions in low frequencies (Dauchez, 1999). In this frequency range, the viscous boundary layer is larger than the pore size, so friction viscous

forces are present in the fluid domain. It is defined as the ratio:

$$\sigma_R = \frac{(p_2 - p_1)}{Ve} \tag{2.1}$$

where p_1 and p_2 are the pressures in both sides of the material, V is the velocity of air flow per unit area, and e is the material thickness. Its value vary between $1000 Nm^{-4}s$ for the "more opened" materials and $100000 Nm^{-4}s$ for the "more closed", or for impermeable films.

Viscous Characteristic length (Λ) describes the viscous effects in high frequencies. In low frequencies, inertial forces dominate viscous shear forces, so the effect is significant only near the skeleton walls (Dauchez, 1999).

Thermal Characteristic length (Λ') describes the thermal exchanges between the two phases in high frequencies. The skeleton has a high thermal inertia, when compared with the fluid. So it tries to modify the fluid incompressibility modulus that varies between the isothermal modulus, in low frequencies, and the adiabatic modulus, in high frequencies.

Generally, the characteristic lengths vary between 10^{-5} and 10^{-3} m.

2.2 Equivalent Fluid Model

The equation for waves propagation in fluids is written as Eq. 2.2 (Allard, 1993), (Allard e Atalla, 2009), (Tanneau, 2002). The scalar displacement potential is represented by $u = \nabla\phi + \nabla \wedge \psi$.

$$\nabla\phi - \frac{1}{c_0^2}\frac{\partial^2 \phi}{\partial t^2} = 0 \tag{2.2}$$

where $c_0 = \sqrt{\frac{K}{\rho}}$ is the sound wave propagation velocity, and K and ρ are fluid characteristics: Bulk modulus and density. However, in the Equivalent Fluid Model of a poroelastic medium, the solid phase presence is expressed as a modification in the fluid characteristics: the propagation velocity changes and dissipative terms are included in the material behavior (volumetric mass and equivalent modulus are complex). In other words, c_0 from Eq. 2.2 is expressed such as:

$c_0 = \sqrt{K/\rho}$. These fluid characteristics can be obtained through semi-empirical formulas and with theoretical considerations. In this work, the mathematical model developed by Johnson, Champoux, and Allard that is named JCA model is applied (Allard, 1993), (Atalla e Panneton, 2005). It considers viscous and thermal coupling between the skeleton and the air. The expression for K is given by Eq. 2.3.

$$K(\omega) = \frac{\gamma P_0}{\gamma - (\gamma - 1)\left(1 + \frac{8\eta}{j\Lambda'^2 N_{Pr}^2 \omega \rho_0}\sqrt{1 + j\rho_0 \frac{\omega N_{Pr}^2 \Lambda'^2}{16\eta}}\right)^{-1}} \tag{2.3}$$

For the equivalent density ρ, the following parameters are defined:

$$\rho = \frac{\tilde{\rho_{22}}}{\phi_P} \tag{2.4}$$

where

$$\tilde{\rho_{22}} = \phi_P \rho_0 + \rho_a + \frac{1}{j\omega}\tilde{b} \tag{2.5}$$

with

$$\tilde{b} = \sigma_R \phi_P^2 \sqrt{1 + \frac{4j\alpha_\infty^2 \eta \rho_0 \omega}{\sigma_R^2 \Lambda^2 \phi_P^2}} \tag{2.6}$$

Finally,

$$\rho_a = \phi_P \rho_0 (\alpha_\infty - 1) \tag{2.7}$$

where ρ_0 is fluid the volumetric mass, μ is the fluid viscosity, N_{Pr} is the Prandt Number, and $\gamma = c_p/c_v$ is the specific heats ratio. This model provides good results for materials with high porosity. The standard numerical values for air parameters are listed in Tab. 2.1 (Atalla e Panneton, 2005), (Dauchez, 1999).

2.3 Biot's Model

Unlike the Equivalent Fluid model, the Biot's model considers the skeleton movements, and consequently includes the relative movements between both fluid and solid mediums. Allard (1993)

Property	Nomenclature, Value and Unit
Temperature	$T_0 = 18C$
Pressure	$p_0 = 1.0132x10^5 Pa$
Volumetric mass	$\rho_0 = 1.213 kg.m^{-3}$
Sound velocity	$c_0 = 342.2 m.s^{-1}$
Adiabatic incompressibility modulus	$K_a = 1.42x10^5 Pa$
Characteristic impedance	$Z_0 = 415.1 Pa.m^{-1}s$
Viscosity	$\mu = 1.84x10^{-5} kg.m^{-1}.s^{-1}$
Prandt number	$N_{Pr} = 0.74$
Specific heats reason	$\gamma = 1.4$

Table 2.1: Saturated Air Fluid Properties. Adapted from Dauchez (1999).

added the viscous effects in Biot's model. The equilibrium equations, written in *UU* form (a function of solid and fluid displacements *u*), for the solid and for the fluid, respectively, are:

$$
\begin{aligned}
\bar{\bar{\sigma}}_{ij,j}^S + \omega^2 \left(\tilde{\rho}_{11} \vec{u}_i^S + \tilde{\rho}_{12} \vec{u}_i^F \right) &= 0 \\
\bar{\bar{\sigma}}_{ij,j}^F + \omega^2 \left(\tilde{\rho}_{12} \vec{u}_i^S + \tilde{\rho}_{22} \vec{u}_i^F \right) &= 0
\end{aligned}
\tag{2.8}
$$

where the convention for the temporal dependence is $e^{j\omega t}$. JCA micro/macro model (ALLARD, 1993) for the parameters involved in Eq. 2.8 are expressed such as shown in Eq. 2.5 and 2.9.

$$
\begin{aligned}
\tilde{\rho}_{11} &= \rho_1 + \rho_a + \frac{1}{j\omega}\tilde{b} \\
\tilde{\rho}_{12} &= -\rho_a - \frac{1}{j\omega}\tilde{b}
\end{aligned}
\tag{2.9}
$$

Considering the vibrations of the solid phase, modeling the material as biphasic and homogenized, and including viscous, inertia and pressure couplings, this model is considered complete in the literature. Therefore, it is commonly used in researches in the porous materials field.

2.4 Constitutive Equations

The field behavior is described by a coupled constitutive equations system (Allard, 1993):

$$\bar{\bar{\sigma}}_{ij,j}^S = ((P - 2\mu_L)\bar{\epsilon}_{kk}^S + Q\bar{\epsilon}_{kk}^F)\delta_{i,j} + 2\mu_L \bar{\epsilon}_{i,j}^S$$
$$\bar{\bar{\sigma}}_{ij,j}^F = (R\bar{\epsilon}_{kk}^F + Q\bar{\epsilon}_{kk}^S)\delta_{i,j} \tag{2.10}$$

The parameters P, Q, and R are complex and related to the stiffnesses of both phases. They consider thermal dissipations effects. Fluid and solid deformations are given by ϵ_{kk}^F and ϵ_{kk}^S, respectively. λ_L and μ_L are Lamé coefficients of the empty skeleton. One considers the hypothesis that the compressibility skeleton modulus when empty or saturated with air are negligible. So, one writes:

$$P = \lambda_L + 2\mu_L + \frac{(1-\phi_P)^2}{\phi_P}K(\omega)$$
$$Q = (1 - \phi_P)K(\omega) \tag{2.11}$$
$$R = \phi_P K(\omega)$$

2.5 Transfer Matrix Method for Transmission Loss and Absorption predictions

The method used is able to evaluate the acoustic performance of a variety of materials: isotropic solids, fluid layers, and porous materials. It consists of combining the transfer matrices of each layer and of each interface. So, it enables researchers to analyze any material combination. The problem is summarized into restricted equations and studies can vary their parameters solving this problem in a reasonable computational time (Allard e Atalla, 2009), (Tanneau, 2002). The method implementation was developed by PhD Olivier Tanneau and PhD Pierre Lamary.

2.5.1 Principle of the method

The system consists of N layers, where the first (1) represents the incident field and the last (N), the receptor field (generally air). Each layer has e_i thickness in the z direction, as observed in Fig. 2.1. The coordinates x and y are considered infinite, generating an infinite transverse section area, so the problem only depends on the z coordinate. A wave propagated in medium 1 has as characteristics: incidence angle (θ_1), wavenumber (k_1), and amplitude(ϕ_1) (Allard e Atalla, 2009), (Tanneau, 2002).

We suppose that in each layer i, m waves propagate with a pulsation frequency ω. The number of waves depends on the type of the medium that they are transversally crossing: 1 wave in fluids, 2 waves in solids and 3 waves in poroelastics (two compression waves and one shear wave) (Tanneau, 2004). All waves with indexes i (layer) and j (wave) can be described by their incidence angle θ_i^j, a wavenumber k_i^j and two amplitudes ϕ_i^{aj} and ϕ_i^{rj} that correspond to the displacement potentials of the incident and of the reflected wave (forward and backward waves).
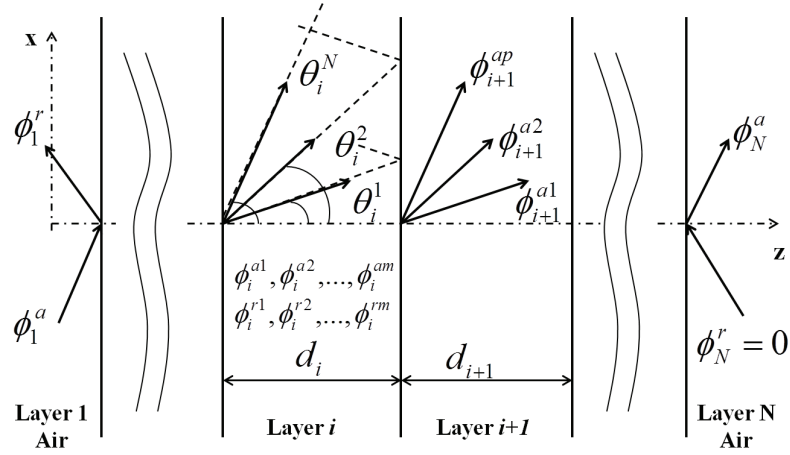
Figure 2.1: Transfer Matrices method schema, adapted from (TANNEAU, 2004).

According to the Snell-Descartes' law, it is possible to relate the layers i and $i+1$ angles as described in Eq. 2.12.

$$k_i sin(\theta_i) = k_{i+1} sin(\theta_{i+1}) \qquad (2.12)$$

The displacement potential at a given position $M(x,y,z)$ of the layer can be written as:

$$\phi_i(M)_{M \in i} = \left(\phi_i^a e^{-jk_i z cos\theta_i} + \phi_i^r e^{jk_i z cos\theta_i} \right) e^{-jk_i x sin\theta_i} \qquad (2.13)$$

To simplify, Eq. 2.13 can be written in matrix form, as shown in Eq. 2.14.

$$\phi_i(z) = [F_i(z)] \begin{bmatrix} \phi_i^a \\ \phi_i^r \end{bmatrix} \tag{2.14}$$

Using a displacement potential (Eq. 2.14) and deformation constraint relations defined by the transverse field, it is possible to establish the following relations.

$$\begin{bmatrix} \vec{u}_i(z) \\ \bar{\bar{\sigma}}_i(z) \end{bmatrix} = [G_i(z)] \begin{bmatrix} \phi_i^a \\ \phi_i^r \end{bmatrix} \tag{2.15}$$

Matrix $[G_i(z)]$ is defined in Sec. 2.5.2 and 2.5.3, for poroelastic, fluid and solid fields. The method's principle consists of imposing on each interface the displacement continuity relations and the restrictions in the frontier point (for instance $z = z_i^{i+1}$, that represents the interface between layers i and $i+1$.), where we can write:

$$[I_i] \begin{bmatrix} \vec{u}_i(z_i^{i+1}) \\ \bar{\bar{\sigma}}_i(z_i^{i+i}) \end{bmatrix} = [I_{i+1}] \begin{bmatrix} \vec{u}_{i+1}(z_i^{i+1}) \\ \bar{\bar{\sigma}}_{i+1}(z_i^{i+i}) \end{bmatrix} \tag{2.16}$$

where $[I]$ is the interface matrix that depends on i and $i+1$ material types. All possible interface matrices are listed in Sec. 2.5.3. Using the relations from Eq. 2.15, it is possible to write:

$$[I_i][G_i(z_i^{i+i})] \begin{bmatrix} \phi_i^a \\ \phi_i^r \end{bmatrix} = [I_{i+1}][G_{i+1}(z_i^{i+i})] \begin{bmatrix} \phi_{i+1}^a \\ \phi_{i+1}^r \end{bmatrix} \tag{2.17}$$

Naming $[A_i(z_i^{i+i})] = [I_i][G_i(z_i^{i+i})]$, the system from Eq. 2.17 becomes

$$\begin{bmatrix} A_i(z_i^{i+1}) & -A_{i+1}(z_i^{i+1}) \end{bmatrix} \begin{bmatrix} \phi_i^a \\ \phi_i^r \\ \phi_{i+1}^a \\ \phi_{i+1}^r \end{bmatrix} = [0] \tag{2.18}$$

18

After, it is necessary to assemble the Eq. 2.18 established for each of the interfaces in a unique system, as shown in Eq. 2.19. Boundary conditions are assigned to the system, so it includes the same number of equations and unknowns. We suppose that the incident wave is known and that there is no reflected wave in the last layer, therefore ϕ_1^a is fixed and $\phi_N^r = 0$.

$$
\begin{bmatrix}
A_1(z_1^2) & -A_2(z_1^2) & 0 & \cdots & 0 \\
0 & A_2(z_2^3) & -A_3(z_2^3) & \ddots & \cdots \\
\vdots & \ddots & \ddots & \ddots & 0 \\
0 & \cdots & 0 & A_{n-1}(z_{n-1}^n) & -A_n(z_{n-1}^n)
\end{bmatrix}
\cdot
\left\{
\begin{array}{c}
\phi_1^a \\
\phi_1^r \\
\phi_2^a \\
\phi_2^r \\
\phi_3^a \\
\phi_3^r \\
\vdots \\
\phi_n^a \\
\phi_n^r
\end{array}
\right\}
= [0]
\qquad (2.19)
$$

The transparency index is given by $\tau = \frac{\rho_N |\phi_N^a|^2}{\rho_1 |\phi_1^a|^2}$. Generally, the TL curve as a function of frequency is calculated as: $TL = 10\log(1/\tau)$.

The transmissibility experimental tests are made using a diffuse field. Therefore, for each frequency and for each incidence angle a computation is required and the TL curve is obtained as a mean of the indexes calculated for a fixed number of incidences (generally between 0^0 and 78^0) as shown by Eq.2.20.

$$
TL_{BD} = 2 \int_0^{\theta_{lim}} \tau(\theta) \sin\theta \cos\theta d\theta
\qquad (2.20)
$$

2.5.2 Applying to the porous media

The wave equations for the porous media are obtained substituting the behavior equations (Eq. 2.10) into the Biot's model equilibrium equations (Eq. 2.8). Decomposing fluid and solid

19

displacements as functions of fluid and solid potentials one obtains: $\vec{u}^S = \nabla\phi^S + \nabla \wedge \psi^S$ and $\vec{u}^F = \nabla\phi^F + \nabla \wedge \psi^F$, where ψ is the displacement potential of the shear wave. From Eq. 2.8, for the scalar potentials it is possible to write:

$$[M]\begin{bmatrix} \Delta\phi^S \\ \Delta\phi^S \end{bmatrix} + \omega^2[\rho]\begin{bmatrix} \phi^S \\ \phi^S \end{bmatrix} = [0] \tag{2.21}$$

with

$$[M] = \begin{bmatrix} P & Q \\ Q & R \end{bmatrix}, [\rho] = \begin{bmatrix} \tilde{\rho}_{11} & \tilde{\rho}_{12} \\ \tilde{\rho}_{12} & \tilde{\rho}_{22} \end{bmatrix} \tag{2.22}$$

The solutions can be expressed as an eigenvector base from the matrix $\omega^2[M^{-1}][\rho]$, as shown in Eq. 2.23.

$$[\phi] = \begin{bmatrix} \phi^S \\ \phi^F \end{bmatrix} = \phi_1\begin{bmatrix} 1 \\ r_1 \end{bmatrix} + \phi_2\begin{bmatrix} 1 \\ r_2 \end{bmatrix} \tag{2.23}$$

The eigenvectors (r_i) and the eigenvalues (k_i^2) are written as displayed in Eq. 2.24.

$$\begin{aligned} r_i &= \frac{\phi_i^F}{\phi_i^S} = \frac{Pk_i^2 - \omega\tilde{\rho}_{11}}{\omega^2\tilde{\rho}_{12} - Qk_i^2}, i = 1,2,... \\ k_{i=1,2}^2 &= \frac{\omega^2}{2(PR-Q^2)}(P\tilde{\rho}_{22} + R\tilde{\rho}_{11} - 2Q\tilde{\rho}_{12} \pm \sqrt{\Omega}) \end{aligned} \tag{2.24}$$

with

$$\Omega = (P\tilde{\rho}_{22} + R\tilde{\rho}_{11} - 2Q\tilde{\rho}_{12})^2 - 4(PR - Q^2)(\tilde{\rho}_{11}\tilde{\rho}_{22} - \tilde{\rho}_{12}^2) \tag{2.25}$$

So, it is possible to write the solution shown in Eq. 2.26.

$$\phi_i = (\phi_i^a e^{-jk_i z cos\theta} + \phi_i^r e^{jk_i z cos\theta})e^{jk_i x sin\theta} \tag{2.26}$$

The displacement resultant from these two potentials are given by the expression:

$$\begin{aligned} \vec{u}_L^S &= \nabla\phi_1 + \nabla\phi_2 \\ \vec{u}_L^F &= r_1\nabla\phi_1 + r_2\nabla\phi_2 \end{aligned} \tag{2.27}$$

Equation 2.27 shows that there are two distinct longitudinal waves propagating in the porous medium, characterized by the complex wavenumbers: k_1 and k_2.

The terms with the vector potentials reduce to:

$$\mu\Delta\psi^S + \omega^2\left(\tilde{\rho}_{11}\psi^S + \tilde{\rho}_{12}\psi^F\right) = 0$$
$$\omega^2\left(\tilde{\rho}_{12}\psi^S + \tilde{\rho}_{22}\psi^F\right) = 0 \tag{2.28}$$

with

$$k_3^2 = \frac{\omega^2}{\mu}\left(\frac{\tilde{\rho}_{11}\tilde{\rho}_{22} - \tilde{\rho}_{12}^2}{\tilde{\rho}_{22}}\right), r_3 = -\frac{\tilde{\rho}_{12}}{\tilde{\rho}_{22}} \tag{2.29}$$

One unique shear wave with wavenumber k_3 propagates in the material. So the final solid and fluid displacements can be written as displayed in Eq. 2.30.

$$\vec{u}^S = \nabla\phi_1 + \nabla\phi_2 + \nabla\wedge\psi$$
$$\vec{u}^F = r_1\nabla\phi_1 + r_2\nabla\phi_2 + r_3\nabla\wedge\psi \tag{2.30}$$

Finally, the relation among the potentials ϕ_1^a, ϕ_1^r, ϕ_2^a, ϕ_2^r, ψ^a, and ψ^r and the variables (3 displacements and 3 constraints) $u_x^S, u_z^S, u_z^F, \sigma_{xz}^S, \sigma_{zz}^S$, and σ_{zz}^F are summarized in Eq. 2.31.

$$
\begin{bmatrix} \sigma_{zz}^F \\ \sigma_{zz}^S \\ \sigma_{xz}^S \\ u_z^F \\ u_z^S \\ u_x^S \end{bmatrix} =
\begin{bmatrix}
(Rr_1 + Q)k_1^2 e^{-jk_1 z\cos\theta_1} & (Rr_1 + Q)k_1^2 e^{jk_1 z\cos\theta_1} \\
-[2\mu sin^2\theta_1 - (P + r_1 Q)]k_1^2 e^{-jk_1 z\cos\theta_1} & -[2\mu sin^2\theta_1 - (P + r_1 Q)]k_1^2 e^{jk_1 z\cos\theta_1} \\
\mu k_1^2 sin2\theta_1 e^{-jk_1 z\cos\theta_1} & -\mu k_1^2 sin2\theta_1 e^{jk_1 z\cos\theta_1} \\
-jk_1 r_1 cos\theta_1 e^{-jk_1 z\cos\theta_1} & jk_1 r_1 cos\theta_1 e^{jk_1 z\cos\theta_1} \\
-jk_1 cos\theta_1 e^{-jk_1 z\cos\theta_1} & jk_1 cos\theta_1 e^{jk_1 z\cos\theta_1} \\
-jk_1 sin\theta_1 e^{-jk_1 z\cos\theta_1} & -jk_1 sin\theta_1 e^{jk_1 z\cos\theta_1}
\end{bmatrix} \cdots
$$

$$
\cdots
\begin{array}{cc}
(Rr_2 + Q)k_2^2 e^{-jk_2 z\cos\theta_2} & (Rr_2 + Q)k_2^2 e^{jk_2 z\cos\theta_2} \\
-[2\mu sin^2\theta_2 - (P + r_2 Q)]k_2^2 e^{-jk_2 z\cos\theta_2} & -[2\mu sin^2\theta_2 - (P + r_2 Q)]k_2^2 e^{jk_2 z\cos\theta_2} \\
\mu k_2^2 sin2\theta_2 e^{-jk_2 z\cos\theta_2} & -\mu k_2^2 sin2\theta_2 e^{jk_2 z\cos\theta_2} \\
-jk_2 r_2 cos\theta_2 e^{-jk_2 z\cos\theta_2} & jk_2 r_2 cos\theta_2 e^{jk_2 z\cos\theta_2} \\
-jk_2 cos\theta_2 e^{-jk_2 z\cos\theta_2} & jk_2 cos\theta_2 e^{jk_2 z\cos\theta_2} \\
-jk_2 sin\theta_2 e^{-jk_2 z\cos\theta_2} & -jk_2 sin\theta_2 e^{jk_2 z\cos\theta_2}
\end{array} \cdots
$$

$$
\begin{array}{cc}
0 & 0 \\
\mu k_3^2 sin2\gamma e^{-jk_3 z cos\gamma} & \mu k_3^2 sin2\gamma e^{jk_3 z cos\gamma} \\
-\mu k_3^2 cos2\gamma e^{-jk_3 z cos\gamma} & -\mu k_3^2 cos2\gamma e^{jk_3 z cos\gamma} \\
\cdots \quad -jk_3 r_3 sin\gamma e^{-jk_3 z cos\gamma} & -jk_3 r_3 sin\gamma e^{jk_3 z cos\gamma} \\
-jk_3 sin\gamma e^{-jk_3 z cos\gamma} & -jk_3 sin\gamma e^{jk_3 z cos\gamma} \\
jk_3 cos\gamma e^{-jk_3 z cos\gamma} & -jk_3 cos\gamma e^{jk_3 z cos\gamma}
\end{array}
\cdot
\begin{bmatrix}
\phi_1^a \\
\phi_1^r \\
\phi_2^a \\
\phi_2^r \\
\psi^a \\
\psi^r
\end{bmatrix}
\tag{2.31}
$$

2.5.3 Continuity relations

The continuity relations depend on the material types next to the interfaces. The continuity relations derived from combining fluids, solids and poroelastic media are defined in this section.

1. **Fluid-fluid interface**

   When an interface between two fluids is observed, the continuity exists in displacement and in pressure: $u_z^i(z_i^{i+1}) = u_z^{i+1}(z_i^{i+1})$ and $p^i(z_i^{i+1}) = p^{i+1}(z_i^{i+1})$. Having as basis Eq. 2.18 and including these continuity relation, we obtain

   $$
   \begin{bmatrix} A_i(z_i^{i+i}) & -A_{i+1}(z_i^{i+i}) \end{bmatrix}
   \begin{bmatrix}
   \phi_i^{Fa} \\
   \phi_i^{Fr} \\
   \phi_{i+1}^{Fa} \\
   \phi_{i+1}^{Fr}
   \end{bmatrix} = 0
   \tag{2.32}
   $$

   or

   $$
   [A_i(z_i^{i+1})] = \begin{bmatrix} 1 & 0 \\ 0 & 1 \end{bmatrix} [G_i^F(z_i^{i+1})]
   \tag{2.33}
   $$

   where

   $$
   [G_i^F] = \begin{bmatrix}
   \rho c_0^2 e^{-jzkcos\theta} & \rho c_0^2 e^{jzkcos\theta} \\
   -jkcos\theta \rho e^{-jkzcos\theta} & jkcos\theta \rho e^{jkzcos\theta}
   \end{bmatrix}
   \tag{2.34}
   $$

   where c_0 is the wave propagation velocity. We have $c_0 = \sqrt{K/\rho}$, K is the incompressibility modulus and ρ is the volumetric mass of the fluid.

2. **Solid-solid interface**

Continuity is present in the displacements and in the constraints, so

$$
\begin{bmatrix} A_i(z_i^{i+i}) & -A_{i+1}(z_i^{i+i}) \end{bmatrix}
\begin{bmatrix}
\phi_i^{Sa} \\
\phi_i^{Sr} \\
\psi_i^{Sa} \\
\psi_i^{Sr} \\
\phi_{i+1}^{Sa} \\
\phi_{i+1}^{Sr} \\
\psi_{i+1}^{Sa} \\
\psi_{i+1}^{Sr}
\end{bmatrix} = 0
\tag{2.35}
$$

with

$$
[A_i(z_i^{i+1})] = [G_i^S(z_i^{i+1})]
\tag{2.36}
$$

where

$$
G_i^S =
\begin{bmatrix}
k_L^2(\lambda + 2\mu cos^2\theta)e^{-jk_L z cos\theta} & k_L^2(\lambda + 2\mu cos^2\theta)e^{jk_L z cos\theta} \\
-jk_L cos\theta e^{-jk_L z cos\theta} & jk_L cos\theta e^{-jk_L z cos\theta} \\
k_L^2 \mu sin2\theta e^{-jk_L z cos\theta} & -k_L^2 \mu sin2\theta e^{jk_L z cos\theta} \\
-jk_L sin\theta e^{-jk_L z cos\theta} & -jk_L sin\theta e^{-jk_L z cos\theta}
\end{bmatrix} \quad \dots
$$

$$
\begin{matrix}
k_T^2 \mu sin2\gamma e^{-jk_T z cos\gamma} & -k_T^2 \mu sin2\gamma e^{jk_T z cos\gamma} \\
-jk_T sin\gamma e^{-jk_T z cos\gamma} & -jk_T sin\gamma e^{jk_T z cos\gamma} \\
-k_T^2 \mu cos2\gamma e^{-jk_T z cos\gamma} & -k_T^2 \mu cos2\gamma e^{jk_T z cos\gamma} \\
jk_T cos\gamma e^{-jk_T z cos\gamma} & -jk_T cos\gamma e^{jk_T z cos\gamma}
\end{matrix}
\tag{2.37}
$$

3. **Fluid-solid interface**

Continuity is in normal displacements and constraints, what means: $u_z^i(z_i^{i+1}) = u_z^{i+1}(z_i^{i+1})$, $-p^i(z_i^{i+1}) = \sigma_{zz}^{i+1}(z_i^{i+1})$, and $0 = \sigma_{xz}^{i+1}(z_i^{i+1})$. Therefore, we write Eq. 2.38.

$$
\begin{bmatrix} A_i(z_i^{i+i}) & -A_{i+1}(z_i^{i+i}) \end{bmatrix}
\begin{bmatrix}
\phi_i^{Fa} \\
\phi_i^{Fr} \\
\phi_{i+1}^{Sa} \\
\phi_{i+1}^{Sr} \\
\psi_{i+1}^{Sa} \\
\psi_{i+1}^{Sr}
\end{bmatrix} = 0
\tag{2.38}
$$

with

$$[A_i(z_i^{i+i})] = \begin{bmatrix} -1 & 0 \\ 0 & 1 \\ 0 & 0 \end{bmatrix} [G_i^F(z_i^{i+i})] \tag{2.39}$$

and

$$[A_{i+1}(z_i^{i+i})] = \begin{bmatrix} 1 & 0 & 0 & 0 \\ 0 & 1 & 0 & 0 \\ 0 & 0 & 1 & 0 \end{bmatrix} [G_{i+1}^S(z_i^{i+i})] \tag{2.40}$$

4. **Porous-porous interface**

Describing the porous material by Biot's model, the continuity relations are written as:

$$
\begin{aligned}
u_z^{Si} &= u_z^{Si+1} \\
u_x^{Si} &= u_x^{Si+1} \\
\phi_P^i(u_z^{Fi} - u_z^{Si}) &= \phi_P^{i+1}(u_z^{Fi+1} - u_z^{Si+1}) \\
\sigma_{zz}^{Si} + \sigma_{zz}^{Fi} &= \sigma_{zz}^{Si+1} + \sigma_{zz}^{Fi+1} \\
\frac{\sigma_{zz}^{Fi}}{\phi_i^P} &= \frac{\sigma_{zz}^{Fi+1}}{\phi_{i+1}^P} \\
\sigma_{xz}^{Si} &= \sigma_{xz}^{Si+1}
\end{aligned}
\tag{2.41}
$$

These relations express the solid phase continuity and the air flow conservation between both layers. The matrix becomes

$$[A_i(z_i^{i+i})] = \begin{bmatrix} \frac{1}{\phi_P^i} & 0 & 0 & 0 & 0 & 0 \\ 1 & 1 & 0 & 0 & 0 & 0 \\ 0 & 0 & 1 & 0 & 0 & 0 \\ 0 & 0 & 0 & \phi_P^i & -\phi_P^i & 0 \\ 0 & 0 & 0 & 0 & 1 & 0 \\ 0 & 0 & 0 & 0 & 0 & 1 \end{bmatrix} [G_i^P(z_i^{i+i})] \tag{2.42}$$

where G_i^P is displayed in Eq. 2.32.

5. **Porous-fluid interface**

24

The relations between fluid and porous layers are

$$
\begin{aligned}
(1 - \phi_P^i)u_z^{Si} + \phi_P^i u_z^{Fi} &= u_z^{Fi+1} \\
\frac{\sigma_{zz}^{Fi}}{\phi_P^i} &= \sigma_{zz}^{Fi+1} \\
\frac{\sigma_{zz}^{Si}}{(1-\phi_P^i)} &= \sigma_{zz}^{Fi+1} \\
\sigma_{xz}^{Si} &= 0
\end{aligned}
\tag{2.43}
$$

This results in Eq. 2.44 and 2.45.

$$
[A_i(z_i^{i+i})] =
\begin{bmatrix}
1 & 0 & 0 & 0 & 0 & 0 \\
0 & 1 & 0 & 0 & 0 & 0 \\
0 & 0 & 1 & 0 & 0 & 0 \\
0 & 0 & 0 & \phi_P^i & 1-\phi_P^i & 0
\end{bmatrix}
[G_i^P(z_i^{i+i})]
\tag{2.44}
$$

and

$$
[A_{i+1}(z_i^{i+i})] =
\begin{bmatrix}
\phi_P^i & 0 \\
1-\phi_P^i & 0 \\
0 & 0 \\
0 & 1
\end{bmatrix}
[G_i^F(z_i^{i+i})]
\tag{2.45}
$$

6. **Porous-solid interface**

The interface satisfies the following conditions:

$$
\begin{aligned}
u_z^{Si} &= u_z^{Si+1} \\
u_z^{Fi} &= u_z^{Si+1} \\
u_x^{Si} &= u_x^{Si+1} \\
\sigma_{xz}^{Fi} + \sigma_{zz}^{Si} &= \sigma_{zz}^{Si+1} \\
\sigma_{xz}^{Si} &= \sigma_{xz}^{Si+1}
\end{aligned}
\tag{2.46}
$$

So

$$
[A_i(z_i^{i+i})] =
\begin{bmatrix}
1 & 1 & 0 & 0 & 0 & 0 \\
0 & 0 & 1 & 0 & 0 & 0 \\
0 & 0 & 0 & 1 & 0 & 0 \\
0 & 0 & 0 & 0 & 1 & 0 \\
0 & 0 & 0 & 0 & 0 & 1
\end{bmatrix}
[G_i^P(z_i^{i+i})]
\tag{2.47}
$$

and

$$[A_{i+1}(z_i^{i+i})] = \begin{bmatrix} 1 & 0 & 0 & 0 \\ 0 & 0 & 1 & 0 \\ 0 & 1 & 0 & 0 \\ 0 & 0 & 0 & 1 \end{bmatrix} [G_i^S(z_i^{i+i})] \tag{2.48}$$

Tanneau (2004) presents a scheme of his implementation of the Transfer Matrix method. First, the data file is read, then it starts picking up an angle and a frequency. The matrices G are calculated for the specific material, the assembly is made, and boundary conditions are considered. Finally, loading is included and the solution is calculated through a linear system similar to $k.x = F$. So, the transmission loss can be obtained.

2.6 Characterization tests

In this work, the acoustic panels are composed of three types of felt: hard, intermediate, and soft felts, as stated in Section 1.4. These felt layers and the mineral layer were experimentally characterized at the *CTTM* (Centre de Transfert de Technologie du Mans), in Le Mans, France.

Porosity, tortuosity, and viscous characteristic length were measured in the same device. The sample was subjected to an ultrasound acoustic excitation: transmission coefficient measure enabled tortuosity and the characteristic length determination and reflection coefficient measure was used to obtain surface porosity. For flow resistivity the measurement process followed ISO 9053 (ISO 9053,1991) standard. The sample was subjected to a continue air flow and the parameter was deduced from the volume flow and from the pressure drop between two free surfaces of the sample. Young modulus was obtained through stress-strain curve that was experimentally obtained in a compressive mechanical characterization bench. Loss factor was also measured in this bench. After that, the sample absorption performance was experimentally obtained in a Kundt tube of 45mm of diameter. Next, all parameters values obtained previously were used as input values for *Maine 3A*, a software based on the Equivalent Fluid model. Thermal characteristic length was adjusted comparing experimental and simulated curves, so that, all parameters were obtained.

Three measure results were made for each layer. As the thickness of the porous materials are not constant along their surface, significant variations in the measures were displayed when
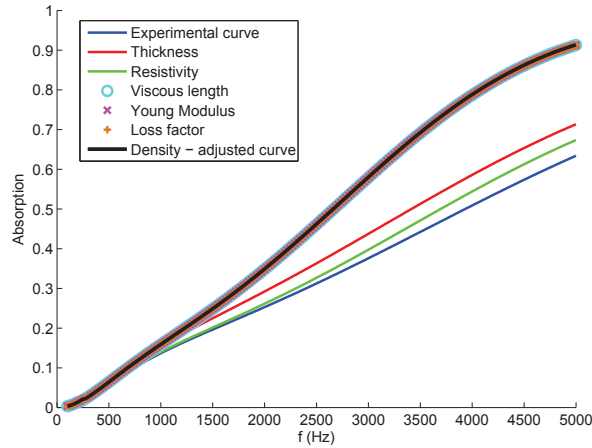
Figure 2.2: Adjust process of the intermediate felt, sample 3.

analyzing the different samples.

To confirm the experimental data, absorption curves were simulated with the *Maine 3A* software using the measured parameters as inputs. They were compared with the measured absorption curves made in the Kundt tube. The measured parameter values were adjusted in the software, one by one, so the simulated curves could fit the experimental ones.

Figure 2.2 shows the parameters adjusted for the intermediate felt, sample 3. This case was chosen for the adjust demonstration, because its absorption curve is the most different from its measured curve among the tested samples. The parameters were adjusted one by one, in this sequence: thickness, resistivity, viscous length, Young Modulus, loss factor and density. Observing this sequence, it is possible to observe the sensitivity of the model related to each parameter. Thickness, resistivity and viscous length adjusting showed a significant change in the curve, while the other parameters did not have the same importance.

After achieving the measured curve, adjusted parameters were obtained for each sample of each felt. Tables 2.2, 2.3 and 2.4 show the experimental and the adjusted results of the characterization tests for hard, intermediate, and soft felts.

The adjusted curve is the closest approximation obtained to the experimental curve in relation to the measured absorption curve in Kundt tube. Figure 2.3 shows the measured and the final

Table 2.2: Experimental and adjusted data parameters of the hard felt characterization.

Properties	Sample 1	Sample 2	Sample 3	Mean
Exp. Thickness (mm)	5	5	5	5
Adj. Thickness (mm)	5.2	6	5.5	5.57
Exp. Weight(g)	1.34	2.02	1.76	1.71
Adj Weight(g)	-	-	-	-
Exp. Specific mass (kg/m^3)	172.3	259.8	226.3	219.5
Adj. Specific mass (kg/m^3)	220	220	220	220
Exp. Resistivity (rayl/m)	128421	203375	231510	187768.67
Adj. Resistivity (rayl/m)	140000	220000	250000	203333.33
Exp. Porosity	1	1	1	1
Adj. Porosity	1	1	1	1
Exp. Tortuosity	1	1	1	1
Adj. Tortuosity	1	1	1	1
Exp. Viscous Characteristic Lenght (μm)	16.2	13.9	10.9	13.67
Ad. Viscous Characteristic Lenght (μm)	14	14	14	14
Exp. Thermal Characteristic Lenght (μm)	-	-	-	-
Adj. Thermal Characteristic Lenght (μm)	42	42	42	42
Exp. Young Modulus (kPa) [1]	83	667	280	343.33
Adj. Young Modulus (kPa) [1]	50	220	50	106.67
Exp. Loss Factor (%) [1]	0.08	0.004	0.011	0.033
Adj. Loss Factor (%) [1]	0.1	0.1	0.1	0.1

Table 2.3: Experimental and adjusted data parameters of the intermediate felt characterization.

Properties	Sample 1	Sample 2	Sample 3	Mean
Exp. Thickness (mm)	10	10	10	10
Adj. Thickness (mm)	11	11	11	11
Exp. Weight(g)	1.17	1.15	1.02	1.11
Adj. Weight(g)	-	-	-	-
Exp. Specific mass (kg/m^3)	75.2	73.9	65.6	71.58
Adj. Specific mass (kg/m^3)	72	72	72	72
Exp. Resistivity (rayl/m)	20760	20703	19195	20219,33
Adj. Resistivity (rayl/m)	20000	20000	20000	20000
Exp. Porosity	1	1	1	1
Adj. Porosity	1	1	0.95	0.98
Exp. Tortuosity	1	1	1	1
Adj. Tortuosity	1	1	1	1
Exp. Viscous Characteristic Lenght (μm)	45.8	46.9	55.8	49.5
Adj. Viscous Characteristic Lenght (μm)	30	30	27	29
Exp. Thermal Characteristic Lenght (μm)	-	-	-	-
Adj. Thermal Characteristic Lenght (μm)	150	200	140	163.33
Exp. Young Modulus (kPa) [1]	5	13	6	8
Adj. Young Modulus (kPa) [1]	10	10	10	10
Exp. Loss Factor (%) [1]	0.118	0.0067	0.088	0.07
Adj. Loss Factor (%) [1]	0.05	0.05	0.05	0.05

Table 2.4: Experimental and adjusted data parameters of the soft felt characterization.

Properties	Sample 1	Sample 2	Sample 3	Mean
Exp. Thickness (mm)	22	22	18	20.67
Adj. Thickness (mm)	25	25	18	22.67
Exp. Weight(g)	3.3	4.27	2.16	3.24
Adj. Weight(g)	-	-	-	-
Exp. Specific mass (kg/m^3)	96.4	124.8	77.2	99.47
Adj. Specific mass (kg/m^3)	96.0	125.0	77.0	99.33
Exp. Resistivity (rayl/m)	28552	50251	28813	35872
Adj. Resistivity (rayl/m)	28000	51000	23000	34000
Exp. Porosity	1	1	1	1
Adj. Porosity	1	1	1	1
Exp. Tortuosity	1	1	1	1
Adj. Tortuosity	1	1	1	1
Exp. Viscous Characteristic Lenght (μm)	35.7	29.1	42.4	35.73
Adj. Viscous Characteristic Lenght (μm)	36	30	40	35.33
Exp. Thermal Characteristic Lenght (μm)	-	-	-	-
Adj. Thermal Characteristic Lenght (μm)	150	150	150	150
Exp. Young Modulus (kPa) [1]	43	125	24	64
Adj. Young Modulus (kPa) [1]	43	450	24	172.33
Exp. Loss Factor (%) [1]	0.009	0.004	0.027	0.01
Adj. Loss Factor (%) [1]	0.01	0.005	0.03	0.015
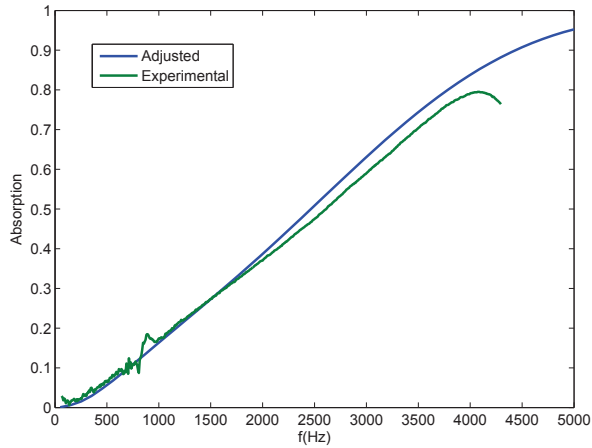
Figure 2.3: Adjusted and measured curves for Intermediate felt, sample 3.

adjusted curves for intermediate felt, sample 3.

The adjusted curves will be used as reference curves for the comparisons between *Maine 3A* and *TMTX* simulations. As both softwares apply the Equivalent Fluid porous material model, their results must be exactly the same.

2.7 Multilayered panel absorption conditions

The panel acoustic measurements were performed according to their application necessities. At *General Motors*®, absorption, transmission loss and insertion loss performances are considered in the acoustic analysis. However, added to the standard absorption configuration commonly used in the Kundt tube, another specific configuration is used in the measurements. To organize the analyzes, the absorption configurations were classified as Free absorption and Blocked absorption, and they are explained in the Sec. 2.7.1 and 2.7.2.

2.7.1 Free absorption

This configuration simulates the real working condition of the panel. Diffuse noise comes from the engine, passes through a steel plate and through the acoustic panel, arriving in the pas-

sengers' cabin, as illustrated in Figure 2.4. Transmission loss and insertion loss are also measured with the free absorption configuration.

2.7.2 Blocked Absorption

This configuration represents the standard Kundt's tube: the noise is emitted as plane waves, then it passes through the panel, it reflects at the end of the tube, and it does its way back. When received, it is finally measured, as shown in Figure 2.5.
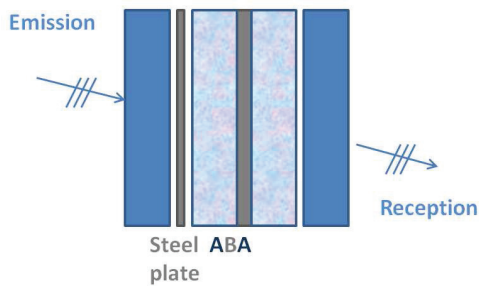
Figure 2.4: Free absorption schema of the ABA-cotton panel.
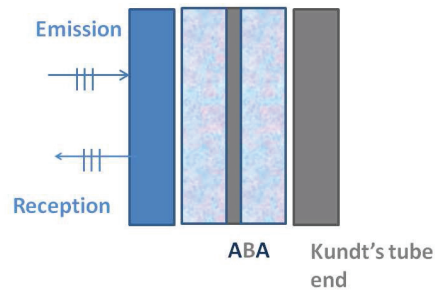
Figure 2.5: Blocked absorption schema of the ABA-cotton panel.

Before studying the panels, the reference curves of each felt layer were used to validate the *TMTX* simulations. The adjusted characterization parameters were inserted in the *TMTX* software and blocked absorption curves were calculated for all samples of the three felts. Figures 2.6, 2.7, and 2.8 show *TMTX* and *Maine 3A* absorption curves comparison for hard, intermediate, and soft felts, respectively.

For all felts, it was possible to observe that *Maine 3A* and *TMTX* results were identical for all samples, using the adjusted data. This validated *TMTX* simulations and the complete panel simulations could start.

2.8 Acoustic panels simulations

Free absorption, blocked absorption, transmission loss and insertion loss performances of both panels were analyzed and compared using the *TMTX* software. The DL-PU panel is not in-
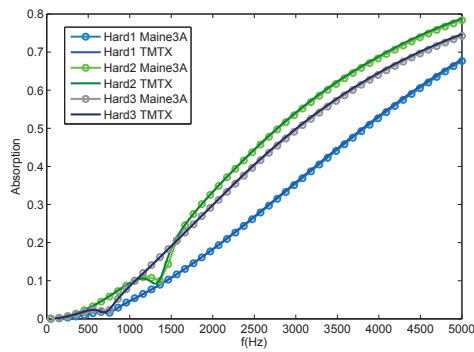
Figure 2.6: *TMTX* and *Maine 3A* absorption simulations comparison for hard felt.
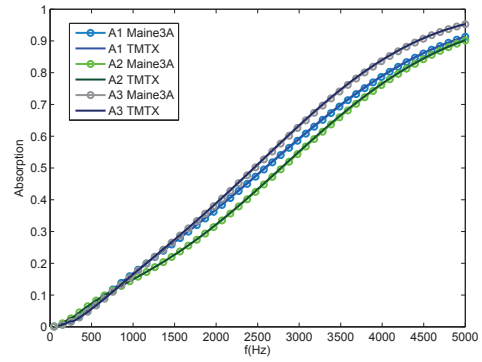
Figure 2.7: *TMTX* and *Maine 3A* absorption simulations comparison for soft felt.
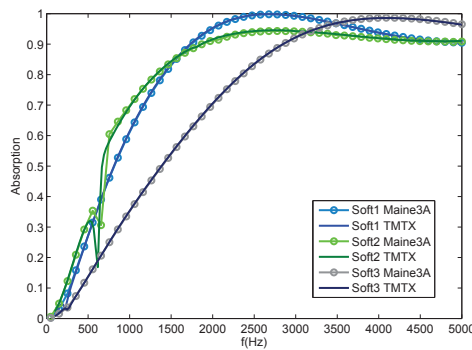
Figure 2.8: *TMTX* and *Maine 3A* absorption simulations comparison for intermediate felt.

cluded in the simulations, because its parameters were not characterized. Moreover, certainly it guarantees the acoustic performance required by the automaker, because before ABA-cotton and DL-cotton designs, it was the initial solution applied in the vehicle.

2.8.1 Absorption

Figure 2.9 shows free absorption performances of both panels. For frequencies below 5000 Hz, DL-cotton panel has a better absorption; however, in high frequency regime, the panels present almost the same absorption level. The DL-cotton panel is only composed of cotton fiber reinforced composite, and the natural fibers present a good acoustic performance in low frequencies, so the present result is consistent.

Figure 2.10 shows blocked absorption performances of both panels. As observed in Figure 2.9, in frequencies below 5000 Hz, DL-cotton panel has a better absorption. From 5000 to 7000 Hz approximately, ABA-cotton panel achieves the DL-cotton absorption level; however on higher frequencies, a decline is observed in the ABA-cotton curve, while DL-cotton continues with almost the same absorption level.
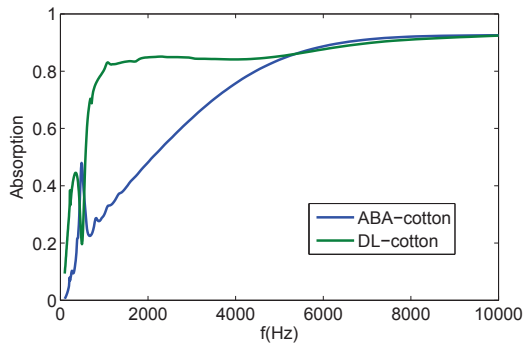
Figure 2.9: Free absorptions of DL-cotton and ABA-cotton panels.
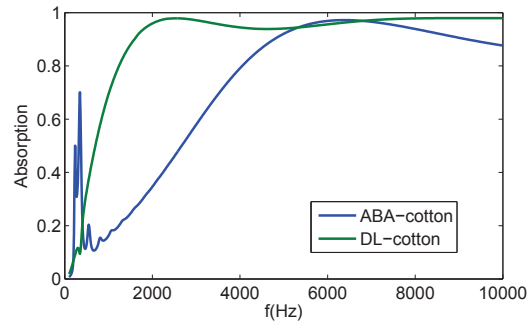
Figure 2.10: Blocked absorptions of DL-cotton and ABA-cotton panels.

2.8.2 Transmission Loss and Insertion Loss

Figure 2.11 shows the transmission loss performance of both panels. After the breathing frequency, ABA-cotton panel displays a better performance then DL-cotton panel.

Figure 2.12 shows the insertion loss performance of both panels. After the breathing frequency, ABA-cotton panel displays a better performance then DL-cotton panel, as observed in Figure 2.11.

When installed in the vehicle, the acoustic panel guarantees the required sound level for the passenger. This is confidential, and it is defined by *General Motors*®. However, it is known that even with the worse TL performance, after tests made in a vehicle prototype, they chose the DL-cotton instead of the ABA-cotton panel to apply in the automobile model called *Agile*®. Therefore, it is possible to conclude that the DL-cotton panel provides the required sound comfort for the passengers.
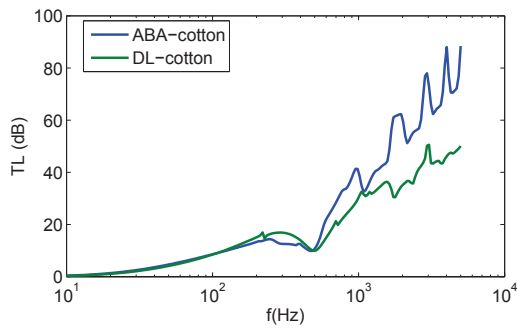
Figure 2.11: Transmission Losses of DL-cotton and ABA-cotton panels.
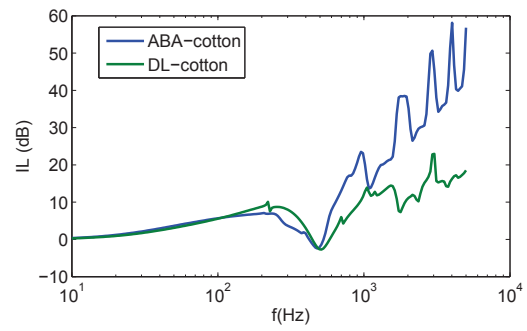
Figure 2.12: Insertion Losses of DL-cotton and ABA-cotton panels.

3 Life Cycle Assessment background

3.1 Life Cycle Assessment

This chapter contains basic notions about the LCA methodology, so readers who are familiar with the subject can disregard it.

According to ISO (2006a), the LCA methodology consists of "compilation and evaluation of the inputs, outputs and the potential environmental impacts of a product system throughout its life cycle". Its first publications date from the 60's (JENSEN *et al.*, 1997) with studies focusing on raw material consumption, energy efficiency and waste disposal.

In 1969, the *Coca Cola Company* funded a study to compare resource consumption and environmental emissions associated with beverage containers (JENSEN *et al.*, 1997). In 1972, (BOUSTEAD, 1996) calculated the total energy used in different types of beverages containers. His methodology became notorious and was applied in other types of systems. This research field attracted people and a significant number of works were published in 3 decades.

The LCA Sourcebook, developed in Europe, was published in 1993 (JENSEN *et al.*, 1997). This publication could spread the methodology to other regions outside Europe and the methodology started to consolidate. As until nowadays this is a relatively new research field, there is not a great quantity of guidebooks, standard case studies, unquestionable impact assessment methods or specific databases for all study cases. ISO 14040 (ISO, 2006a) and ISO14044 (ISO, 2006b) are the main references for LCA practitioners.

The main functions of an LCA are to quantify and to compare environmental performances of products.

3.2 LCA steps

Figure 3.1 shows the four steps of the LCA methodology and the relations among them. They are be described in Subsections 3.2.1, 3.2.2, 3.2.3, and 3.2.4.
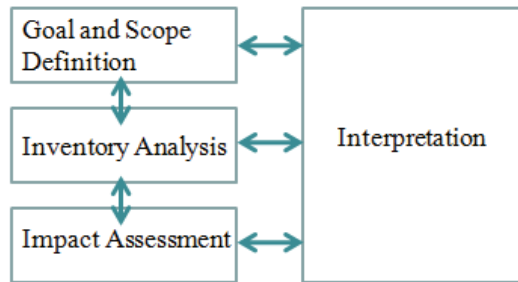
Figure 3.1: LCA steps.

3.2.1 Step 1: Goal and Scope Definition

In this step, the study objectives are defined containing: study reasons, concerned public, and conclusions applications. All hypothesis, limitations, and frontiers of the system should be registered, moreover the exigency about data source quality should be defined.

Another important definition is the **functional unit** that "describes and quantifies those properties of the product, which must be present for the studied substitution to take place. These properties (the functionality, appearance, stability, durability, ease of maintenance etc.) are in turn determined by the requirements in the market in which the product is to be sold" (WEIDEMA *et al.*, 2004). Some examples of functional unit are:

- o to travel a 100km car trip, comparing two fuel options: 6.3 kg of biodiesel and 5.7 kg of fossil diesel;

- o a paint that covers $100m^2$ of walls with an opacity of 0.98, during 20 years;

- o to prepare hot coffee for 10 people of a department that arrive from 8:00 until 9:30 during 5 years.

This first step seems to be clear and simple, however, when performing an LCA defining goal and scope is not an easy task. First, it is important to observe if the study is being made for a comparison purpose among more then two products or services, or for a single product analysis. Generally, the hypothesis and the limitations are made according to the possibilities related to data

collection: are there enough and reliable data sources about a certain point, or not? So, the LCA practitioner already starts to make choices and to simplify the real case study.

The case defined in Sec. 1.4 had a few limitations related to data collection that resulted in a few simplifications and limitations. Specific data about the suppliers production process, or about their own suppliers could not be easily collected. Moreover, each supplier had different data quality, and for each one of them an specific limitation needed to be made. The LDPE provider imported raw material from China, therefore no reliable specific data about its production could be found, and the most recent LDPE data available in the database was chosen. Another example is the landfill end-of-life. *Coplac*® informed that this is the end-of-life of their product. Furthermore materials that are similar to the ones applied in acoustic panels were found in landfills, and recycled material collectors informed that this kind of product arrives in landfills really often. However, any acoustic panel could be detected in the two visited landfills. Even without verifying the panel final destiny, the landfill was considered.

The real case study functional unit definition took around one year. Research was necessary until we were able to establish that a vehicle in Brazil travels 180.000 km during 10 years, on average, before being discarded, as stated in Sec. 4.3. A difficulty was also faced when dealing with only one component of the vehicle, because only the contributions related to it could be considered in the whole life cycle, and the functional unit needs to support that too.

3.2.2   Step 2: Inventory Analysis

In this step all life cycle process is identified and described in detail. Data is collected, the modeling starts and an LCA software is chosen containing databases. Practitioners need to explore the database, reading the documentation available on it, so they are able to choose the best data. They can also modify an available data, or create their own data based on their specific collected information. In this work, *Ecoinvent* database is used.

Generally, this is the longer step of an LCA study, because researchers need to explore all points of the product life cycle and the functionalities and the database of the software.

In the real case study, more than one database was analyzed and used in the panels modeling,

because only trying data it is possible to observe if they represent what the practitioner needs. The difficulties of this phase were related to: recycled cotton fiber and use phase modelings. There is no specific data for recycled Brazilian cotton fibers or for the Brazilian fuel, so they needed to be created and adjusted, in order to generate a coherent result, when compared to the other impact contributors. This is detailed in Tab. 4.5.

3.2.3   Step 3: Impact Assessment

In this step, a Life Cycle Impact Assessment (LCIA) method is chosen. These methods are available in softwares as well as the databases, some examples are: *CML, Eco-indicator 99*, *EDIP*, *ReCiPe*, and *IMPACT 2002*. Each LCIA method includes a different set of potential impact categories, so the choice is made according to the study objective. In this work, seven potential impacts from *CML 2002* LCIA method were chosen (the reasons for this choice are presented in Section E): vbbbb

- **Abiotic depletion (AD)**: This impact category indicator is related to extraction of minerals and fossil fuels due to inputs in the system. The Abiotic Depletion Factor (ADF) is determined for each extraction of minerals and fossil fuels based on remaining reserves and on the rate of extraction. Its unit is kg of Sb equivalent/kg emission.

- **Acidification (A)**: The Acidification Potential (AP) is expressed in relation to the acidifying effect of the SO_2. Other known acidifying substances are nitrogen oxides and ammonia (Goedkoop *et al.*, 2008). Its unit is kg of SO_2 equivalent/kg emission.

- **Eutrophication (E)**: The Nutriphication potential (NP) is set at 1 for phosphate (PO_4). Other emissions also influence eutrophication, notably nitrogen oxides and ammonium (Goedkoop *et al.*, 2008). Its unit is kg of PO_4 equivalent/kg emission.

- **Global warming (GW)**: The Global Warming Potential (GWP) is the potential contribution of a substance to the greenhouse effect. The characterization model as developed by the Intergovernmental Panel on Climate Change (IPCC) is selected for development of characterization factor. This value has been calculated for a number of substances over periods of 20, 100 and 500 years because it is clear that certain substances gradually decompose and will become inactive in the longrun. GWP over a 100-year period is the most common choice (Goedkoop *et al.*, 2008). Its unit is kg of CO_2 equivalent/kg emission.
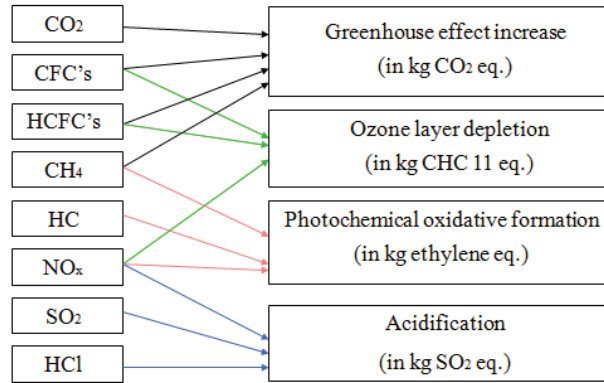
Figure 3.2: Flows associated with potential impacts.

○ **Ozone layer depletion (OLP)**: This impact category is related to the harmful effects of the stratospheric ozone depletion that permits a larger fraction of UV-B radiation reaches the earth surface. OLD values have been established mainly for hydrocarbons containing combined bromine, fluorine and chlorine, or CFC's. One of the substances the CFC-11 has been adopted as a reference. The characterization model is developed by the World Meteorological Organization (WMO) (Goedkoop *et al.*, 2008). Its unit is kg of $CFC - 11$ equivalent/kg emission.

○ **Fresh water aquatic ecotoxicity (FWAE)** and **Terrestrial ecotoxicity (TE)**: These categories refer to the impact on fresh water and on terrestrial ecosystems, as a result of emissions of toxic substances to water and soil. The main substances are heavy metals. They receive toxicity scores related to emissions to the water and to the soil (Goedkoop *et al.*, 2008). Its unit is kg of $1,4 - DB$ equivalent/kg emission.

The impact assessment is composed of: classification, characterization and valuation (normalization, weighting, grouping, etc) (SETAC, 1992), (SETAC, 1993). Classification is illustrated in Figure 3.2 (reproduced from (Santos *et al.*, 2013)) that shows the association between Elementary Flows (EF's) - "material or energy entering the system being studied that has been drawn from the environment without previous human transformation, or material or energy leaving the system being studied that is released into the environment without subsequent human transformation" (ISO, 2006a) - and potential impacts. Characterization consists of transforming EF's into common equivalence values through LCIA characterization factors.
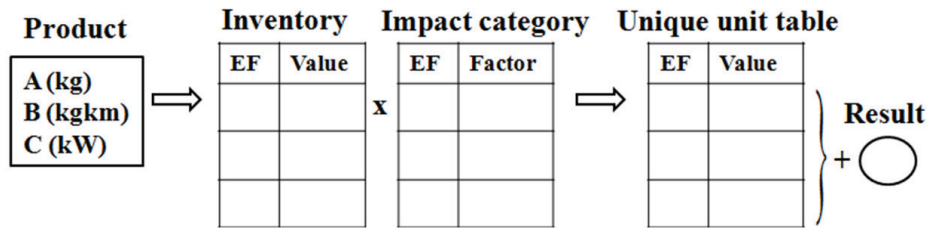
Figure 3.3: LCA mathematical model.

The valuation phase is also made according to LCIA models that normalize, weight or group impact categories according to: a panel of experts, political opinions, impacts of a universal set (impacts of a country, a continent or the world), regional concerns, etc. Therefore this phase is fundamentally subjective, so if the study is aligned to concepts valued by the method, this step makes sense, otherwise, no.

Figure 3.3 shows a resume of LCA mathematical model. The input data that constitutes a material or a product is inserted. Data can be: raw material, energy, transport, production process, end-of-life treatment and so on, and it is composed of EF's. When summing respectively the different EF's of each data, it is possible to obtain the inventory table of the complete product. This table is multiplied by the impact category table from the LCIA method chosen and all EF's turn into the same unit - the unit related to the calculated impact category - and they can be summed. This sum is the LCA result of this impact category.

In this phase, ISO (2006a) recommends practitioners to perform a sensitivity analysis and uncertainty calculations before making conclusions. This is due to cumulative effects of model imprecisions, input uncertainties and data variabilities.

3.2.4 Step 4: Interpretation

The interpretation phase should involve an iterative process of reviewing and revising the scope of the LCA (ISO, 2006a), as shown in Figure 3.1, because all decisions made during the LCA process (the modeling, the data quality, the methodology of data collection, etc.) influence the results.

The interpretation depends on all definitions presented in Step 1. Only based on the LCA objective, this phase is able to generate conclusions, explain limitations and provide recommendations. ISO (2006a) also recommends an specialist critical feedback of the LCA report, and this was made for the real case study. Furthermore, discussions with other LCA researchers were precious to generate questions, and to signal possible modeling errors. There are also some polemic points such as: to consider or not to consider the virgin cotton production in the recycled cotton fibers created process? This is a choice made by the LCA practitioner that will always generate discussions, however in this work this production was not considered, because if considered, its contribution in relation to the use phase of the product is discrepant, and the results become meaningless.

4 Real case study LCA

This Chapter is the author version of the article entitled: Use of recycled natural fibres in industrial products: A comparative LCA case study on acoustic components in the Brazilian automotive sector. It was published in Resources, Conservation & Recycling, in 2014, volume 84, pages: 1-14.

4.1 Introduction

4.1.1 Natural fibres in industrial products: technical benefits and market potentials

There is a growing interest in using natural fibres in industrial products (ALVES *et al.*, 2010). According to John e Thomas (2008), who reviewed the various aspects of cellulosic biofibres and biocomposites, the main advantages of the use of natural fibres are: economical production with few requirements for equipment, low specific weight, nonabrasive to molding equipment, lesser environmental impact, carbon dioxide neutral, little energy needed for production, worldwide availability, and possible energy recovery at end-of-life.

Natural fibers offer numerous technical advantages when compared to synthetic materials. This has been demonstrated, for example, by Yang e Yan (2012), who compare natural (flax, ramie, and jute) and synthetic (glass and carbon) fibers for sound absorption as well as for use in reinforced composites. They concluded that sound absorption property of natural fibers is always superior to synthetic fibers. Moreover, the superiority of natural fibers was also observed for the reinforced composites, especially at high frequencies, which can be interesting for aeronautical applications.

However, for the use as composite reinforcement, natural fibers present several technical disadvantages. It is in particular difficult to guarantee a uniform dispersion of the natural fibers within the matrix. Besides, the molding cannot be made at high temperatures because this type of fiber would lose its properties (JOHN E THOMAS, 2008). Furthermore, natural fiber composites manufactured nowadays generally mix natural fibers and synthetic polymers, which results in a composite that, at its end-of-life, is hard to recycle, since it requires a sequence of processes and a large quantity of energy (ALVES *et al.*, 2010).

Many natural fibers are widely available in tropical regions. A country like Brazil has a huge potential to produce vegetable fibers. In 2010, the production numbers were, for example: 3 million tons of cotton, 9 million tons of jute, and 250 thousand tons of sisal (IBGE, 2010).

4.1.2 Environmental pros and cons of the use of renewable materials in the automotive sector

The automotive industry faces the challenge of reducing extraction from nature and emissions to the environment during the whole life cycle of products (Parliament (2000); Simic e Dimitrijevic (2012); Puri *et al.* (2009); Schmidt *et al.* (2004)). Reducing the quantity of synthetic materials used in these products is a possible solution. Indeed, the use of natural materials, specifically of natural fibers, is currently becoming more common globally (Alves *et al.* (2010); Luz *et al.* (2010); Zah *et al.* (2006); Uihlein *et al.* (2008)). In Brazil, for example, car manufacturers such as Volkswagen, Ford, Honda and General Motors already apply natural fibres in car seats, dashboard coverings, roofs and trunk lids (OESP, 2004).

According to Niederl-Schmidinger e Narodoslawsky (2006), "processes on the basis of renewable resources always have an intrinsic perception of being environmentally friendly and sustainable". In order to confirm this perception for natural fibers, LCA has been often applied to several types of renewable resources for different products (e.g., Uihlein *et al.* (2008)) and for fuels (e.g., Sander e Murthy (2009)).

LCA has also been used to analyze the environmental performances of renewable resources, especially of natural fibres, in the automotive sector.

Alves *et al.* (2010) analyze the advantages of replacing glass fibers by jute fibers to produce structural frontal bonnets for a type of off-road vehicle ("buggy"). The natural fire reinforced bonnet improved the environmental performance of the whole vehicle, mainly due to its lower weight compared to usual solutions.

Luz *et al.* (2010) substituted talc by sugarcane bagasse fibers as reinforcement in polypropylene composites which constitute automotive components. The detected beneficial aspects of the sugarcane composite are: bagasse carbon absorption during cultivation, which reduces global

46

warming, cleaner production processes, lower weight, and bagasse-PP economic recovery (50% incineration + 50% recycling scenario) at the end-of-life (Luz *et al.*, 2010).

Zah *et al.* (2006) present the environmental perspectives of the use of carauá fibers produced in the Amazon region in the automotive industry. They compared the environmental impact of polypropylene composites using carauá fibers with traditional glass fiber composites in automotive applications over the whole life cycle of the product. Their results showed that the natural fiber advantages are due to their higher thermal recovery rate and to the potential weight reduction. The negative aspects are the environmental impact caused by carauá fiber monocultures (especially in the Eutrophication impact category) and the lower carauá fiber composite strength. Because of the latter, carauá composite parts require more material mass to match the structural performance of glass fiber components. Their conclusion is that, overall, the use of carauá fibers in automotive parts does not bring improvements to their environmental performance.

Corbière-Nicollier *et al.* (2001) compared the environmental performance of glass fiber and China reed fiber reinforcements in plastics for pallet construction. Using this natural fiber, energy consumption and other environmental impacts were strongly reduced, mainly due to the pallet weight reduction, the substitution of glass fiber production by natural fiber cultivation and the polypropylene use reduction (a higher proportion of Chine reed fiber was applied in the natural fiber reinforced pallet).

4.1.3   Aim of this work

The goal of this case study is to assess and compare the environmental impacts during the whole life cycle of three alternative acoustic panels usable in passenger vehicles produced, used and disposed of in Brazil. One "status-quo" panel is made of polymeric material (PU) while two innovative alternatives are mainly made of recycled natural (cotton) fibers. In order to calculate the environmental performance of these products, the LCA methodology (as defined in ISO (2006a) was used. This analysis aims at identifying environmental hot-spots of the innovative designs and at deriving improvement opportunities. This aim is totally in line with LCA, whose "results may be useful inputs to a variety of decision-making processes", including product development and improvement (ISO, 2006a).

The paper is organized as follows. In section 4.2, the case study is defined. Section 4.3 introduces the LCA model and the associated inventory considering three phases of the life cycle: production, use and end-of-life (considering two scenarios: landfilling and incineration with energy recovery). The results of the analysis are presented in Section 4.4. Finally, a discussion about the improvement opportunities for these products and further research needs is presented.

4.2 Case study definition

4.2.1 Context of the case study

The case study presented in this paper was performed within a larger research project aiming at enhancing the design of industrial products containing natural fibers presenting both high technical (acoustic properties in this particular case) and environmental performances. During this project, several types of natural fibers (e.g., cotton and indigenous fibers such as carauá) are to be analyzed and many characterization tests are to be made in order to obtain key acoustic parameters such as porosity, resistivity, and tortuosity. This research project involves several research centers and companies that already use natural fibers in products put on the Brazilian market. The case study reported in this paper was led during the first phase of the project, where acoustic and LCA models have been initially tested on "status-quo" (using polymers) and innovative (using recycled cotton fibers) options.

4.2.2 System definition

This section was already presented in Sec. 1.4.

4.3 LCA model

4.3.1 Goal and scope definition

The aim of the LCA model is to evaluate and compare the potential environmental impacts of the three acoustic panels previously described considering the environmental concerns of the automotive industry in Brazil. In this section, the LCA model will be developed in a structured way after ISO (2006a).

A) Functions of the product systems:

The panels behave as acoustic barriers for the noise coming from the front of the vehicle. Thus, they guarantee an acceptable noise level for the passengers, as shown in Fig. 1.2.

B) Functional unit:

The functional unit of this study is maintaining an acceptable acoustic level inside a vehicle during 10 years (or 180,000 km, the mean distance traveled by a vehicle in Brazil in this time period). No variation of the acoustic level during the component's life was considered.

C) Systems:

The three systems to be compared and to fulfill the functional unit are the DL-PU panel, the ABA-cotton panel, and the DL-cotton panel.

Three phases of their life cycle were considered: production (including extraction of raw materials and manufacturing of parts), use and end-of-life. While the first two phases are usually addressed for automotive components, the latter phase (end-of-life) is of particular importance in the Brazilian context: nowadays, 21% of the Brazilian solid waste is disposed in open dumps, 37% in controlled landfills and 36% in non-controlled landfills (IBGE, 2000). In 2010, a new law project was endorsed to establish a national policy for solid waste (SILVA, 2010). Among other objectives, it encourages the development of reuse and recycling practices and the application of Life Cycle Assessment (LCA) methodology in waste management.

The design phase was disregarded, because of its low contribution to the environmental impacts (MUNOZ et al., 2006).

The panels are produced, used and disposed of in Brazil.

D) Limitations and hypotheses:

The product under study being produced, used and disposed of in Brazil, the analysis should, in principle, use datasets that are relevant for this specific geographical context. Nevertheless, some specific data were not available in the *EcoInvent* database or they were considered too old (older than 2000). This lack of data is common in Brazilian LCA studies, as observed, for example, in Ribeiro e Silva (2009), Eicker *et al.* (2009), Luz *et al.* (2010), and Ugaya e Walter (2004). Therefore, for our study, some datasets (e.g., the Brazilian energetic mix) have been updated.

Most of the data used in the model are average data valid for Europe, extracted from the *EcoInvent* database. This approach can be assumed as valid in this study for two reasons: first, it can be assumed that the performances of most industrial processes considered in the analysis do not vary with the location; second, as reported by Ugaya e Walter (2004) for the use of steel in Brazilian automobiles, although variations between foreign and national data concerning manufacturing processes exist, the influence of these variations on the LCA results for automotive applications is minor because the life cycle impacts are usually dominated by the use phase.

E) Impact categories selected and methodology of impact assessment:

Selection of impact categories has to be done considering the goal and objectives of the study, but also considering the environmental concerns of the geographical context, as argued by Wood *et al.* (2010).

Brazil is a country with a fast industrialization, rapid urban growth, and based on a large-scale intensive agriculture, fostering environmental problems, such as deforestation, air and water pollution, land degradation, increase of the number of endangered species, and waste management issues. These issues are directly related to acidification impact categories, mainly due to pollution. Moreover, the question of mineral resource availability is of key importance anywhere in the world, and so also in Brazil, one of the largest worldwide exporters of minerals. The impact of this activity on the environment can be measured by the abiotic depletion category.

Moreover, one of the major environmental concerns in Brazil is climate change, as presented in the National Plan on Climate Change (Government of Brazil, 2007). This document reports on the climate change topic and establishes some mitigation opportunities related to energy (e.g., higher contributions from renewable sources), biodiversity, soil and water.

Today, there is no specific LCIA (Life Cycle Inventory Analysis) method recommended for the loss of biodiversity (see, for instance, the review by Curran et al. (2011)). Some end-point

LCIA methods exist, but there is little consensus on them. However, several existing impact categories and associated mid-point LCIA characterization methods currently cover the main drivers of biodiversity losses. This includes global warming, acidification, eutrophication, and ecotoxicity impact categories. The concern about water and soil protection can be evaluated through fresh water aquatic ecotoxicity and terrestrial ecotoxicity categories.

Considering all the above, the impact categories considered in this work are: Abiotic Depletion (AD), Acidification (A), Eutrophication (E), Global Warming (GW), Ozone Layer Depletion (OLD), Fresh Water Aquatic Ecotoxicity (FWAE) and Terrestrial Ecotoxicity (TE).

The ILCD recommendations for Life Cycle Impact Assessment (COMISSION, 2010) were the support for the choice of the LCIA impact methods. Although they were developed for the European context, the recommendations have been developed by international experts and considering methods available globally. They should be considered as internationally recommended and, therefore, applicable to the Brazilian context as well. For each impact category, the methods are rated against the criteria defined in the LCIA Framework and Requirements (COMISSION, 2010). For AD, GW and OLD, the CML 2002 LCIA method is recommended. For E and A, Sepalla's method is recommended, but it is not yet implemented in LCA software, while the CML 2002 method is rated as the second best method. The USEtox model is recommended for the TE, although, in the FWAE case, no LCIA method is currently recommended. Considering the latter, the CML 2002 impact assessment method seems a good compromise between recommendations and software implementations, and it was therefore chosen in our study. Only the characterization phase of the LCI was carried out and is reported in this paper.

4.3.2 Software and data

In this study, SimaPro® software version 7.3.3 was used together with the *EcoInvent* V2 database, from 2007.

4.3.3 Production phase model

The steps of the life cycle considered in this study, with a special focus on the production processes, are illustrated in Fig. 4.1. Raw materials are extracted and transported to the suppliers, then the felt and the mineral layers are produced in the city of Itu and taken to the city of Taubaté
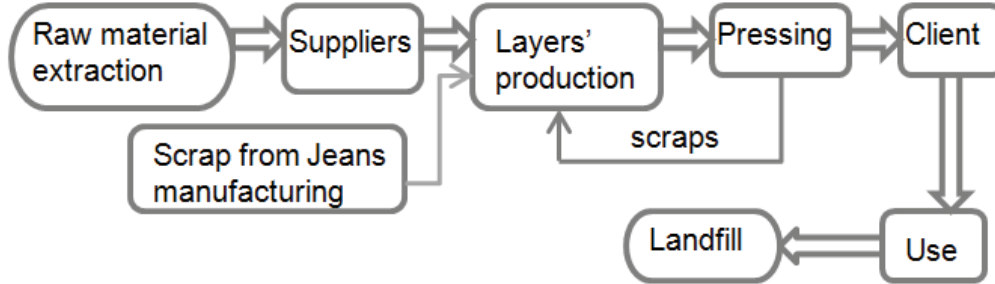
Figure 4.1: Acoustic panel life cycle scheme.

Felt layers	Mineral Layers
1) To shred the jeans fibbers	1) To mix cement, calcite and PE
2) To mix PE, cotton, and jeans	in the correct proportion;
3) To deposit the mixture on a mat	2) To calender the mass;
(thickness and width)	3) To cut the piece
4) To cook the mat in oven	

Table 4.1: Simplified manufacturing process of felts and mineral layers.

(230km distant from Itu) in order to be pressed together, generating the final panels. In this pressing phase, scraps are generated because the panel geometry includes empty holes[1]. This obtained scrap is shredded and reused in felt and mineral material mixtures of the production process. From Taubaté, the panels are transported to the client, to be installed in the vehicles.

Table 4.1 contains the simplified manufacturing process of felt (left) and mineral (right) layers. PU foams were not produced at *Coplac®*; they were directly used in the pressing step. In the calendering process the felt mixture is pressed into a smooth, united and consistent layer.

In the model, the calcite C_aCO_3 was approximated as "limestone C_aCO", because these minerals are quite similar and they are extracted from the same rock. The cement was modeled as "unspecified cement", because there is no specific information about it. However, the considered energy mix for production was the Brazilian one, which was created for this case study according to the Brazilian energetic mix (ANEEL, 2012).

---

[1]An anti flame film is applied in all panel models during the pressing phase. This treatment was neglected in this LCA study

Since the life cycles of the products under study are characterized by original features such as consumption of recycled fibers during production and energy recovery at end-of-life, the so-called "50/50 allocation split" was used. This approach consists of splitting 50% of credits/burdens associated to the use of recycled materials and 50% to the end-of-life recovery between previous and following life cycles. This approach was initially recommended by the method developed in France under the laws Grenelle I of 2009 and Grenelle II of 2010, published in June 2011 (AFNOR, 2011).

It is now also required by the European Commission's Product Environmental Footprint methodology (COMMISSION, 2013a), published as an annex of the recommendation linked to the Communication "Building the Single Market for Green Products - Facilitating better information on the environmental performance of products and organizations" (COMMISSION, 2013b). This method is currently the only method that allows considering burdens/credits of both input of recycled materials and outputs of scraps and recovered energy, while still avoiding double counting at the system level (ALLACKER et al., 2014). This means that the panels under study assume a share of the impacts of the virgin cotton production (although they only consume cotton fibers scraps) and also benefits from the avoided disposal of the scrap of cotton fibers and from the production of recovered energy.

The following energy necessary to shred cotton fibers was considered as 11.75kWh per ton of scrap. This value was approximated from the shredding of jute fibers (ALVES et al., 2010), because specific data for cotton fibers were not found.

The scraps of the panel material were modeled only considering the energy necessary for the shredding process, as cited in this section. This energy value was doubled because fibers are shredded twice (the first time when they are treated as scraps of jeans and the second time when they are already scraps of panels).

Table 4.2 shows details of the transportation processes from the suppliers to *Coplac*® considered in the model. For the truck transportation, a lorry fleet average of 20-28 tons was chosen, because there is no specific information available. For the ship transportation present in the LDPE case, transoceanic freight was selected.

Other considered transportation steps include: layers transportation to Taubaté, where the pressing phase occurs; scraps return to Itu; panel distribution to the client.

Raw Material	Means of transportation (dataset used)	Distance (km)
Cotton	Truck (lorry 20-28 t fleet average)	145
Jeans	Truck (lorry 20-28 t fleet average)	145
LDPE	Truck (lorry 20-28 t fleet average)	100
	Ship (transoceanic freight)	17,600
Cement	Truck (lorry 20-28 t fleet average)	227
Calcite	Truck (lorry 20-28 t fleet average)	300

Table 4.2: Information about the suppliers' transportation: raw material, means of transport and distance.

Layer	Energy (kWh)
Hard felt	1.345
Soft felt	2.153
Mineral ABA	0.1492
Intermediate felt	1.077

Table 4.3: Energy quantity necessary for the production of each layer.

The energy used for the layers production is listed in Table 4.3. This information was collected at the production plant of *Coplac*® through the average power consumption of the machines involved in the layers' production. Moreover, the pressing phase consumes 0.5kWh of electricity per panel.

4.3.4   Use phase model

Brazil is the unique nation that fully incorporates ethanol as an alternative for fossil fuels in the transport sector (FARINELLI *et al.*, 2009). On average, vehicles use as much as 20% of ethanol (DIGEST., 2012).

Since the objective of this work is a comparison of three panel alternative solutions, only the contributions of the panels to the vehicle's fuel consumption and air emissions were considered for the use phase. A refined fuel consumption model specifically addressing the lightening of vehicles through reduction of the vehicle weight and motor size, such as the one proposed by Duflou *et al.* (2009), could have been considered. However, since the potential for lightening the vehicle brought by the fibers of an acoustic panel is far below the one discussed by Duflou *et al.* (2009) (around 0.5% against 6,1% of the vehicle weight in the case of the reference), such a refined consumption

Panel Share	(%)
DL-PU	1.08
ABA-cotton	1.11
DL-cotton	0.63

Table 4.4: Share of the weight of each panel compared to the weight of the car.

model was judged as unnecessary.

A share proportional to the weight of the acoustic components of the process "operation of passenger car" using Ethanol/Gasoline fuel available in the *EcoInvent* 2.2 database was therefore used for the modeling. Ugaya e Walter (2004) adopted a similar approach.

The share (kg of panel/kg of vehicle) related to each panel was calculated considering a vehicle mass of 912kg (Duflou *et al.*, 2009). This share was multiplied by the 180,000km of the use phase and the kilometers only associated with the panel mass were obtained. Table 4.4 shows the shares associated to each panel use phase.

4.3.5 End-of-life phase model:

The acoustic panel should reach its end-of-life together with the end-of-life of the vehicle. In some rare cases, the end-of-life of the panel could happen before, if the component is changed during the life of the vehicle. However, considering that *Coplac*® does not sell replacing panels, this latter option was not considered.

A comprehensive analysis of the recoverability of the product should be done, as recommended by Mathieux e Brissaud (2010). Such an analysis could be done by calculating some recoverability indicators, as defined, for instance, by ISO (2002). However, considering that there is no known process (at least at the pilot stage) to recycle these specific components and materials at the end-of-life, and that no robust data can hence support the calculations, it was decided not to try to do such a comprehensive analysis at this stage. Therefore, in order to analyze the end-of-life of the components, it was decided to apply the LCA methodology considering the relevant end-of-life scenarios. Current and possible end-of-life scenarios for this component can be identified based on the discussion of the so-called "Waste Hierarchy" (Prevent/Re-use/Recycle/Recover/Dispose of

safely), as defined, for example, in the Waste Framework Directive (PARLIAMENT, 2000). The prevention option is, to some extent, addressed because innovative panels bring a reduction of mass of raw material compared to the original panel. This is especially true for the DL-cotton panel, because it has a final mass of half of the mass of the ABA-cotton panel with similar acoustic performance. This should reduce not only the overall mass of residual waste to be handled, but also other environmental aspects (such as fuel consumption during reverse logistics). The re-use option is currently not available for the component and might hardly be available in the future. In Brazil, from the existing 40 million passenger vehicles (DETRAN, 2013), only a very small share of end-of-life vehicles would contain the panel in a foreseeable future, and the market for re-used components would be too small. With such a small market, prohibitive dismantling costs and logistics problems (high costs and energy consumption for long distance transportation) might occur.

Similarly, the recycling option is currently not available, due to the same reasons as for the re-use option, and also due to unavailability of a widely available recycling technology. Organizing reverse logistics to the producer that already has the proper technology (used for the production of scraps) might imply too high costs and environmental impacts. No reason for this situation to change in a foreseeable future was identified.

As stated in the EU ELV Directive **??**, the energy recovery option is an alternative to landfill. This is especially true for many organic materials and this option is therefore considered in our analysis. However, incineration with energy recovery is not currently widely available in Brazil, as this scenario is applied in less than 1% of the national waste (IBGE, 2010). Within the framework of the recent legislation on solid waste (SILVA, 2010), efforts are being made in order to spread this waste treatment option, and this scenario can be considered as possible in Brazil in the future, when components currently put on the market will reach their end-of-life.

The safe disposal option is currently the only option applicable to the panels. Thanks to recent policy development in Brazil, controlled landfills should be widely available when the components reach their end-of-life.

For the LCA analysis of the end-of-life, two scenarios of end-of-life treatment have therefore been considered:

○ Scenario 1: Dispose of in controlled landfills (current scenario);

○ Scenario 2: Energy recovery (future scenario).

It is considered that the materials contained in the panels, after manual dismantling or after shredding (in which case they would be included in the automotive shredder residues), will be disposed of in one of the two scenarios. Due to a lack of information, the emissions and removals of these two pre-treatments are, however, not considered in the LCA modeling.

As explained in Sec. 4.3.3, the "50/50" allocation split was applied to the LCA model and the panels to be recovered by incineration inherited from 50% of the benefits/burdens associated to the avoided virgin energy production.

Table 4.5 summarizes the unit processes used to model production, use and end-of-life phases in the LCA model, using original datasets available in the *EcoInvent* database. In a few cases, considering the high influence of energy in the production and in the end-of-life phase, the original datasets were modified in order to use either more recent data or to use more relevant data: for example, the energy mix from Switzerland considered for the energy recovery at the end-of-life was replaced by the Brazilian energy mix, as presented in Table 4.5.

Name of unit processes created in the LCA model	Original datasets	Description
Recycled (kg)	Electricity, low voltage, production BR, at grid/ BR U Modified to follow ANEEL (2012)	Energy quantity used by shredding of jeans scraps: 11.75 kWh (ALVES *et al.*, 2010)
Scraps (kg)	Electricity, low voltage, production BR, at grid/ BR U Modified to follow ANEEL (2012)	Energy quantity used by reused scraps from the panel production process: 2*11.75 kWh (ALVES *et al.*, 2010), because this material is shredded twice
PU (kg)	Polyurethane, flexible foam, at plant/RER U [2]	Resources consumption and emissions of PU production
PE (kg)	Polyethylene, LDPE granulate, at plant/RER U[2]	Resources consumption and emissions of PE production

---

[2]Energy mix modified to the Brazilian mix.

Energy (kWh)	Electricity, low voltage, production BR, at grid/BR U Modified to follow ANEEL (2012)	Resources consumption and emissions of production of energy
Transport (kg.km)	Transport, lorry >28t, fleet average/CH S	Resources consumption and emissions of *Coplac*® intern transport
Ed (kg)	Disposal, paper, 11.2% water, to sanitary landfill/CH S	Avoided resources consumption and emissions from yarn cotton disposal in landfill
Cotton vigin (kg)	Yarn, cotton, at plant/GLO S	Resources consumption and emissions of virgin yarn cotton production
Cement (kg)	Cement, unspecified, at plant/CH U^2	Resources consumption and emissions of cement production
Calcite (kg)	Limestone, milled, packed, at plant/CH U^2	Resources consumption and emissions of calcite production
Use phase (km)	Operation, passenger car, ethanol 5%/CH S	Resources consumption and emissions of the use phase
Yarn cotton landfill (kg)	Disposal, paper, 11.2% water, to sanitary landfill/CH U	Resources consumption and emissions of yarn cotton disposal in landfill
PE (kg) landfill	Disposal, polyethylene, 0.4% water, to sanitary landfill/CH S	Resources consumption and emissions of PE disposal in landfill
Cement or calcite landfill (kg)	Disposal, inert material, 0% water, to sanitary landfill/CH S	Resources consumption and emissions of calcite or cement disposal in landfill
Yarn cotton incineration (kg)	Disposal, textiles, soiled, 25% water, to municipal incineration/CH U^3	Resources consumption and emissions of yarn cotton incineration
	Heat, natural gas, at industrial furnace low-NO_x >100kW/RER S	Heat generated by yarn cotton incineration

---

[3]Energy recovered from incineration added in the process.

	Electricity, low voltage, production BR, at grid/BR U ANEEL (2012)	Energy generated by yarn cotton incineration
PE incineration (kg)	Disposal, polyethylene, 0.4% water, to municipal incineration/CH U[3]	Resources consumption and emissions PE incineration
	Heat, natural gas, at industrial furnace low-NO_x >100kW/RER S	Heat generated by PE incineration
	Electricity, low voltage, production BR, at grid/BR U ANEEL (2012)	Energy generated by PE incineration

Table 4.5: Summary of production, use and end-of-life LCI unit processes created.

4.4 Results and discussion

4.4.1 LCA results for the panel production phase

Figure 4.2 shows the parameter contributions for impact assessment results of raw material extraction and manufacturing, i.e., the production phase. Virgin cotton and PU extraction appear as the greatest contributors [4]. The plastic contributes mostly to the abiotic depletion and global warming categories, because of the polyols and toluene present in the PU, while virgin cotton has more impact on the toxicity categories, because of the fertilizers applied in its cultivation.

In the production phase, there are two important parameters: the mass of materials applied in each panel and the energy necessary to make these materials achieve the desired geometry. Comparing the recycled textile panels, the ABA-cotton panel has almost twice the DL-cotton mass; however, it consumes 65% of the energy used in the DL-cotton production, as it is possible to observe in Tab. 1.1 and 4.3 for mass and energy, respectively. However, the DL-cotton model requires

---

[4]All LCA results presented in the paper are normalized to the maximum absolute value, set to 100% (or -100% if negative).
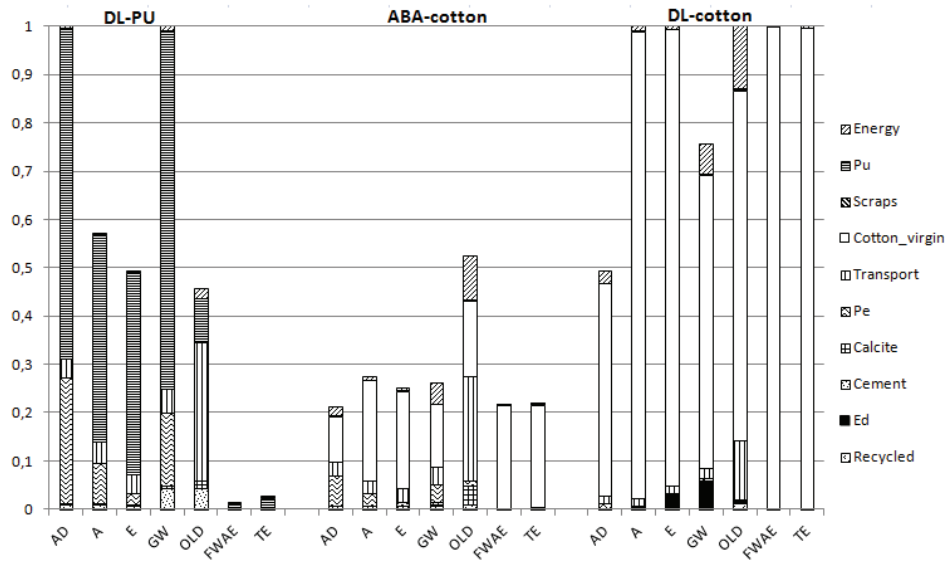
Figure 4.2: Comparison and analysis of main contributors to DL-PU, ABA-cotton, and DL-cotton impact assessment results. Energy refers to "energy consumed in the manufacturing process".

approximately 40% more textile than the ABA-cotton model, so its impacts are higher.

With the LCA analysis, it was possible to identify the that DL-cotton panel is the most impacting in five of the seven analyzed impact categories in the production phase, especially because of the high quantity of cotton applied. The toxicity values are the most discrepant. For instance, in the fresh water aquatic ecotoxicity, the DL-cotton is 11.4kg 1.4DB eq., while the DL-PU is 5.82kg 1.4DB eq. At the same time, the DL-PU panel has the highest impact in two important categories for the Brazilian context: abiotic depletion and global warming.

The energy significantly contributes to the global warming and ozone layer depletion categories. To better understand this, the Brazilian energetic mix according to ANEEL was investigated (Tab. 4.6[5] shows the Brazilian energetic matrix including the processes used in the created process, all from *EcoInvent*). The biomass is mainly composed of sugarcane bagasse and scraps of vegetal coal and wood. The enormous hydroelectric potential is exploited, as it can be seen in Tab. 4.6, with around 80% of the energy sources being renewable in Brazil.

---

[5]mainly hydroelectric power plants are in South America.

Type	%	Process
Hydro	65.72	Electricity, hydropower at reservoir power plant/ BR S
Natural gas	9,75	Electricity, natural gas, at power plant/ UCTE S
Industrial gas		1,44 Electricity, industrial gas, at power plant/ UCTE S
Biomass	7.17	Electricity, bagasse, sugarcane, at fermentation plant/ BR S
Imports	6.50	Electricity, hydropower at reservoir power plant/ BR S
Petrol	5.70	Electricity, at cogen 200kWe diesel CSR, allocation exergy/ CH S
Nuclear	1.60	Electricity, nuclear, at plant/ CH S
Mineral Coal	1.55	Electricity, hard coal, at power plant/ UCTE S
Eolic	1.17	Electricity, wind power plant/ RER S

Table 4.6: Percentage use to create the LCI dataset for the Brazilian Energetic Matrix (ANEEL, 2012), and associated processes from Ecoinvent.

4.4.2   LCA results for the panel production, use and end-of-life phases

In the use phase, the fuel consumption of the car associated to the three panels has to be considered. The impacts of the use phase change proportionally to the panel's mass, as explained in Sec. 4.3.4. The results are presented in Fig. 4.3, which also includes the end-of-life phase. For the end-of-life phase, two scenarios have been considered.

1. Scenario 1: disposal (current scenario)

   Figure 4.3 shows the impact assessment results considering production, use (fuel consumption) and end-of-life of DL-PU, ABA-cotton and DL-cotton panels, considering Scenario 1.

   Observing Fig. 4.3, it is possible to see that, in all impact categories, the use phase represents a dominant share of the panels' environmental impacts. This profile is confirmed in the literature by Munoz *et al.* (2006), Duflou *et al.* (2009), Alves *et al.* (2010), and Luz *et al.* (2010).

   Considering the design evolution of the products, starting with DL-PU, followed by ABA-cotton, and finally DL-cotton panels, it is possible to observe a relative improvement in the product environmental performance.

   In the DL-PU panel case, no natural or recycled material is applied; instead, polyurethane foam is used. Moreover, it includes the heavy mineral layer, what results in a high final weight, so the use phase impacts are also high. The landfill end-of-life scenario contribution

Figure 4.3: Comparison among DL-PU, ABA-cotton, and DL-cotton whole life cycle impact assessments with landfill end-of-life scenario, with the "50/50" allocation split.

is observed mainly in the eutrophication category due to the landfilling of PU. This "status-quo" option presents the highest impacts in four of the seven categories: AD, A, E, and GW. Furthermore, OLD result is really close to the worse one, i.e., ABA-cotton. In the two toxicity categories, DL-PU impacts are the best ones, because it does not apply natural cotton fiber.

The ABA-cotton panel presents intermediate results. This model employs recycled cotton fibers; however, its weight is also high, because of the mineral layer presence. Therefore, the use phase contribution is large. The landfill end-of-life scenario contribution is observed in eutrophication and in the global warming categories, especially because of cotton fibers and polyethylene disposals, respectively. An increase is observed in the toxicity categories when comparing with DL-PU panel results, due to natural fiber use, which require a significant quantity of pesticides for cultivation.

Finally, the DL-cotton panel combines recycled and natural materials use with lower weight. As its mass is almost half of the other ones, the use phase does not increase its impacts as much as it increases for the other two panels. Nevertheless, the virgin cotton production impact is still significant in the fresh water aquatic ecotoxicity and in the terrestrial ecotoxicity categories. Therefore, the DL-cotton panel continues to be the most impacting in these two categories. Similarly to the ABA-cotton panel, the landfill end-of-life scenario contribution is observed in the eutrophication and in global warming categories, mainly because of cotton fibers and polyethylene disposals, respectively.
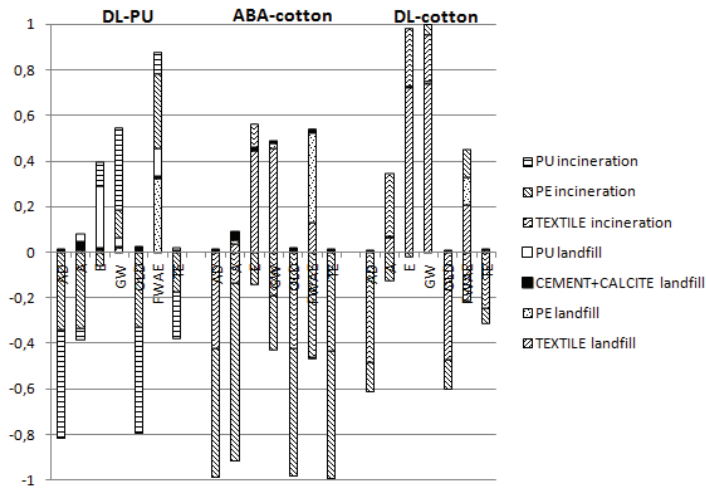
Figure 4.4: Comparison between incineration and landfill end-of-life scenarios.

Comparing the total results for the three panels, the worst performances are observed for DL-PU and ABA-cotton, but the first one achieves the highest impacts because it associates larger weight and non-recycled raw materials. As the recycled textiles are associated to lower weight, up to this stage of this case study analysis, it is possible to conclude that they are a beneficial alternative for the environment.

2. Scenario 2: incineration with energy recovery (prospective scenario)

As cited in Sec. 4.3.5, the incineration with energy recovery scenario can be supposed as available in Brazil in a near future and a comparison with the landfill scenario is therefore made here. Figure 4.4 shows the comparison between landfill and incineration with energy recovery end-of-life scenarios for the three panels. First, it is possible to conclude that textiles, PU and PE have good energy recovery potentials. So, the recovered energy and heat produced through incineration can bring some environmental benefits.

A new analysis of the whole life cycle was made, in order to observe the contribution of each phase considering the incineration with energy recovery scenario. Results are shown in Figure 4.5. In the abiotic depletion, ozone layer depletion and terrestrial ecotoxicity categories, negative results represent the benefits associated to recovered energy and heat and avoided disposal.

Scenario 2 results also illustrate the significant contribution of the use phase and the secondary importance of the production phase for the LCA results. The DL-PU panel presents higher environmental impacts in all categories, except for the two toxicity categories. How-
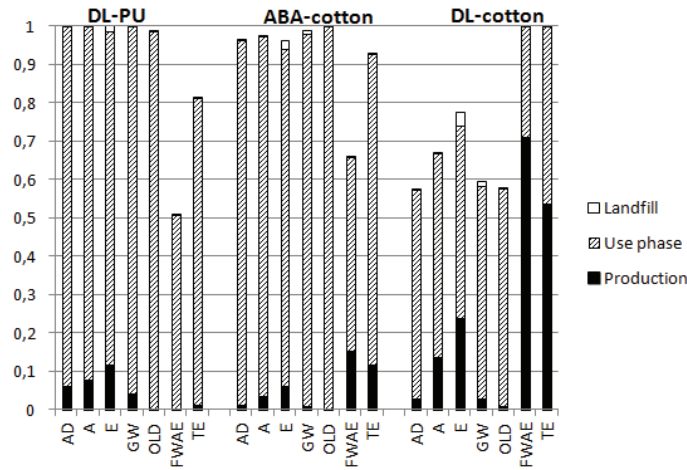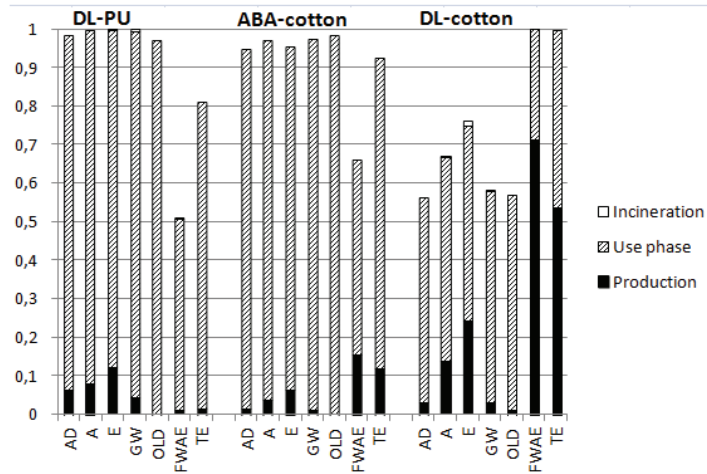
Figure 4.5: Comparison among DL-PU, ABA-cotton, and DL-cotton whole life cycle impact assessment with incineration end-of-life scenario, with the "50/50" allocation split.

ever, it has potential for energy recovery. The ABA-cotton panel is the most benefited by the incineration end-of-life, because it combines textile and PE energy recovery potentials.

Comparing Scenarios 1 and 2, considering the whole life cycle, the difference between them is not so visible. However, the recovery brings some reduction of the environmental impacts. The impact categories need to be carefully analyzed according to the context, and it is not simple to state which scenario is the most adequate. However, as the automotive industry is under pressure to increase the share of the mass of vehicles that is actually recovered at the end-of-life, Scenario 2 could be encouraged, because it provides recovered energy and also reduces the volume of residual waste.

Observing the three options, and knowing that they ensure the desired vehicle interior noise level, it is possible to conclude that the DL-cotton is the best available option, independently of the chosen end-of-life scenario, for all impact categories, except FWAE and TE. The latter can mainly be explained by the high contribution of the production of renewable fibers (See Fig.4.2). Overall, this alternative can be judged as better because it combines lower weight, virgin material economy, energy recoverability at end-of-life and residual waste landfilling reduction. The results of this case study on a specific component and using specific raw materials are coherent with general findings published in literature concerning the use of renewable materials in automotive parts.

Finally, a sensitivity analysis regarding the "50/50" (as presented in Fig. 4.3 and Fig. 4.5) and

the "100/0" allocation splits was developed. The "100/0" allocation split modeling allocates the benefits of recycling only to the production stage, and does not give any credit to the recycling phase. For such a modeling, considering that only scrap cotton is used in the production of the panels, no impact of the production of virgin cotton is considered. However, 100% of the processes associated to scrap jeans (e.g., shredding and logistics) are allocated to the production stage. Moreover, this modeling considers 100% of landfilling for end-of-life Scenario 1 and 100% of incineration without energy recovery for end-of-life Scenario 2. The results of this alternative modeling are presented Fig. 4.6 and Fig. 4.7, respectively.

Both figures show the impacts of virgin cotton production. The credits associated to energy recovery are not considered, so that the relative contribution of the use phase automatically increases. This is especially true for several impact categories, including E, FWAE and TE, while almost no influence can be seen on the other impact categories (i.e., GW, AD). The use phase being predominant, this modeling slightly emphasizes the environmental advantages of using the DL-cotton option compared to other options, in particular for the E, FWAE and TE impact categories. Non-normalized LCA results of Scenarios 1 and 2 are available in Tab. 4.7 and Tab. 4.8. In addition, an uncertainty analysis is presented in Annex C, Sec. 4.8.

4.4.3 Discussion: how such LCA results can be used in an R&D context

The acoustic panels' life cycle assessment results can provide support for some design / production improvement opportunities, because the magnitude of the contribution of several parameters of the component (material mass, composition, processes, etc.) to the environmental impacts can be calculated for each phase of the life cycle.

A design evolution was already observed: starting with DL-PU and ending with DL-cotton. It was based on weight reduction by replacing synthetic materials by recycled natural fibers, and it brought some noticeable environmental improvements. Another opportunity can also be derived from the LCA analysis, i.e., to reduce internal transportation by improving logistics or substituting suppliers by closer ones and to simplify the end-of-life treatment of the felt mixture.

4.4.4   Further research opportunities

Looking at the results presented in this study, it can be concluded that relevant environmental improvement can be achieved by design taking into account LCA. LCA results have shown that going from DL-PU, to DL-cotton represented a design evolution in terms of environmental performance. The environmental models are currently mainly parameterized as functions of the layer thickness (through the mass). Considering a constant functional area for the panel, design alternatives with constant acoustic characteristics can be developed by modifying parameters such as the structure of the layers, their thickness and the materials used, for example, using other natural fibers (see, for instance, Lamary *et al.* (2011)). Further research is needed to develop acoustic models as functions of the same parameters (structure of layers, thicknesses and materials used). When this will be done, a multi-objective optimization, addressing weight, acoustic and some environmental performances will be possible, and design options with high performance for all these criteria will be identified.

Moreover, when such alternative panels and additional design parameters (geometry, accessibility, etc.) will be available, a comprehensive recoverability analysis of the components will be possible with the objective of identifying further ecodesign opportunities in order to make the recyclability higher. An idea that could even improve the DL-cotton panel performance would be to replace the traditional cotton by the organic cotton. The reciclability rate increase will be possible using either a multicriteria recoverability analysis of complex products (as defined by Huisman *et al.* (2003)) or Mathieux *et al.* (2008)), a simplified integration of material recycling constraints during design of components (FROELICH *et al.*, 2007), or a product and material specific Material Flow Analysis (MATHIEUX E BRISSAUD, 2010)). This analysis will, however, only be possible when efficient recovery processes applicable to this type of components and materials (including composting processes) are developed.

4.5   Conclusions

This LCA case study analyzed the use of recycled cotton fibers in automotive acoustic components in replacement of components made mainly of polyurethane. The so-called "DL-cotton panel" option, which combines two layers of recycled fibers of different densities and for which natural fibers represent a majority of its raw materials, was identified as the most environmentally

friendly option, on average 30% less impacting than the other two solutions. This component combines good acoustic performance with lower weight, economy of fossil resources, heat and energy saving during production, and it also avoids textile disposal in landfills. The paper therefore confirms the advantages of the cotton fibre and the performances of natural fibres in general used in vehicle applications, in particular thanks to lower weight, as reported in other publications.

The research reported in this paper goes beyond previously published work by highlighting the particular behavior in LCA of recycled fibers compared to virgin ones (in terms, e.g., of shared contribution of agriculture production and of avoidance of landfilling), thanks to the application of the "50/50" allocation rules. As the automotive industry faces the challenge of reducing waste mass at the end-of-life vehicles, incineration seems to be most feasible futuristic recovery scenario for the moment in the Brazilian context for the component. Moreover, this work demonstrates the limited performances of current and future possible end-of-life scenarios and highlights the necessity to work on future scenarios based on recycling. Furthermore, it shows how the environmental analysis results can be used for ecodesign purposes. In particular, this justifies the need for leading multi-objective (coupling technical and environmental performances) optimization for the ecodesign of these acoustic components coupling environmental and acoustic models. This will be developed in the future.

These results, although very dependant of the Brazilian scenario, should also be valid in other regions sharing the same production, use and end-of-life infrastructures. In emerging countries, for example Thailand, that are characterized by large automotive industry, large natural fiber production, significant use of biofuels and similar (emerging) waste treatment facilities (cf. e.g. UNEP (2011)) similar environmental behavior could probably be observed.

Further work may also include the test of the models on other components and other fibers (recycled or not), especially coming from tropical regions. If replicated for many automotive components, this strategy could bring some noticeable weight reduction. Similar analysis will also be carried out on other transportation applications, e.g. in aeronautics.

Figure 4.6: Comparison among DL-PU, ABA-cotton, and DL-cotton whole life cycle impact assessment with landfill end-of-life scenario,with the "100/0" allocation split.

	DL-	PU			ABA-	cotton			DL-	cotton	
	Total	P	Use	L	Total	P	Use	L	Total	P	Use	L
AD	3.17	0.19	2.98	0.00	3.06	0.04	3.02	0.00	1.8	0.09	1.72	0.00
A	1.07	0.08	0.98	0.00	1.04	0.04	1.00	0.00	0.71	0.14	0.57	0.00
E	0.13	0.02	0.12	0.00	0.13	0.01	0.12	0.00	0.10	0.03	0.07	0.00
GW	483.84	20.92	462.41	0.51	477.58	4.79	468.96	3.82	287.66	14.50	267.31	5.85
OLD	0.00	0.00	0.00	0.00	0.00	0.00	0.00	0.00	0.00	0.00	0.00	0.00
FWAE	5.82	0.08	5.71	0.02	7.56	1.75	5.79	0.03	11.44	8.12	3.30	0.02
TE	1.39	0.02	1.37	0.00	1.59	0.20	1.39	0.00	1.71	0.92	0.79	0.00

Table 4.7: Non-normalized LCA results with end-of-life Scenario 1 (P = production and L = landfill).

4.6 Appendix A: Sensitivity analysis

In order to compare "50/50" and "100/0" allocation splits, a sensitivity analysis was developed. In the "100/0" allocation spit modeling, virgin cotton production was neglected and only impacts related to jeans manufacturing and logistics were considered. Figures 4.6 and 4.7 illustrate landfill and incineration without energy recovery end-of-live results, with "100/0" allocation split.

4.7 Appendix B: Non-normalized results

The non-normalized LCA results with Scenarios 1 and 2 are contained in Tab. 4.7 and 4.8, respectively.
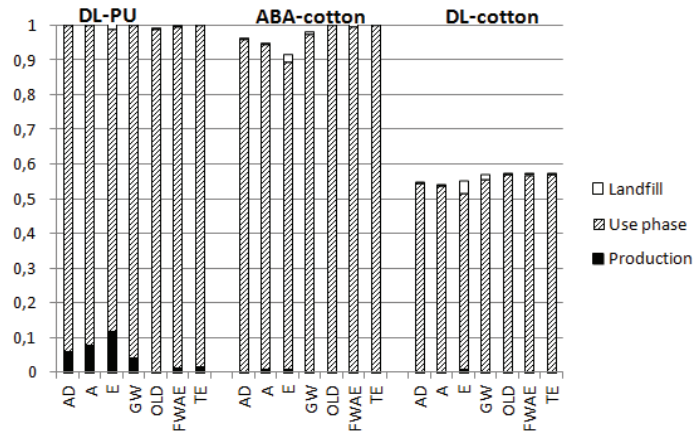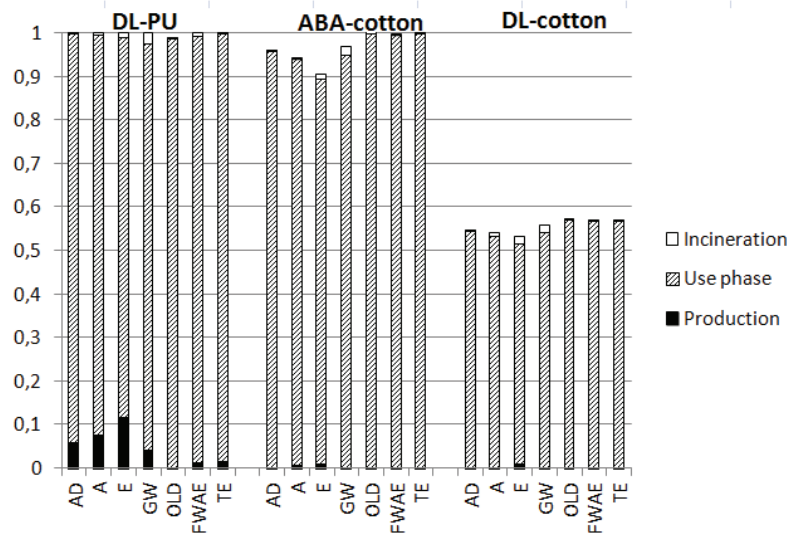
Figure 4.7: Comparison among DL-PU, ABA-cotton, and DL-cotton whole life cycle impact assessment with incineration end-of-life scenario, with the "100/0" allocation split.

	DL-	PU			ABA-	cotton			DL-	cotton		
	Total	P	Use	L	Total	P	Use	L	Total	P	Use	L
AD	3.11	0.19	2.98	-0.06	2.98	0.04	3.02	-0.08	1.76	0.09	1.72	-0.05
A	1.06	0.08	0.98	0.00	1.03	0.04	1.00	-0.01	0.72	0.14	0.57	0.00
E	0.13	0.02	0.12	0.00	0.13	0.01	0.12	0.00	0.10	0.03	0.07	0.00
GW	487.10	20.92	462.41	3.77	470.41	4.79	468.96	-3.35	283.79	14.50	267.31	1.98
OLD	0.00	0.00	0.00	0.00	0.00	0.00	0.00	0.00	0.00	0.00	0.00	0.00
FWAE	5.81	0.08	5.71	0.02	7.51	1.75	5.79	-0.02	11.42	8.12	3.30	0.00
TE	1.38	0.02	1.37	-0.01	1.56	0.20	1.39	-0.03	1.70	0.92	0.79	-0.01

Table 4.8: Non-normalized LCA results with end-of-life Scenario 2 (P = production and I = incineration).

4.8   Appendix C: Uncertainty analysis

Uncertainty analysis was performed as recommended by ISO (2006a) and the LCA conclusions could be enriched. Uncertainty in the input data was considered in this approach. Moreover, as only system processes were chosen in the panel modeling, all input data treated as random variables are related to the specific case study.

According to deterministic results from Sec. 4.4 production and use are the most relevant life cycle phases. Moreover, raw material quantity directly influences the use phase fuel consumption because it varies the panel final mass. At this point, it was important to note that, as the panel modeling is parameterized, the variation in these masses influences all LCA quantities, including the use phase. Therefore, raw material quantities were chosen as random variables.

At SimaPro®, a variation of 10% in mass is accepted in the felt and in the mineral mixtures manufacturing. As no more information about these random variables was available, PE, cotton, calcite, and cement mass quantities were modelled with the triangular probability density function, having as minimum and maximum values minus and plus 10% of their known mean values.

Monte Carlo simulation was performed with SimaPro®. The software offers two stop criteria: a fixed number of runs and a standard error value that is defined as the reason between the standard deviation and the square root of the number of realizations. However, neither criteria can guarantee statistical convergence. A large number of realizations does not assure convergence and the standard deviation is not dimensionless, so the user needs to establish a standard error that is proportional to the order of magnitude of the analyzed result. In order to verify the convergence of the mean value of the impact categories, 2000 realizations were computed. Fig. 4.8 shows the evolution of the average for the TE result of the DL-panel case. It can be seen that around 900 realizations are sufficient to assure convergence in this case.

Mean and coefficient of variation values for the three panels LCA with Scenario 1 are listed in Tab. 4.9 Mean values are similar to deterministic values listed in Table 4.7 and the coefficients of variation vary between 6.85% and 2.44%. To explore these values, the Probability Density Functions (PDF's) of impact categories were put together as shown in Fig. 4.9 for the TE case.

In Fig. 4.9 it is possible to observe that the PDF's curves intersect each other. This behavior
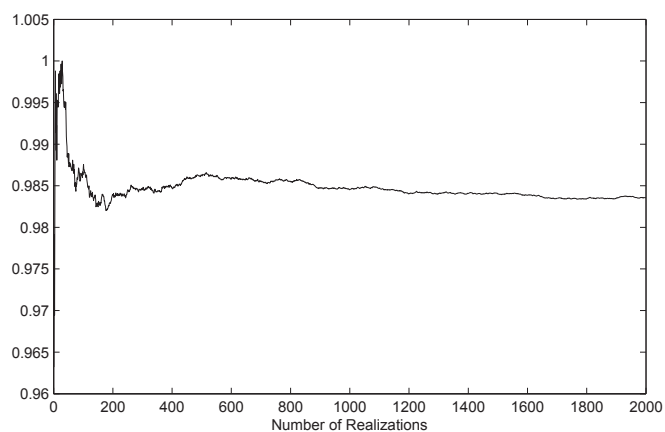
Figure 4.8: Monte Carlo simulation convergence of TE impact category result mean for the DL-cotton panel case.

		DL-	PU	ABA-	cotton	DL-	cotton
	Unit	Mean	CV (%)	Mean	CV (%)	Mean	CV(%)
AD	kg Sb eq	3.16	3.89	3.08	3.18	1.81	3.86
A	kg SO2 eq	1.07	3.83	1.05	3.16	0.71	3.41
E	kg PO4 eq	0.13	2.96	0.15	4.41	0.12	6.85
GW	kg CO2 eq	483.00	3.96	481.00	3.18	285.00	3.86
OLD	kg CFC-11 eq	0.00	4.13	0.00	3.18	0.00	4.01
FWAE	kg 1,4-DB eq	5.79	2.44	7.95	4.01	12.50	5.32
TE	kg 1,4-DB eq	1.40	4.07	1.61	3.17	1.70	3.54

Table 4.9: Means and coefficients of variation of the three panel's uncertainty analysis.
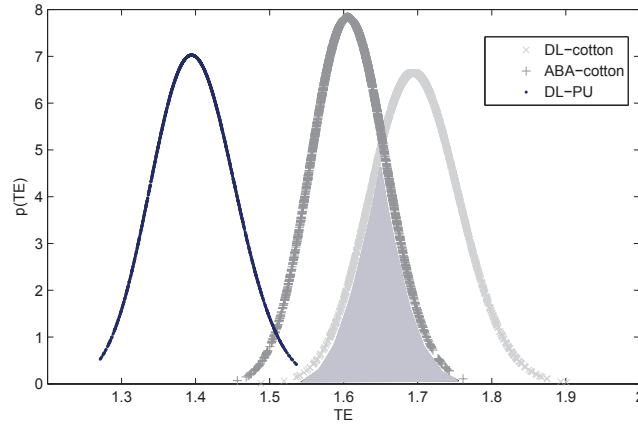
Figure 4.9: DL-PU, ABA-cotton, and DL-cotton probability density functions of TE impact category.

was observed only in FWAE and in TE impact categories. The intersection interval in the horizontal axis indicates values that can be obtained by both panel solutions. For example, both ABA-cotton and DL-cotton can generate TE values between 1.5 and 1.8 approximately. The DL-cotton PDF area minus the shaded area represents the probability of DL-cotton panel to be the most impacting: 57.95%. For FWAE, the curves tendency is similar to Fig. 4.9 and in 94.75% of the cases, DL-cotton is the most impacting.

Excluding FWAE and TE, deterministic results were confirmed by the uncertainty analysis, because no variation in the comparisons occurred. Moreover, information was included, because, considering uncertainties, it is possible to calculate the probability of the DL-cotton panel to be the most impacting in toxicity categories.

5 Uncertainties in poroelastic materials' acoustic performance

This chapter is the author version of the article entitled: Uncertainty analysis of porous material parameters using random fields. It was presented at Uncertainties 2014, in Rouen, France. When treating the acoustic performance of the multi-layered acoustic panel case study, a complete uncertainty analysis would would include variations on material properties, materials sequence and layers thickness. However this work is an initial approach that treats the flow resistivity of the poroelastic material as a random variable and analyses its influence on the transmission loss curve. Future work can be developed to improve the uncertainty analysis of the acoustic model.

5.1 Introduction

The pollution caused by use of plastics and emissions at end-of-life treatments is affecting the air, the soil, and the water (JOHN E THOMAS, 2008). A solution being explored nowadays is the natural fiber composite material. Mixing natural fibers with synthetic or natural plastics provides an enormous variety of composites in terms of: tensile strength, density, stiffness, etc. Therefore they are widely used in civil constriction, furniture and automotive industry, etc.

These composites are generally modeled as poroelastic materials because during the production process empty spaces are left between the fibers. This type of material is composed of a skeleton (also called matrix or frame) and pores. The pores are generally filled with a fluid that can be liquid or gas, while the skeleton is solid (generally constituted by fibers or by a polymeric matrix) (ALLARD, 1993). The interaction between the solid and the fluid phases generate energy losses that are welcome in acoustic applications. So, poroelastic materials are widely used as acoustic materials.

If the displacements of the skeleton are neglected, the porous material can be simply studied as an equivalent fluid medium. However, the Biot-Allard model (ALLARD, 1993), (ALLARD E ATALLA, 2009) is more commonly used. It considers the solid displacements, includes all interactions between fluid and solid phases, and treats energy losses due to viscous and thermal coupling.

As it is difficult to guarantee the homogeneity of a natural fiber composite during its production process, parameter variability is common in this type of medium. The pore size and shape are not easily controlled, so density varies causing a fluctuation in all other parameters: porosity, tortuosity, etc. When uncertainties are considered in the models, the method most usually used is the Monte Carlo (MC) simulation. It is a sampling method that consists on generating independent realizations of random variables based on their probability distributions. By solving the deterministic problem for each realization, and collecting an ensemble of solutions, statistical moments can be calculated (SOBOL, 1994). Another method with wide application when considering random fields is the Karhunen-Loève (KL) expansion (PAPOULIS E PILLAI, 2002), (GHANEM E SPANOS, 2003), (XIU, 2010). The KL expansion may be used to discretize the random field by representing it by scalar independent random variables and continuous deterministic functions. By truncating the expansion the number of random variables becomes finite and treatable numerically. Several authors use the KL expansion to model Gaussian random processes. Adhikari e Friswell (2010) proposed an expansion-based model updating for linear structural dynamical systems. Poirion e Soize (1999) and Schevenels *et al.* (2004) present the Karhunen-Loève expansion for non-Gaussian processes.

This work aims at analyzing the variability of the transmission loss of a poroelastic acoustic panel when variations in its parameters are included. These variations are treated as uncertainties. A transfer matrix method implementation in Matlab® is used to simulate the multilayered poroelastic acoustic panel (TANNEAU *et al.*, 2006). The flow resistivity parameter of the poroelastic material is modeled as a random variable throughout its thickness. How the variation of this parameter influences the panel transmission loss is investigated. The uncertainty propagation is performed using a Monte Carlo approach. The discretization of the random field is done directly and using the Karhunen-Loève expansion. The spatial discretization is necessary for the computation of the transmission loss using the available software. The convergence of the mean and standard deviation of the acoustic transmission loss curve are evaluated. The KL decomposition truncation allows decreasing the number of random variables and, therefore, the computational cost.

5.2 Poroelastic acoustic model

This text was already presented in Sec. 2.1.

5.3 Deterministic model

The acoustic deterministic model schema is observed in Fig. 5.1. A Matlab® program which deals with the transmissibility of flat multi-layered panels with infinite extension called *TMTX* is used. It has two default air layers: incidence of the wave and reception of the wave. An acoustic wave starts from the first default air layer, the incident medium, passes through a thin steel plate of $0.8mm$ and then over a second air layer with $10mm$, achieving the poroelastic material layer of $80mm$. The wave is finally received in the receptor default air layer.
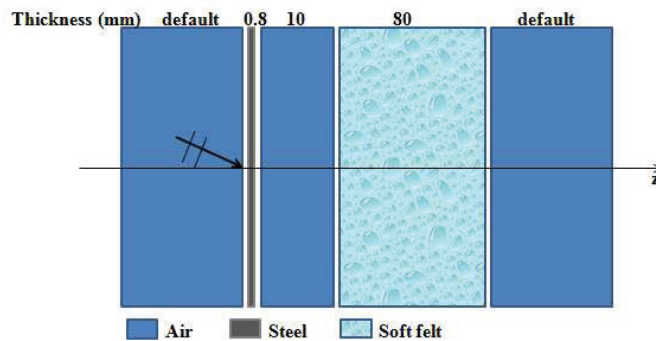
Figure 5.1: Acoustic model schema.

Table 5.1 contains the poroelastic material properties, called Soft felt, and the flow resistivity mean value.

Table 5.1: Parameters of the Soft felt.

Properties	Mean value
Specific mass (kg/m^3)	99.333
Flow resistivity (rayl/m)	34000
Porosity	1
Tortuosity	1
Viscous Characteristic Lenght (μm)	35.3333
Thermal Characteristic Lenght (μm)	150
Young Modulus (kPa)	172333
Loss Factor (%)	0.015

5.4 Stochastic models

In the stochastic analysis, the poroelastic acoustic panel flow resistivity parameter varies throughout its thickness, in z dimension. In both methods, the unique poroelastic material layer of $80mm$ was replaced by a sequence of N poroelastic material layers (N depends on the thickness discretization). This strategy permitted the spacial flow resistivity variation using the transfer matrix method.

5.4.1 Stochastic approach with random variables

Monte Carlo method was used as stochastic solver. It consists in solving the problem repeated times, each one of them with a new random input. The mean and the standard deviation of the result are calculated through the samples generated. In each realization i, a vector of N gaussian random flow resistivity values is generated and each random value is associated with a poroelastic thin layer, provoking the spacial variation. To be more realistic, a suavization in the flow resistivity spacial variation is made: each component of the random vector is calculated as a combination of its neighbors, as explained in Eq. 5.1.

$$\sigma_R(i) = \frac{1}{2}\sigma_R(i) + \frac{1}{4}\sigma_R(i-1) + \frac{1}{4}\sigma_R(i+1) \tag{5.1}$$

With a standard deviation of 5% a random vector of the flow resistivity parameter is generated. The suavization is applied 8 times and Fig. 5.2 shows smoothed and non smoothed flow resistivity vectors. After that, the stantard deviation of this random variable decreased to around 2%, depending on its discretization along the panel thickness.

Let $X(\xi, \omega_k)$ be the frequency response of the stochastic system calculated for a realization ξ, generated by the Monte Carlo method (RUBINSTEIN E KROESE, 2008). The mean-square convergence analysis with respect to independent realizations of the random variable X, denoted by $X_j(\xi, \omega_k)$, is carried out studying the function $n_S \mapsto conv(n_S)$ defined by:
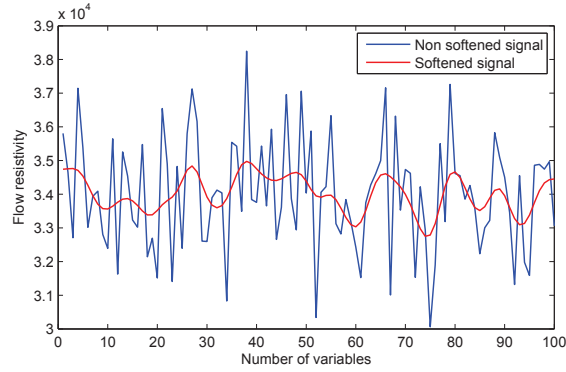
Figure 5.2: Flow resistivity variation suavization along the acoustic panel thickness.

$$conv(n_S) = \frac{1}{n_S} \sum_{j=1}^{n_S} \int_B \|X_j(\xi, \omega)\|^2 \, d\omega \tag{5.2}$$

Mean and standard deviation square convergence are displayed in Figs. 5.3 and 5.4 for 1000 realizations and 20 thin poroelastic layers of $4mm$. The mean converges fast, however around 800 realizations are necessary for the standard deviation convergence.
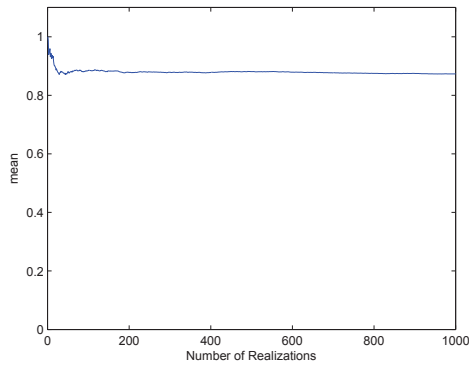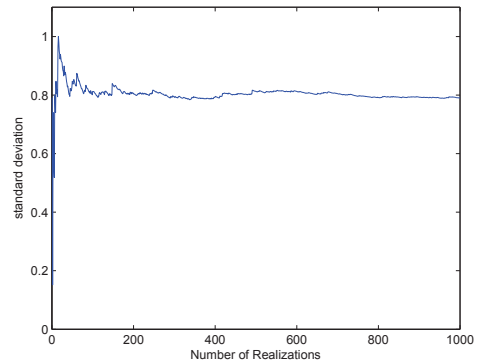

Figure 5.4: Monte Carlo standard deviation convergence.

Figure 5.3: Monte Carlo mean convergence.

Figure 5.5 shows MC mean value, its confidence interval, and the deterministic transmission loss curve. In frequencies close to 10^4 Hz, the statistical curves become more oscillating, and the deterministic curve overcomes the mean value, but it stays inside the confidence interval.
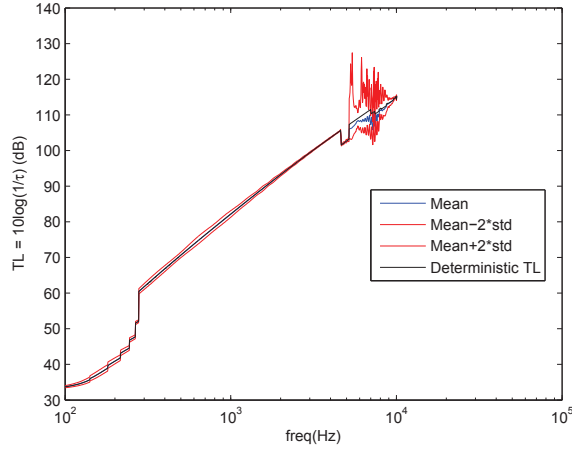
Figure 5.5: Deterministic TL response, Monte Carlo simulation mean, and confidence interval.

5.4.2 Stochastic approach with random fields

One difficulty in using random process is to directly associate the model, mathematically or numerically, with a theory in question. For this reason a discretization of the random fields in terms of random variables is made. Theoretically the random field is described by various points (random variables). For a good approximation, a large number of points is required. This concept is close to the Fourier-type series. Conditioning that a covariance function is finite, symmetric and positive, it is possible to describe a spectral decomposition in a generalized Fourier-type series as:

$$\varpi(x,\theta) = \bar{\varpi}(x) + \sum_{j=1}^{M} \xi_n(\theta)\sqrt{\lambda_j}\varphi_j(x) \tag{5.3}$$

where $\varpi(x,\theta)$ is a random field with a covariance function $C_{\varpi}(x_1,x_2)$ defined in a space $\mathcal{D}$. Here θ denotes an element of the (random) sample space Ω, so that θ is into Ω; $\xi_j(\theta)$ are uncorrelated random variables, and the constants λ_j and functions $\varphi_j(x)$ are eigenvalues and eigenfunctions that satisfy the integral equation:

$$\int_{\mathcal{D}} C_{\varpi}(x_1,x_2)\varphi_j(x_1)dx_1 = \lambda_j\varphi_n(x_2) \quad \forall = 1,2,... \tag{5.4}$$

The eigenvalues and eigenfunctions can be sorted in descending order so that Eq. 5.3 is

78

truncated at M terms. So, it is possible to approach the autocorrelation function by the following spectral decomposition:

$$\hat{C}(x_1,x_2) = \sum_{j=1}^{M} \lambda_j \varphi_j(x_1)\varphi_j(x_2)$$ (5.5)

A one-dimensional autocorrelation function with a Gaussian random field and exponentially decaying can be express as:

$$C(x_1,x_2) = e^{-|x_1-x_2|/b}$$ (5.6)

where b is correlation length. An analytical solution in the interval $-a < x < a$ is assumed with a zero mean, then the underlying random field $\varpi(x,\theta)$ can be expanded using the Karhunen-Loève expansion as:

$$\varpi(x,\theta) = \sum_{j=1}^{\infty} \xi_j(\theta)\sqrt{\lambda_j}\varphi_j(x)$$ (5.7)

Defining that $c = 1/b$, the corresponding eigenvalues and eigenfunctions for odd j are given by:

$$\lambda_j = \frac{2c}{\omega_j^2 + c^2}; \quad \varphi_j(x)\frac{cos(\omega_j x)}{\sqrt{a + \frac{sin(2\omega_j a)}{2\omega_j}}} \quad \text{where} \quad tan(\omega_j a) = \frac{c}{\omega_j}$$ (5.8)

and for even j are given by

$$\lambda_j = \frac{2c}{\omega_j^2 + c^2}; \quad \varphi_j(x)\frac{sin(\omega_j x)}{\sqrt{a - \frac{sin(2\omega_j a)}{2\omega_j}}} \quad \text{where} \quad tan(\omega_j a) = \frac{\omega_j}{-c}$$ (5.9)
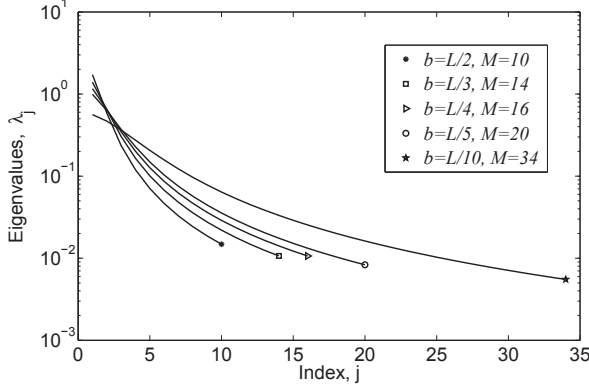
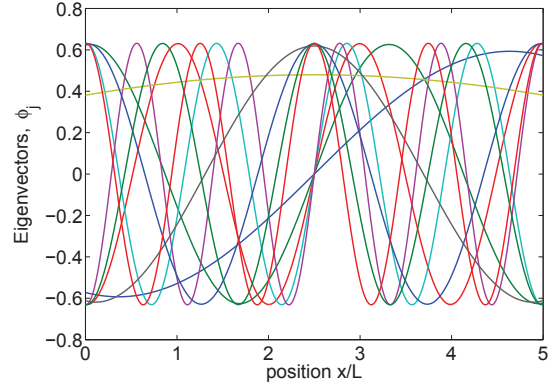Figure 5.6: Eigenvalues with different values of correlation length.

Figure 5.7: Eigenvectors associated with the 10 first modes.

For theory presented in this section, a numerical test has been done to demonstrate the eigenvalues and eigenvector behavior. Eigenvalues are simulated with different values of correlation length related to truncated modes numbers, and arranged in decreasing order as shown Fig. 5.6. Eigenvectors associated with the 10 first modes are illustrated in Fig. 5.7.

As mentioned before, the flow resistivity parameter is assumed a random variable in this present study. In the context of random fields theory, which is the approach used in this section, the flow resistivity parameter is a random field of the form:

$$\sigma_R(x,\theta) = \sigma_{R_0}(1 + \varepsilon \varpi(x,\theta)) \tag{5.10}$$

The flow resistivity is assumed to be an homogeneous Gaussian random field. To illustrate, 6 terms used in the KL expansion are shown in Fig. 5.8, with correlation length $b = 1/2$ and strength parameter $\varepsilon = 0.05$.

In order to be able to compare MC and KL results, an equivalence between them was made. An approximate correlation length was calculated by visually comparing theoretical Eq. 5.6 and smoothed signal correlation function (C_{xx}) curves as shown in Fig. 5.9. The value $b = L/35$ was the one that best approximated these curves, so it was established as the correlation length for KL simulation. Moreover, when smoothing the random variable signal, its standard deviation was reduced and this updated value was calculated by computing the square root of the mean square
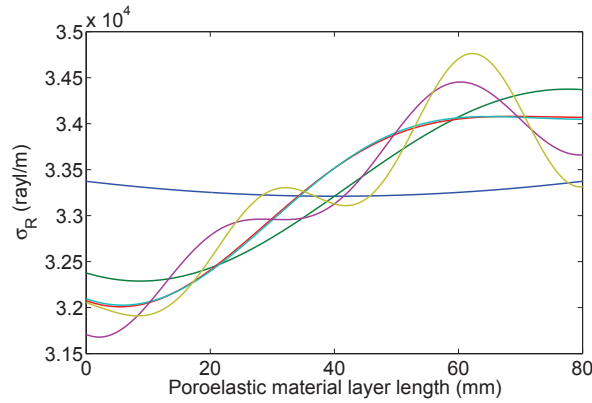
Figure 5.8: Illustration of the first 6 terms of the KL expansion.

value of the realizations divided by the mean, after smoothing.
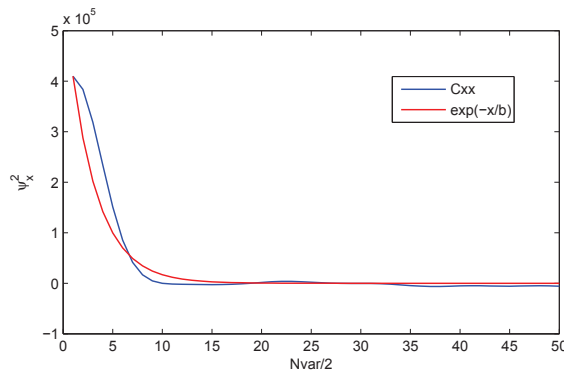
Figure 5.9: Correlation length visual approximation.

The same simulation from Sec. 5.4.1 was performed with KL expansion with 10 modes, 1000 realizations, and a thickness discretization of 20 thin layers. Figu. 5.10 and 5.11 display mean and standard deviation convergence. In this case, convergence is achieved with around 600 realizations. So, the KL expansion with proper truncation allows a faster convergence compared with the direct discretization of the random field.

In Fig. 5.12, mean, confidence interval, and deterministic transmission loss curve are shown. The confidence interval is similar to the one observed in Fig. 5.5 and mean and deterministic curves also diverge in frequencies close to 10^4 Hz.

Fig. 5.13 shows a TL curve calculated with 1% of error in the flow resistivity parameter
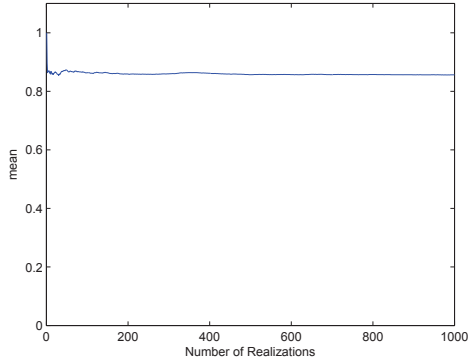
Figure 5.10: Karhunen-Loève mean convergence.
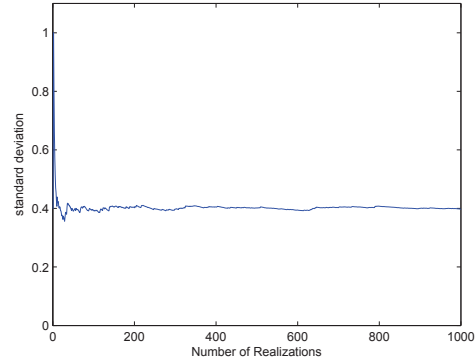
Figure 5.11: Karhunen-Loève standard deviation convergence.

compared with the deterministic TL curve. It is possible to observe that slight variations in the flow resistivity of the layers decrease significantly the TL in high frequencies. This behavior needs to be further investigated.

5.5 Discussion and conclusion

This work aimed at analyzing the influence of parameters variations in the transmission loss curves of poroelastic materials. It was possible to observe that uncertainties influence the acoustic performance, mainly in high frequencies, above 10^3 Hz. The transmission loss curve confidence interval increases dramatically. Comparing direct discretization and Karhunen-Loève expansion with 10 modes, the standard deviation of the TL converges first for the latter. In both simulations, in high frequencies, the mean curve tends to be below the deterministic curve.
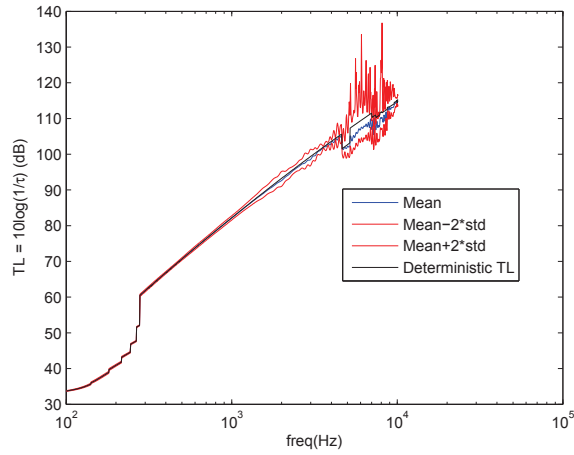
Figure 5.12: Deterministic TL response, Karhunen-Loève simulation mean, and confidence interval.
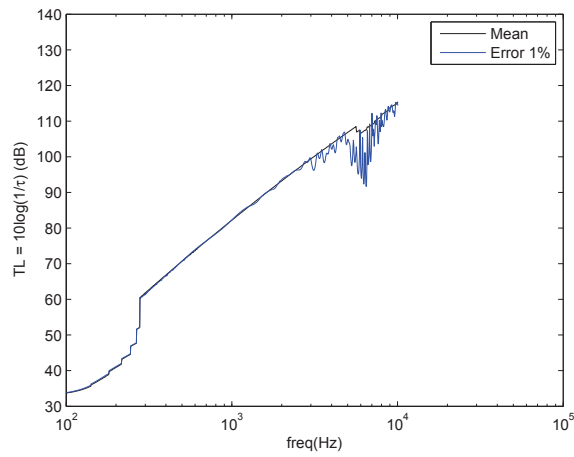
Figure 5.13: Deterministic TL response, Karhunen-Loève simulation mean, and confidence interval.

6 Optimization

6.1 Multi-objective Optimization

Optimize is to select the best element (based on some criteria) from a group of alternatives, is to project something new maximizing its efficiency and minimizing its cost (Deb, 2001). The main goal of an optimization with one objective is to find the global optimum that satisfies all project restrictions. However, in multi-objective problems (Sawaragy *et al.*, 1985), (Chankong e Haimes, 1983) a unique point is not obtained, but a solution set that aims at preserving the diversity of this project (Deb, 2001). Moreover, practitioners deal with variables and objective spaces, what is not trivial when trying to maintain diversity in both of them. Ordinarily, the objectives are conflicting among themselves, therefore an improvement in one dimension does not imply in a general improvement of the other objectives.

Mathematically, a multi-objective optimization problem (MOOP) is defined such as (Deb, 2001):

$$
\begin{aligned}
\text{Minimize/Maximize} \quad & f_m\left(\vec{x}\right), & m &= 1,2,3,\ldots,M; \\
\text{subject to} \quad & g_j\left(\vec{x}\right) \geq 0, & j &= 1,2,3,\ldots,J; \\
& h_k\left(\vec{x}\right) = 0, & k &= 1,2,3,\ldots,K; \\
& x_i^{(L)} \leq x_i \leq x_i^{(U)}, & i &= 1,2,3,\ldots,n.
\end{aligned}
\tag{6.1}
$$

where $\vec{x} = (x_1,x_2,\ldots,x_n)^T$ is the decision variables vector, $x_i^{(L)}$ is x_i lower bound and $x_i^{(U)}$ is its upper bound.

Once the problem is defined, a solution strategy should be defined. There are 3 main approaches (Lobato, 2008):

- *A Posteriori* Methods: they are applied after the optimization process. Pareto criterion is used to identify the optimum solutions set. The objectives are not unified. The preference of one objective in relation to other is established at the end of the optimization process.

- Progressive Methods: they are applied during the optimization process. They consist of Heuristic methods, based on biological evolution principles and models.

- *A Priori* Methods: they are applied before the optimization process. Objectives are weighted,

so one unique objective is obtained. A multi-objective optimization is transformed into an optimization with a unique objective.

6.1.1 Pareto Concept

According to Edgeworth-Pareto (Deb, 2001), (Lobato, 2008) a x^* point is considered an optimum if "none used criterion can improve the solution without worsening at least one criterion". This optimum concept provides a set of non-dominated solutions.

Definition 1: A solution x_1 dominates a solution x_2 if both conditions are satisfied:

○ The solution x_1 is no worse than x_2 in all objectives , or $f_j(x_1) \rhd f_j(x_2)$, for all $j = 1,2,...,M$.

○ The solution x_1 is strictly better than x_2 in at least one objective , or $f_j(x_1) \lhd f_j(x_2)$ for at least one $j \in \{1,2,...,M\}$.

Definition 2: Given a solution set P^1, the non-dominated group P^2 is composed of non-dominated solutions by any P^1 element.

Definition 3: The non-dominated group belonging to the feasible space is called global Pareto optimal.

Definition 4: The Pareto front is composed of the objective functions vector set $f(x) = (f_1(x), f_2(x),...f_M(x))$, for each solution x that belongs to the optimum Pareto set.

The two main metrics used to evaluate multi-objective optimization performance are to find the solutions that are as near as possible to the Pareto front and to obtain the greatest diversity of solutions in the barrier. They are respectively named: convergence and diversity. Figure 6.1 illustrates both metrics. It is important to note that convergence and diversity can be conflicting metrics, so using only one of them does not completely evaluate the algorithm performance (Deb, 2001), (Lobato, 2008). Deb (2001) presents a series of quantitative metrics such as: the error tax, the convergence metric, etc.

86
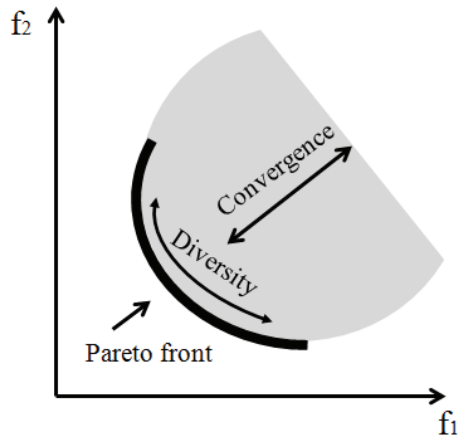
Figure 6.1: Performance metrics of the multi-objective optimization (Reproduced from (Deb, 2001)).

The uncertainties of the models were not included in the optimization. However, in an industrial design process, uncertainties highly affect the final prototype performance, so it is interesting to research a methodology in order to deal with such case in a future work.

6.1.2 Mixed variables optimization

Two types of variables can be present in the an optimization problem: discrete and continuous variables. Discrete variables are generally a code for a finite number of data listed in a database, for instance: possible values of Young's modulus of a mechanical structure element that depends on the material choice, and possible positioning coordinates of a bar that composes a framework. Continuous variables represent the value of the variable itself, for example in a structure, the area, the thickness, etc. Generally, commercial optimization algorithms deal with continuous variables. However they permit the user to modify key functions, by rounding the continuous values generated for the discrete variables, so it becomes a mixed variables algorithm.

6.1.3 Genetic Algorithm (GA)

"Genetic algorithms are search algorithms based on the mechanics of natural selection and natural genetics" (Goldberg, 1989). It finds application in computational science, engineering, economy, mathematics, etc. Genetic Algorithm's main steps are:

1. Initialization: Generate a random population of n individuals, also called chromosomes;

2. Fitness evaluation: Evaluate the fitness $f_m(x)$ of each chromosome x_i in the population;

3. Selection: Select parent chromosomes from the previous population according to their fitness (the better the fitness, the bigger the chance to be selected). The user can choose to include these selected parents in the new population;

4. Crossover: With a crossover probability, combine the parents to form a new population. For example, if parent 1 (p_1) and parent 2 (p_2) are defined such as:

$$
\begin{aligned}
p_1 &= \begin{bmatrix} a & b & c & d & e \end{bmatrix} \\
p_2 &= \begin{bmatrix} 1 & 2 & 3 & 4 & 5 \end{bmatrix}
\end{aligned}
\tag{6.2}
$$

a possible child resultant from the crossover is:

$$
child1 = \begin{bmatrix} a & 2 & 3 & d & 5 \end{bmatrix}
\tag{6.3}
$$

5. Mutation: With a mutation probability, mutate parents to generate children. To mutate means to create different values to the chromosome genes. For instance, *child2* can be generated from the mutation of parent 1, such as follows:

$$
child2 = \begin{bmatrix} g & b & c & d & e \end{bmatrix}
\tag{6.4}
$$

This step helps on guaranteeing the population diversity.

6. Replace: Use the new population in a new iteration;

7. Test: If the end condition is satisfied, stop and return the best solution;

8. Loop: Go back to Step 2.

Genetic algorithms tend to be computationally expensive and generations number; time limit, and fitness limit are the most used stopping criteria. An important variable that influences simulation time is the population size. Tanneau *et al.* (2006) state that the population size should be between 50 and 100 in order to guarantee diversity. However, the bigger the population, the higher the computational cost.

The genetic algorithm is sensitive to the initial population, to the mutation and the crossover rates, and to the population size, as stated before. Therefore, a sensitivity analysis was made and the best combination among these criteria was established:

○ Initial population randomly generated;

○ 80% of crossover rate;

○ 20% of mutation rate;

○ population size of 100 individuals.

With this arrangement, diversity and convergence could be clearly observed in the Pareto front.

6.2 Multi-objective optimization advantages

In this work, multi-objective optimization was developed using Matlab® Optimization Toolbox, modifying creation, crossover and mutation functions in order to deal with mixed variables. The discrete variables were derived from rounding the continuous variables.

To evaluate the algorithm, the work from Olivier Tanneau was used as basis for comparison (TANNEAU, 2004), (TANNEAU *et al.*, 2006). It optimizes a multilayered acoustic panel, having as criteria the transmission loss (E) and the mass (G). However, it consists in an *a Priori*, or in a single-objective optimization, because the objective function is calculated doing $F = E + k.G$, where k is a weighting factor. The chromosome is defined as:

$$[M_1 \quad e_1 \quad M_2 \quad e_2 \quad ... \quad M_n \quad e_n]$$ (6.5)

where M is the material type code, a discrete variable, e is the layer thickness, a continuous variable, and n is the number of layers. In the database, there are 11 materials: air, steel, aluminum, heavymass, rubber, glass wool 1, glass wool 2, foam 1, foam 2, foam 3, and foam 4. Moreover, objectives are established for mass and TL. For the mass, $M_{obj} = 5kg/m^2$ and the mass score (G) is calculated as detailed in Eq. 6.6.

$$
\begin{aligned}
G_i &= 0 & if \quad M_i < M_{obj} \\
G_i &= log_{10}\left(\frac{M_i}{M_{obj}}\right) & if \quad M_i \geq M_{obj}
\end{aligned}
\tag{6.6}
$$

For the acoustic criterion, on each octaveband an objective TL (TL_i^{obj}) is defined. The TL of each individual is evaluated for three frequencies in each octaveband, providing a mean value TL_i that is compared to TL_i^{obj}. This number of points was arbitrarily chosen. The acoustic score (E_i) of each bandwidth is calculated as shown in Eq. 6.7. The final acoustic score (E) is calculated by doing: $E = max(E_i)$.

$$
\begin{aligned}
E_i &= 0 & if \quad TL_i > TL_i^{obj} \\
E_i &= TL_i^{obj} - R_i & if \quad TL_i \leq TL_i^{obj}
\end{aligned}
\tag{6.7}
$$

A panel with seven layers and total thickness fixed at $80mm$ is optimized. A frequency range between 112 and 11200 Hz is randomly chosen, and incidence angles between 0 and 80 degrees are considered.

In order to compare the single and the multi-objective optimizations, the same case was simulated, first with a bi-objective optimization, and after with single-objective objective analyses and varying k value. Pareto front and single-objective optimal solutions are observed in Fig. 6.2. Is is clear to see that single-objective optimal solutions are contained in the Pareto front. Talking about the single-objective analysis, increasing k value, the solution tends to the top left of the Pareto curve, because more importance is given to the mass criterion. Moreover, the opposite happens if k value decreases. It is possible to conclude that the bi-objective modeling, provides to decision makers an optimal solutions set that contains diversity among the individuals. Based on that, and adding their concerns in the decision moment, they can choose the best solution.
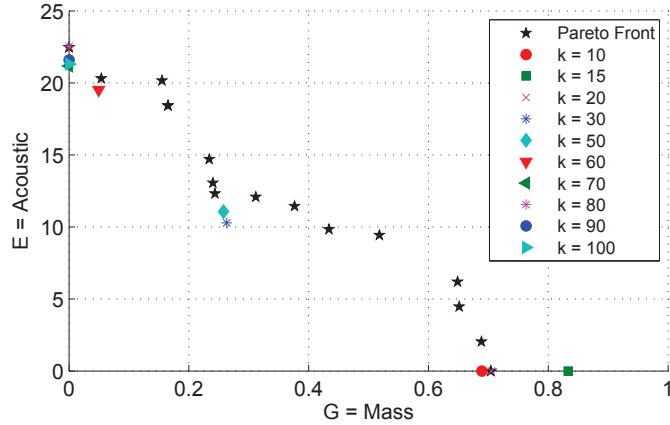
Figure 6.2: Pareto Front and single-objective optimization results.

| Layer | (Tanneau *et al.*, 2006) | | Single-objective | |
	Material	Thickness (mm)	Material	Thickness (mm)
1	Loaded rubber	4	Heavy mass	4.9
2	Foam 3	32.6	Glass Wool 1	14.2
3	Air	0.8	Air	9
4	Foam 3	22.2	Glass Wool 1	18.5
5	Foam 2	7	Glass Wool 1	12.6
6	Heavy mass	3.8	Heavy mass	6.1
7	Glass wool 1	9.6	Foam 3	11.3
Total Thickness		80		76.6
Score		14.3095		6.7662

Table 6.1: Comparison between Tanneau *et al.* (2006) and the single-objective algorithm solutions.

In Tab. 6.3 the multilayered panel solution provided by the single-objective optimization with $k = 10$ is compared with Tanneau *et al.* (2006) result. The score represents the objective function ($F = E + k.G$) value. We can see that the solutions are not exactly the same, however they present the same tendency: the first layer is a thin elastic solid, the third layer is fulfilled by air, the sixth layer is again a thin elastic solid, and the other layers are composed of Foam 3, Foam 2, and Glass Wool 1. Moreover, Foam 2 is not present in the single-objective solution, however there is an infinite number of combinations that result in the defined limits. The advantage of the single-objective solution is that its score is less then half of Tanneau *et al.* (2006) solution score.

Figure 6.3 displays a comparison between Tanneau *et al.* (2006) and the single-objective

transmission loss curves. For each solution, the TL curves in 1/3 octave bands are displayed, so it is easier to analyze their performance in relation to the objective TL. As expected from the score values observed in Tab. 6.3, in the acoustic criterion, the single-objective optimal solution presents a better performance. The final panels' masses are: $4.5490kg/m^{-2}$ for Tanneau *et al.* (2006) solution and $8.9271kg/m^{-2}$ for the single-objective optimal solution. So, the single-objective solution presents a worse mass score, justifying the smaller TL difference.
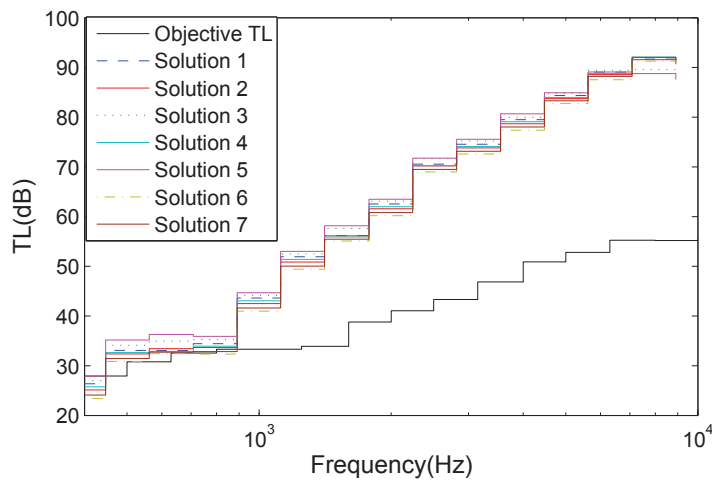
Figure 6.3: Comparison between the TL of (TANNEAU *et al.*, 2006) and the single-objective algorithm solutions.

So it was possible to observe that a multi-objective optimization provides a set of solutions distributed along the Pareto front. Observing this curve, solutions with better performance in one objective and worse in the other can be selected. If weighting is made before the optimization, it is not possible to obtain the diversity of solutions present in the Pareto front.

After concluding that the developed algorithm was able to provide good optimal solutions, in relation to this case presented in the literature, the analysis of the real case study was performed.

6.3   Real case analysis

The real case study consists of optimizing the product presented in Chapter 4, maximizing its transmission loss and minimizing its environmental impact. The acoustic and the environmental models descriptions are detailed in Chap. 2 and 4, respectively.

6.3.1   Surface Response

As the optimization tool was developed in Matlab® environment, the environmental model needed to be integrated in it.

To integrate *SimaPro®* with Matlab®, a surface response model was developed. Ten thickness points were used for the adjustment and the best polynomial degree was chosen according to the model error. Figure 6.4 shows the quadratic error of the Global Worming surface response in function of the polynomial degree.
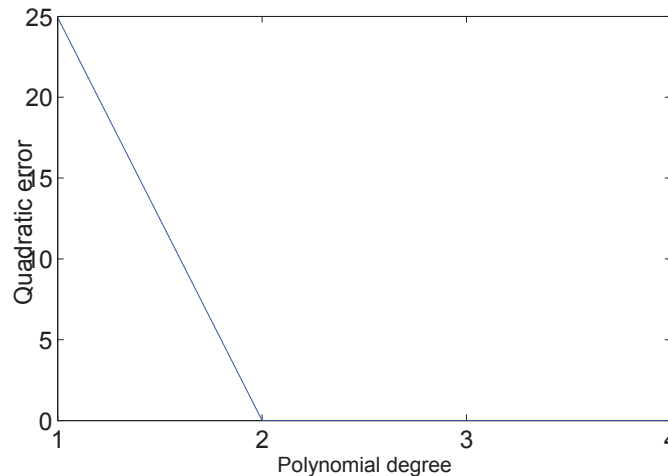
Figure 6.4: Surface response error in function of the polynomial degree.

At this point, a simplification was made: the environmental impact of the multilayered panel was calculated as the sum of the impacts of each one of its layers. So, even with surface response errors in the 10^{-8} order, around 15% of error was obtained in the multilayered panel impact calculation.

Observing Fig. 6.4 it is possible to conclude that the second degree polynomial was able to fit the *SimaPro®* model, for the felt and for the mineral layers. The same analysis was made for the other two impact categories and the same polynomial was also the best adjustment.

6.3.2 Objective functions

The acoustic score is calculated as shown in in Eq. 6.8, however the experimental DL-cotton TL provided by *General Motors*® was chosen as the TL_{obj}, because this is the most modern dash produced by *Coplac*®, and the less environmentally impacting. The objective TL stairs graph is shown in Fig. 6.5, where vertical axis values are not shown for confidentiality reasons.

$$
\begin{aligned}
E_i &= 0 & if \quad TL_i &> TL_i^{obj} \\
E_i &= TL_i^{obj} - R_i & if \quad TL_i &\leq TL_i^{obj}
\end{aligned}
\qquad (6.8)
$$
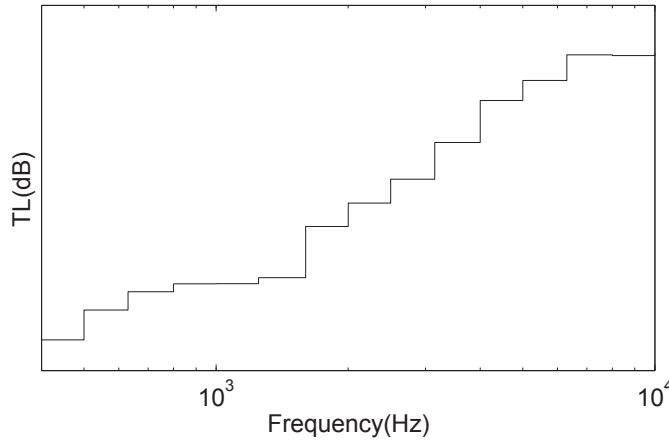
Figure 6.5: Acoustic criterion of the optimization, the experimental DL-cotton panel TL curve.

In this optimization the absorption behavior is not considered. For its calculation a different configuration is necessary, so the TL computation cannot be used. Therefore, considering the absorption performance doubles the computational cost of the acoustic criteria calculation.

Three impact categories were chosen for the optimization, instead of considering the seven criteria from Chap. 4. Global Warming (GW) was selected because of its importance for the automotive industry, and Abiotic Depletion (AD) and Fresh Water Aquatic Ecotoxicity (FWAE) were chosen due to global concerns in general and Brazilian concerns in particular. The environmental score is also calculated as shown in Eq. 6.6, for each impact category. Objectives for GW, AD, and FWAE environmental criteria were settled as detailed in Eq. 6.9. These are results for the DL-cotton multilayered panel, already presented in Chap. 3. However, during the optimization, solutions eas-

ily achieved the objectives for AD and FWAE. Therefore, the analysis was made considering only the GW environmental criterion.

$$[GW_{obj} \quad AD_{obj} \quad FWAE_{obj}] \quad = \quad [287.7 \quad 1.8 \quad 11.4] \qquad (6.9)$$

The environmental score is calculated as shown in Eq. 6.10, where $GW_{obj} = 287.7 kgCO_2 eq..$

$$\begin{aligned} G_i &= 0 & if \quad GW_i &< GW_{obj} \\ G_i &= log_{10}\left(\frac{GW_i}{GW_{obj}}\right) & if \quad GW_i &\geq GW_{obj} \end{aligned} \qquad (6.10)$$

6.3.3 Design variables

The optimization is limited by the following design variables:

○ Maximum multilayered panel thickness settled of $30mm$.

○ A fixed number of 7 layers was established.

○ A database containing 7 materials was provided.

Table 6.2 contains the 7 materials and their respective properties. Moreover, Fig. 6.6 shows the materials' color map that is used when displaying the solutions in the following section. The chromosome was coded as described in Eq. 6.5.

6.3.4 Results

The Pareto front of the real case study is presented in Fig. 6.7. The algorithm aims at filling with points the curve that connects two extreme solutions: null GW and null TL. The vertical axis is log scaled and the horizontal axis represents the maximum difference between the objective and the solution TL, therefore, its scale unit is dB. The DL-cotton and the ABA-cotton panels are included

Material	ϕ_P	σ_R	α_∞	Λ	Λ'	ρ	E	ν	η	c_0
Unit		$N.s/m^4$		μm	μm	Kg/m^3	Pa			m/s
Air	-	-	-	-	-	1.225	-	-	-	342
Loaded rubber	-	-	-	-	-	1240.9	$14.4.10^6$	0.3	0.123	-
Glass Wool 1	0.98	35.10^3	1	60	150	9.5	10.10^3	0	0.2	-
Foam 1	0.81	55.10^4	1.5	10.5	31.5	211	344.10^3	0.33	0.15	-
Intermediate felt	0.98	20.10^3	1	29	163	72	10.10^3	0	0.05	-
Hard felt	1	20.10^4	1	14	42	220	10.10^4	0	0.1	-
Soft felt	1	34.10^3	1	35	150	99.3	17.10^4	0	0.15	-

Table 6.2: Real case materials' database and their properties.
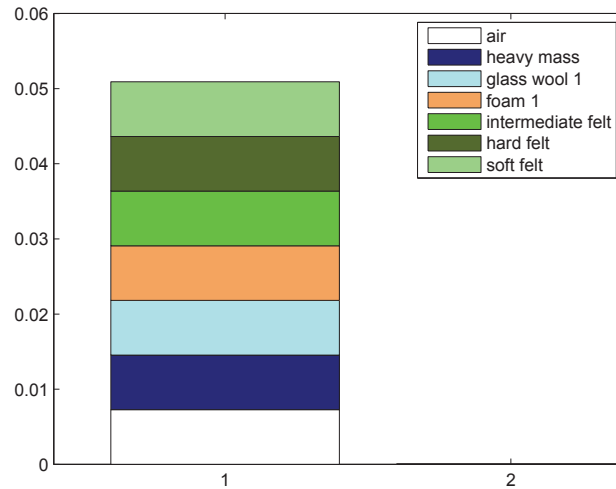
Figure 6.6: Real case database and materials' color map.

in Fig. 6.7, however their environmental and acoustic scores do not permit them to be part of the Pareto front. This means that the optimal set has better scores then these panels. Theoretically, the DL-cotton panel should be located in the horizontal axis, because its environmental performance was chosen as the objective value. However, the surface response model calculated the DL-cotton panel environmental score with 15% of error. So as the the adopted environemtal objective is lower then the DL-cotton panel performance calculated through the surface response, it is siffer then the DL-cotton score.

Analyzing the acoustic criterion, listeners are sensitive to a TL difference of 5dB. Therefore, the twelve solutions with a TL difference below 5dB were analyzed in detail. Their acoustic and

environmental linear scores and their total thicknesses are listed in Tab. 6.3.

Figure 6.7: Pareto front of TL vs GW optimization of the real case study.

Solutions of Tab. 6.3 are listed in a increasing acoustic score order, such as observed in the Pareto front of Fig. 6.7, from the left to the right. It is possible to observe that the lower the acoustic value, the higher the environmental one, what shows the optimizat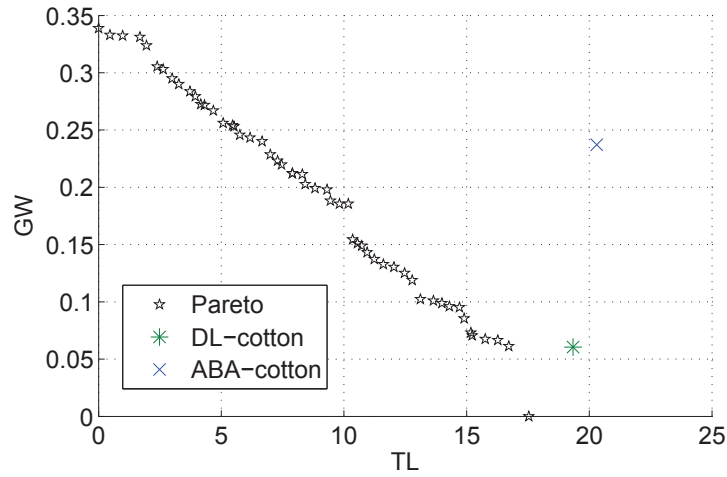ion duality between these objective functions. The thicknesses of solution 1 is larger than $30mm$ that was the maximum established for this optimization. However, numerical approximations of the results compilation can generate small variations of these values, and, in practice, a tolerance is settled for the thickness of the panel.

Figure 6.8 shows three material sequences observed in the solutions. The combination 1 is related to solutions 1, 3 and 5, the combination 2 is the material sequence of solutions 2 and 4 and the other solutions follow the combination 3. They only apply the recycled cotton foams and the loaded rubber materials, combined with air gaps, as observed in the unique objective solution of Sec. 6.2.

Figure 6.9 displays the objective TL and the multi-objective optimal solutions' TL curves, all in function of third octavebands. All the twelve solutions present a better TL performance up to 1000 Hz, but in lower frequencies, with the exception of Solution 1, all solutions have worse acoustic performance then TL objective, and this is why they do not have null acoustic score.

In Tab. 6.4, the thicknesses of the layers of the multi-objective optimal solutions are listed.

Solution	Acoustic score (dB)	Environmental score (kg CO_2 eq.)	Thickness (mm)
1	0	628.7619	30.3
2	0.4650	620.3130	30.0
3	0.9786	619.4215	29.8
4	1.6851	617.6424	27.1
5	1.9520	607.4189	27.3
6	2.3903	580.3013	29.1
7	2.6313	577.1882	27.7
8	2.9984	568.7172	26.2
9	3.2736	562.0463	24.7
10	3.9469	548.2311	27.8
11	4.1671	537.9831	29.6
12	4.3174	536.6480	29.1

Table 6.3: Linear scores and total thicknesses of the real case study solutions.

The thicknesses sequence observed from solutions 1 to 5 form a pattern, with the exception of layer 4 that is an air gap. Another pattern is observed from solutions 6 to 12.

It is curious to note the inversion of the loaded rubber position from combinations 1 and 2 to combination 3. In combinations 1 and 2, the noise achieves the recycled cotton layers and the air gaps, and finally the loaded rubber. The opposite way happens in combination 3. The loaded rubber is important in the transmission loss performance of the panel, and generally it is the first layer faced by the noise and it tries to prevent the sound waves passage. After passing, the noise is absorbed by the foam layers, as observed in the DL panel model. However, in this optimization, the absorption behavior was not considered, so the designer cannot know the solutions absorption performance by checking the Pareto front. With this purpose, a detailed analysis would be required. At that time, adding absorption criteria to the optimization would be an interesting strategy.

The scores observed in Tab. 6.3 for solutions 6 to 12 show that combining the same materials, in the same sequence, it is possible to obtain completely different scores, only by varying the material quantity of each layer.
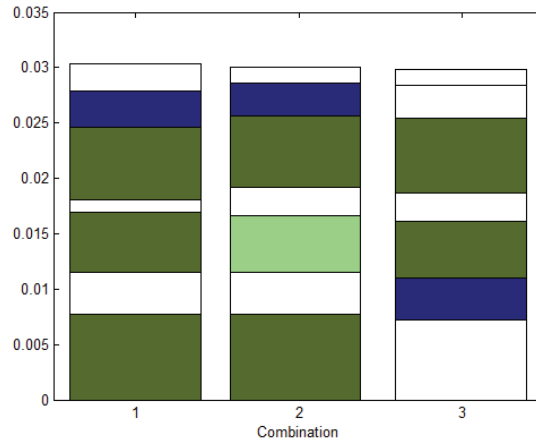
Figure 6.8: Materials' sequences of the multi-objective optimal solutions with TL difference lower than 5 dB. Combination 1: solutions 1, 3, and 4; combination 2: solutions 2 and 4, the remaining solutions follow combination 3.
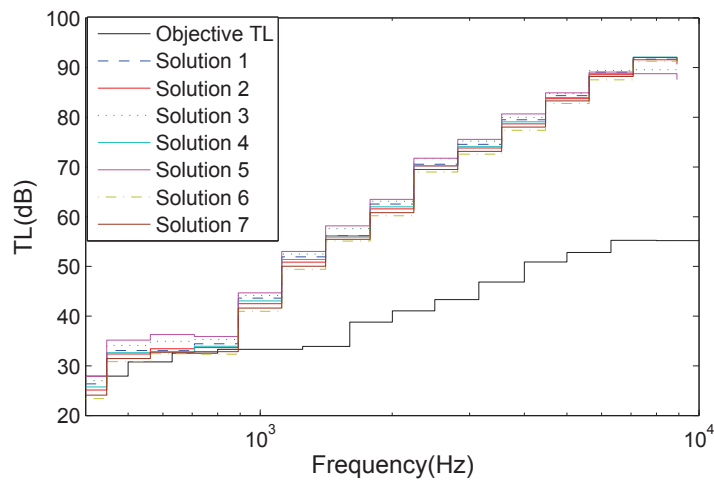
Figure 6.9: Comparison among the multi-objective optimal solutions and the objective TL curve.

Solution	Layer 1	Layer 2	Layer 3	Layer 4	Layer 5	Layer 6	Layer 7
1	7.7	3.8	5.4	1.2	6.5	3.3	2.4
2	7.7	3.8	5.1	2.6	6.4	3.0	1.4
3	7.2	3.8	5.1	2.6	6.7	3.0	1.4
4	7.1	3.8	5.1	0.3	6.4	3.0	1.4
5	7.7	3.8	4.8	0.3	6.8	2.4	1.5
6	0	7.0	6.4	4.9	7.4	2.0	1.4
7	0	7.0	6.0	4.7	7.1	1.4	1.5
8	0	6.5	6.3	3.2	7.4	1.4	1.4
9	0	6.5	6.3	3.2	5.9	1.4	1.4
10	0	5.7	6.0	4.7	7.1	2.3	2.0
11	0	5.0	6.9	4.9	7.4	3.9	1.5
12	0	5.0	6.9	4.7	7.1	3.9	1.5

Table 6.4: Thicknesses (mm) of the layers of the multi-objective optimal solutions.

7 Conclusion

This work aimed at developing a methodology that could help designers to include environmental criteria in the design phase of an acoustic panel applied in passenger vehicles. Without any design methodology, designers tend to follow their previous experience, generally choosing solutions that are similar to existing ones.

The advantages of this design methodology are:

- to quantitatively evaluate the design criteria, based on theoretical models;

- the diversity among the solutions set that can provide unexpected and innovative solutions;

- other objectives can be included in the analysis, such as: cost, social impact, etc. and a Pareto front with more dimensions will be generated;

- to join all criteria scores in a single Pareto front, making easier the developer's choice;

- this idea can be applied to any other product design, provided a numerical model can be used to calculate its performance.

After selecting optimal solutions from the Pareto front, the design team can evaluate them more in detail, in order to combine the quantitative scores with others, and finally choose the best panel design solution.

The real case study could be explored in detail. The acoustic performances of the DL-cotton and the ABA-cotton panels were compared in Chap. 2, based on the Equivalent Fluid acoustic model. The DL-cotton panel has the best blocked and free absorption behaviors, while in high frequencies the transmission loss curve of the ABA-cotton panel is significantly higher then the DL-cotton panel one. However, as when the panel is installed in the vehicle a combination between these two performances is required, after making tests in a vehicle prototype, the automaker decided that the DL-cotton panel is able to provide adequate sound comfort for the passenger.

The environmental performance of the real case study was analyzed in Chap. 4. With the LCA of DL-PU, ABA-cotton, and DL-cotton panels it was possible to observe that the design

evolution of the panel really guaranteed an improvement in its environmental impact, mainly due to the decrease of its weight. Moreover, advantages of the replacement of synthetic materials by recycled natural fibers cannot be neglected. However the end-of-life phase can still be improved by the incineration with energy recovery or by the reuse of the cotton fibers reinforced composite material in the own *Coplac*® production of acoustic panels or other products.

The preliminary uncertainty analysis performed in this work allowed to show how the manufacturing tolerances can modify the final conclusions related to the comparison among different design solutions. Furthermore, when including in the models more variations that are implicit in the production process of the acoustic panel, their influence in the results tends to increase, and the design team needs to be aware of that. A more thorough uncertainty analysis of both acoustic properties and LCA is recommended.

Observing the developed work, it is possible to say that its main objective was achieved. Moreover secondary works could also be derived from the thesis, such as: the acoustic and the environmental models uncertainty analysis and the poroelastic material inverse characterization methodology, which is still under development.

7.1 Future work

Future works that derived from this work are listed below:

1. As the acoustic model can also calculate the multilayered panel absorption, this performance could be easily included in the optimization analysis. A combination of absorption and transmission loss could be relevant for the automaker. However, one more criterion would increase the computational cost of the optimization.

2. In the acoustic model uncertainty analysis, the ideal would be to evaluate the influence on the transmission loss curve of the material properties, the layers' sequence, and the layers' thickness.

3. It would be interesting to search a way how to include uncertainties in the optimization analysis and in the Pareto front result.

4. It would be interesting to investigate why slight variations in the flow resistivity of the layers decrease significantly the TL curve in high frequencies.

7.2 Publications

The publications that occurred during this work are listed below.

1. PEGORETTI, T. S., MATHIEUX, F., EVRARD, D., BRISSAUD, D., ARRUDA, J. R. F., Use of recycled natural fibres in industrial products: A comparative LCA case study on acoustic components in the Brazilian automotive sector. Resources, Conservation and Recycling., v.84, p.1 - 14, 2014.

2. PEGORETTI, T. S., MACHADO, M. R., ARRUDA, J. R. F., dos SANTOS, J. M. C., Uncertainties in poroelastic materials' acoustic performance, Uncertainties 2014, Rouen, 2014.

3. PEGORETTI, T. S., CÓSER, L. F. , SIVIERO, D, HUALLPA, B. N., ARRUDA, J. R. F., LAMARY, P., Inverse characterization of acoustic poroelastic materials using an impedance tube: numerical issues. 14th Pan-American Congress of Applied Mechanics, Santiago, 2014.

4. SANTOS, T. B., ARRUDA, J. R. F., BRISSAUD, D., Treating input data uncertainty in LCA: Monte Carlo and Fuzzy approaches. 4th International Workshop - Advances in Cleaner Production, São Paulo, 2013.

5. SANTOS, T. B., ARRUDA, J. R. F., EVRARD D., BRISSAUD, D., Uncertainty evaluation of LCA models input data using Monte Carlo Method. 6th SETAC World Congress / SETAC Europe 22nd Annual Meeting, Berlin, 2012.

6. SANTOS, T. B., ARRUDA, J. R. F., BRISSAUD, D., Methodology Development to consider Uncertainties in Life-Cycle Assessment. Uncertainties 2012, Maresias, 2012.

7. LAMARY, P., SOUZA NETO, S. L., ARRUDA, J. R. F., SANTOS, T. B., Perforated resonaors and natural fibers for acoustic absorbing applications. COBEM - International Congress of Mechanical Engineering, Natal., 2011.

8. MACHADO, M. R., dos SANTOS, J. M. C., SANTOS, T. B., ARRUDA, J. R. F., Reliability analysis using simple models aiming at a comparison among stochastic methods. ICSV18 - International Congress of Sound and Vibration, Rio de Janeiro, 2011.

9. SANTOS, T. B., ARRUDA, J. R. F., Stochastic analysis for simple and computationally efficient models for tire non-uniformity investigation. International Conference on Noise and Vibration Engineering, Leuven. Proceedings of ISMA 2010., p.5181 - 5194, 2010.

References

ADHIKARI, S. e FRISWELL, M.I. Distributed parameter model updating using the karhunen-loève expansion. **Mechanical Systems and Signal Processing**, v. 24, 326–339, 2010.

AFNOR**Repository of good practices. General principles for an environmental communication on mass market products. Part 0: General principles and methodological framework. BPX-30-310**. Paris. 2011.

ALLACKER, K.; MATHIEUX, F.; MANFREDI, S.; PELLETIER, N.; CAMILLIS, C.D.; ARDENTE, F. e PANT, R. Allocation solutions for secondary material production and end of life recovery: proposals for policy initiatives. **Resources Conservation and Recycling**, v. 88, 1–12, 2014.

ALLARD, J.F. **Propagation of sound in porous media: Modelling sound absorbing materials**. Elsevier Applied Science, 1993.

ALLARD, J.F. e ATALLA, N. **Propagation of Sound in Porous Media Modelling Sound Absorbing Materials**. John Wiley and Sons, 2009.

ALVES, C.; AO, P.M.C.F.; SILVA, A.J.; REIS, L.G.; FREITAS, M.; RODRIGUES, L.B. e ALVES, D.E. Ecodesign of automotive components making use of jute fiber composites. **Journal of Cleaner Production**, v. 18, 313–327, 2010.

ANEEL. Management information bank. 2012.
URL: *http://goo.gl/LDDTr0*

ATALLA, Y. e PANNETON, R. Inverse acoustical characterization of open cell porous mecia using

impedance tube measurements. **Canadian Acoustics**, v. 33, 11–24, 2005.

BARRON, R.F. **Industrial Noise Control and Acoustics**. Marcel Dekker Inc, New York, 2003.

BOUSTEAD, I. Lca - how it came about, the beginning in the uk. **International Journal of Life cycle Assessment**, v. 3, 147–150, 1996.

CHANKONG, V. e HAIMES, Y.Y. **Multiobjective Decision Making: Theory and Methodology**, v. 8. Elsevier Science Publishing Co., 1983.

COMISSION, E. **ILCD Handbook. Framework and Requirements for LCIA models and indicators.** EC- JRC, 2010.
URL: *http://lct.jrc.ec.europa.eu*

COMMISSION, E. **ANNEX II : PRODUCT ENVIRONMENTAL FOOTPRINT (PEF) GUIDE to the COMMISSION. RECOMMENDATION on the use of common methods to measure and communicate the life cycle environmental performance of products and organisations. European**. 2013a.
URL: *http://goo.gl/byjy2c*

COMMISSION, E. **Communication from the Commission to the European Parliament, The Council, The European Economic and Social Committee and the Committee of the Regions: "Building the Single Market for Green Products Facilitating better information on the environmental performance of products and organizations".** Brussels. 2013b.

CORBIÈRE-NICOLLIER, T.; LABAN, B.G.; LUNDQUIST, L.; LETERRIER, Y.; MÂNSON, J.A.E. e JOLLIET, O. Life cycle assessment of biofibres replacing glass fibres as reinforcement in plastics. **Resources Conservation and Recycling**, v. 33, 267–287, 2001.

DAUCHEZ, Nicolas. **Étude Vibroacoustique des Matériaux Poreux par Éléments Finis**. 1999. Tese (Doutorado). Université du Maine and Université de Sherbrooke.

DEB, K. **Multi-objective Optimization using Evolutionary Algorithms**. 2001.

DETRAN. Frota 2013. April 2013.
URL: *http://goo.gl/GoUzTv*

DIGEST., B. Brazil decides to stay at 20in 2012. 2012.
URL: *http://goo.gl/YK1Elr*

DUFLOU, J.R.; MOOR, J.D.; VERPOEST, I. e DEWULF, W. Environmental impact analysis of composite use in car manufacturing. **Manufacturing Technology**, v. 59, 9–12, 2009.

EDER, W.E. Design modelling - a design science approach (and why does industry not use it?). **Journal of Engineering Design**, v. 9, 355–371, 1998.

EICKER, M.O.; HISCHIER, R.; HURNI, H. e ZAH, R. Using non-local database for the environmental assessment of industrial activities: The case of latin america. **Environ Impact Assessment Review**, v. 30, 145–157, 2009.

FARINELLI, B.; CARTER, C.A.; CYNTHIA, L.C.Y. e SUMNER, D.A. Import demand for brazilian ethanol: a cross-country analysis. **Journal of Cleaner Production**, v. 17, S9–S17, 2009.

FROELICH, D.; MARIS, E.; HAOUES, N.; CHEMINEAU, L.; RENARD, H.; ABRAHAM, F. e LASSARTESSES, F. State of the art of plastic sorting and recycling: Feedback to vehicle design. **Minerals Engineering**, v. 20, 902–912, 2007.

GHANEM, R.G. e SPANOS, P.D. **Stochastic Finite Elements A Spectral Approach**. Dover Publications INC, 2003.

GOEDKOOP, M.; OELE, M.; DE SCHRYVER, A. e VIEIRA, M. **SimaPro 7 Database Manual Methods Library**. Pré Consultants, May 2008.
URL: *http://goo.gl/hBKClf*

GOLDBERG, D.E. **Genetic Algorithms in Search, Optimization, and Machine Learning**. Addison-Wesley Publishing Company Inc., 1989.

HUISMAN, J.; BOKS, B. e STEVELS, A. Quotes for environmentally weighted recyclability - the concept of describing product recyclability in terms of environmental value. **International Journal of Production Research**, v. 41, 3649–3665, 2003.

IBGE. National survey of basic sanitation. 2000.
URL: *http://goo.gl/AEOms4*

IBGE. Municipal agricultural production - temporary and parmanent crops. 2010.
URL: *http://goo.gl/yvorJ1*

ISO**ISO 22628 Road vehicles - Recyclability and recoverability - Calculation method.** 2002.

ISO**ISO 14040 Environmental management - Life cycle assessment - Principles and framework**. 2006a.

ISO**ISO 14044 Environmental management - Life cycle assessment - Requirements and guidelines**. 2006b.

JENSEN, A.A.; HOFFMAN, L.; MOLLER, B.T.; SCHMIDT, A.; CHRISTIANSEN, K.; ELKINGTON, J. e SUSTAINABILITY. **Life Cycle Assessment A guide to approaches, experiences and information sources**. European Environment Agency, 6 ed., August 1997.

JOHN, M.J. e THOMAS, S. Biofibres and biocomposites. **Carbohydrate Polymers**, v. 71, 343–364, 2008.

JONES, J.C. **Design methods**. John Wiley & Sons, 1992.

KINSLER, L.E. **Fundamentals of Acoustics**. John Wiley & Sons, 1982.

KOMLY, C.E.; AZZARO-PANTEL, C.; HUBERT, A.; PIBOULEAU, L. e ARCHAMBAULT, V. Multiobjective waste management optimization strategy coupling life cycle assessment and genetic algorithms: Application to pet bottles. **Resources Conservation and Recycling**, v. 69, 66–81, 2012.

LAMARY, P.; NETO, S.L.S.; ARRUDA, J.R.F.; SANTOS, T.B. e MATHIEUX, F. Perforated ressonators and natural fibers for acoustic absorbing applications. COBEM, Natal, 2011.

LEE, J.S. e KIM, Y.Y. Optimal poroelastic layer sequencing for sound transmission loss maximization by topology optimization method. **Journal of Acoustical Society of America**, v. 122, 2097–2106, 2007.

LIND-NORDGREN, E. e GORANSSON, P. Optimising open porous foam for acoustical and vibrational performance. **Journal of Sound and Vibration**, v. 329, 753–767, 2010.

LOBATO, F. S. **Otimização multi-objetivo para o projeto de sistemas de engenharia**. 2008. Tese (Doutorado). Universidade Federal de Uberlândia, Uberlândia.

LUZ, S.; PIRES, A.C. e AO, P.M.F. Environmental benefits of substituting talc by sugarcane bagasse fibers as reinforcement in polypropylene composites: Ecodesign and lca strategy for automotive components. **Resources, Conservation and Recycling**, v. 54, 1135–1144, 2010.

MATHIEUX, F. e BRISSAUD, D. End-of-life product-specific material flow analysis. application to aluminum coming from end-of-life commercial vehicles in europe. **Resources Conservation and Recycling**, v. 55, 92–105, 2010.

MATHIEUX, F.; FROELICH, D. e MOSZKOWICZ, P. Resicled: a new recovery-conscious design method for complex products based on a multicriteria assessment of the recoverability. **Journal of Cleaner Production**, v. 16, 277–298, 2008.

MOORE, B.C.J. e GLASBERG, B.R. A revision of zwicker's loudness model. **Acta Acustica united with Acustica**, v. 82, 335–345, 1996.

MUNOZ, I.; RIERADEVALL, J.; DOMÉNECH, X. e GAZULLA, C. Using lca to assess eco-design in the automotive sector case study of a polyolefinic door panel. **International Journal of Cleaner Production**, v. 5, 323–334, 2006.

NIEDERL-SCHMIDINGER, A. e NARODOSLAWSKY, M. Life cycle assessment as an engineer′s tool? **International Journal of Cleaner Production**, v. 16, 245–252, 2006.

OESP. Country searches more natural fibres for cars. economy. p. b11. 2004.
URL: *http://pib.socioambiental.org/es/noticias?id=37647*

PAHL, G. e BEITZ, W. **Emgineering Design A Systematic Approach**. Springer-Verlag, 1992.

PAPOULIS, A. e PILLAI, S.U. **Probability,Random Variables and Stochastic Processes**. McGraw-Hill, 2002.

PARLIAMENT, E. **DIRECTIVE 2000/53/EC OF THE EUROPEAN PARLIAMENT AND OF THE COUNCIL of 18 September 2000 on end-of life vehicles**. Official Journal of the European Communities, september 2000.

POIRION, F. e SOIZE, C. Monte carlo construction of karhunen loeve expansion for non-gaussian random fields. In N. Jones e R. Ghanem, editores, **13th ASCE Engineering Mechanics Division Conference**. Baltimore, 1999.

POLAK, P. **A Background to Engineering Design**. The Macmillan Press LTD, 1976.

PURI, P.; COMPSTON, P. e PANTANO, V. Life cycle assessment of australian automotive door skins. **International Journal of Life Cycle Assessment**, v. 14, 420–428, 2009.

RIBEIRO, F.M. e SILVA, G.A. Life-cycle inventory for hydroeletric generation: a brazilian case study. **International Journal of Cleaner Production**, v. 18, 44–54, 2009.

RUBINSTEIN, R.Y. e KROESE, D.P. **Simulation and the Monte Carlo Method**. John Wiley & Sons, USA, 2008.

SANDER, K. e MURTHY, G.S. Life cycle analysis of algae biodiesel. **International Journal of Life Cycle Assessment**, v. 15, 704–714, 2009.

SANTOS, T.B.; ARRUDA, J.R.F. e BRISSAUD, D. Treating input data uncertainty in lca: Monte carlo and fuzzy approaches. In **4th International Workshop Advances in Cleaner Production**. São Paulo, May 2013.

SAWARAGY, Y.; NAKAYAMA, H. e TANINO, T. **Theory of Multiobjective Optimization**. Academic Press Inc., Florida, 1985.

SCHEVENELS, M.L.; LOMBAERT, G. e DEGRANDE, G. Application of the stochastic finite element method for gaussian and non-gaussian systems. In **Proceeeding of ISMA**. 2004.

SCHMIDT, W.P.; DAHLQVIST, E.; FINKBEINER, M.; KRINKE, S.; LAZZARI, S.; OS-CHMANN, D.; PICHON, S. e THIEL, C. Life cycle assessment of lightweight and end-of-life scenarios for generic compact class passenger vehicles. **International Journal of Life Cycle Assessment**, v. 6, 405–416, 2004.

SETAC. **Life Cycle Assessment Data Quality: A Conceptual Framework**. SETAC - Society of Environmental Toxicolgy and Chemistry, USA, October 1992.

SETAC. **A Conceptual Framework For Life-Cycle Impact Assessment**. SETAC - Society of Environmental Toxicolgy and Chemistry, USA, March 1993.

SILVA, M. Projeto de lei da política nacional de resíduos sólidos, 2010.

SIMIC, V. e DIMITRIJEVIC, B. Production planning for vehicle recycling factories in the eu legislative and global business environments. **Resources, Conservation and Recycling**, v. 60, 78–88, 2012.

SOBOL, I. **A primer for the Monte Carlo method**. CRC Press, 1994.

TANG, X.; BASSIR, D.H. e ZHANG, W. Shape, sizing optimization and material selection based on mixed variables and genetic algorithm. **Optimization Engineering**, v. 12, 111–128, 2010.

TANNEAU, O. Outil de prédiction d'indice d'affaiblissement par la méthode des matrices de transfert, 2002.

TANNEAU, O. **Modélisation de panneaus d'isolation aéronautiques**. 2004. Tese (Doutorado). Université Pierre & Marie Curie Paris VI.

TANNEAU, O.; CASIMIR, J.B. e LAMARY, P. Optimization of multilayered panels with poroelastic components for acoustical transmission. **Journal of Acoustical Society of America**, v. 120, 1227–1238, 2006.

UGAYA, C.M.L. e WALTER, A.C.S. Life cycle inventory analysis - a case study of steel used in brazilian automobiles. **Int Journal of Life Cycle Assessment**, v. 6, 365–370, 2004.

UIHLEIN, A.; EHRENBERGER, S. e SCHEBEK, L. Utilisation options of renewable resources: a life cycle assessment of selected products. **International Journal of Cleaner Production**, v. 16, 1306–1320, 2008.

UNEP. Waste investing in energy and resource efficiency. 2011.
URL: *http://goo.gl/miEApd*

WEIDEMA, B.; WENZEL, H.; PETERSEN, C. e HANSEN, K. **The Product, Functional Unit and Reference Flows in LCA**. Danish Ministry of the Environment, 70 ed., 2004.

WOOD, M.D.L.; MATHIEUX, F.; BRISSAUD, D. e EVRARD, D. Results of the first adapted design for sustainability project in a south pacific small island developing state: Fiji. **Journal of Cleaner Production**, v. 18, 1775–1786, 2010.

XIU, D. **Numerical Methods for Stochastic Computations: A Spectral Method Approach**. Princeton University Press, USA, 2010.

YANG, W. e YAN, L. Sound absorption performance of natural fibers and their composites. **Science in China Series D**, v. 55, 2278–2283, 2012.

ZAH, R.; HISCHIER, R.; LEAO, A.L. e BRAUN, I. Curauá fibers in the automobile industry - a sustainability assessment. **International Journal of Cleaner Production**, v. 15, 1032–1040, 2006.